NTNU
Faculty of Engineering Science
and Technology
Department of Marine Technology

Advisor: Jørgen Amdahl
Number of pages: 134
Availability: Closed

TMR4900 - Master Thesis

Analysis of the Big Orange XVIII and Ekofisk 2/4W collision in 2009

by

Erik Paulsen

Trondheim, 09.06.2011

NTNU
Dept. of Marine Technology
N-7491 Trondheim

Marinteknisk Senter
O.Nielsens vei 10

Tel. +4773595501
Fax. +4773595697

MASTER THESIS SPRING 2011

for

Stud. Techn. Erik Paulsen

Analysis of the Big Orange XVIII and Ekofisk 2/4-W collision in 2009

Analyse av kollisjonen mellom Big Orange XVIII og Ekofisk2-4/W i 2009

In June 2009 the offshore service vessel Big Orange XVIII sailed into the water injection platform Ekofisk 2/4-W. The kinetic energy was estimated to be in the range of 60 MJ, i.e. six times the standard design impact events for offshore platforms on The Norwegian Continental Shelf. The collision caused major structural damage to the ship and the platform. Several members of the platform were dented, subjected to permanent deformations and/or were torn off. Still, the platform did not collapse.

From a research point of view real accidents represent unite opportunities to learn how the structures behave during extreme actions, to verify the applicability of existing design methods given in codes and guidelines and to introduce improvements, if necessary. For example; after the collision between the Far Symphony and West Venture platform in 2004, the observed energy dissipation in the bow was back-calculated by Moss Maritime using the NORSOK N-004 curve for supply vessel bow impact. Very good agreement was obtained. This confirmed that the design curve, which has been in use from 1981, is realistic.

The objective of the master thesis is to simulate in detail the collision event by means of the nonlinear finite element programs USFOS and LS-DYNA. The structural damage inflicted on the bow of Big Orange XVIII and the platform shall be assessed and compared with the reported damage. The results of the analysis shall also be compared with the damage level predicted with the simplified methods given in NORSOK N-004 Appendix A.

The following topics should be addressed:

1. A review of the collision event with emphasis on the structural damage to the ship and the platform. Reference is made to the report issued by the Norwegian Petroleum Safety Authority: *Investigation of Big Orange XVIII's collision with Ekofisk 2/4-W 8 June 2009* and other information available.

2. On the basis of structural drawings of the upper bow of Big Orange XVIII develop a finite element model for analysis with LS-DYNA. Perform crushing analysis of the bow with a rigid structure of the same shape as the leg/brace connection, which was hit by the bow of Big Orange XVIII.

3. Establish a finite element model of the Ekofisk 2/4-W platform for analysis with USFOS. To the extent possible the repairs and strengthening of the platform which have been undertaken, shall be taken into account. Although

pile-soil interaction probably was not essential with respect to the collision response, it may be considered to include this in the platform model.

4. Perform pushover analyses for environmental loads for the platform in damaged and undamaged condition. Ship collision shall be simulated statically and dynamically with realistic force-deformation curves for the bow of Big Orange XVIII as obtained in part two. The damages obtained shall be compared with the reported damages. Important parameters may be varied in order to see if better agreement can be obtained. It is also of interest to increase the collision energy and/or perform other variations to check what margins the platform had against total collapse. Discuss sources of discrepancy, including the significance of incomplete information. Discuss the relevance of present design procedures for ship collision in view of the findings from the investigations. Improvements may be proposed.

5. Conclusions and recommendations for further work.

Literature studies of specific topics relevant to the thesis work may be included.

The work scope may prove to be larger than initially anticipated. Subject to approval from the supervisors, topics may be deleted from the list above or reduced in extent.

In the thesis the candidate shall present his personal contribution to the resolution of problems within the scope of the thesis work.

Theories and conclusions should be based on mathematical derivations and/or logic reasoning identifying the various steps in the deduction.

The candidate should utilize the existing possibilities for obtaining relevant literature.

Thesis Format

The thesis should be organised in a rational manner to give a clear exposition of results, assessments, and conclusions. The text should be brief and to the point, with a clear language. Telegraphic language should be avoided.

The thesis shall contain the following elements: A text defining the scope, preface, list of contents, summary, main body of thesis, conclusions with recommendations for further work, list of symbols and acronyms, references and (optional) appendices. All figures, tables and equations shall be numerated.

The supervisors may require that the candidate, in an early stage of the work, presents a written plan for the completion of the work. The plan should include a budget for the use of computer and laboratory resources which will be charged to the department. Overruns shall be reported to the supervisors.

The original contribution of the candidate and material taken from other sources shall be clearly defined. Work from other sources shall be properly referenced using an acknowledged referencing system.

The report shall be submitted in two copies:

- Signed by the candidate
- The text defining the scope included
- In bound volume(s)
- Drawings and/or computer prints which cannot be bound should be organized in a separate folder.
- The report shall also be submitted in pdf format along with essential input files for computer analysis, spreadsheets, Matlab files etc in digital format.

Deadline: June 14 2011

Trondheim, January 17th, 2011

Jørgen Amdahl

Abstract

This thesis consists of analyses and discussions regarding the collision between the offshore vessel Big Orange XVIII and Ekofisk 2/4W the 8th of June 2009. The collision caused the bow of Big Orange to deform three meters back from its original position. On the jacket installation, several braces were teared loose and the structure was pushed out of position. Although the installation endured large structural damages, it did not collapse. Based on the reported damage from NPD and the NORSOK design methods, the collision energy was estimated to be 58.7 MJ.

The collision analyses were performed by analyzing Big Orange and Ekofisk 2/4W in two separate uncoupled analyses. A model of Big Orange was made in Patran and analyzed in LS-DYNA. The first model of Big Orange had a $450mm$ mesh, but was refined to a $200mm$ mesh. The model of Ekofisk 2/4W was made and analyzed in USFOS.

The results from LS-DYNA were implemented as non-linear springs in the collision model in USFOS. Technical specifications regarding the vessel were provided by Ulstein Hatlø. Damage reports and structural arrangements regarding Ekofisk 2/4W were provided by Conoco Philips.

The model of 2/4W was analyzed in several conditions:

- Pushover analyses in undamaged and damaged condition
- Static and dynamic ship collision analysis
- Collapse analysis

The pushover analyses were mainly performed to verify that the model behaved as to be expected for this type of structure, and that it could be used for ship impact analysis.

The static and dynamic ship collision analyses in USFOS had the non-linear springs from LS-DYNA implemented at the collision points to simulate the deformation

of the bow in the ongoing collision. Two different dynamic collision models were tested. One model was unsupported, while one model had supports form the north and south bridges. The first collapse analyses were carried out by increasing the collision energy. This was done by increasing the vessel mass or velocity. The last collapse analyses were performed by changing the collision characteristics.

The deformation pattern for the unsupported model was similar to the reported damage both in response and in dissipated energy. Both the static and dynamic analyses dissipated the same collision energy that was estimated following the NORSOK methods. The structure had severe deformations when the collision energy was increased by 10%. The vessel speed would have been $5.019 m/s$ with this energy increase.

The results obtained from the dynamic analysis were not so similar to the recommended design curves in NORSOK, but gave lower forces for displacements. They were however similar to the results Amdahl and Johansen obtained from simulations in 2002. Using LS-DYNA, they obtained load-deformation characteristics for collisions between a ship bow, and vertical leg columns and oblique braces. Improvements proposed to NORSOK could be to update the design curves for collisions with jacket legs and columns of similar diameters. The values for these collisions are the same as for large diameter columns, and are overly conservative if used for smaller diameters.

Because the non-linear springs in USFOS were based on mass and velocity from the actual event, the results from the collapse analysis may deviate from the actual response. To address this problem, the LS-DYNA collision model could be improved to check the results.

Acknowledgments

This is the result of the master thesis work in the spring of 2011. The work has been carried out with the department of Marin Technology at the Norwegian University of Technology and Science.

This master thesis considers ship collisions, the same topic as the project work in the fall of 2011. I find the topic very interesting and I hope this thesis will be useful in feature investigations of ship collisions.

I would like to thank my supervisor Jørgen Amdahl for his time and help during the semester, as well as interesting discussions about the topic.

I would also like to thank PhD- candidate Zhenhui Liu for his assistance regarding modeling in LS-DYNA, Atle Johansen at DNV for help regarding the Ekofisk 2/4W installation, Vidar-Andre Gjerstad at Conoco Philips for useful information and help and Ulstein Hatlø for structural drawings of Big Orange XVIII.

Trondheim, 09.06.2011

Erik Paulsen

Contents

List of Figures

List of Tables

Abrevations

BOXVIII	- Big Orange XVIII
COG	- Center Of Gravity
DNV	- The Norwegian Veritas, Det Norske Veritas.
FE	- Finite Element
GPS	- Global Positioning System
MJ	- Mega Joule
MN	- Mega Newton
Mpa	- Mega Pascal
MWL	- Mean Water Level
NGI	- Norwegian Geotechnical Institute
NORSOK	- Technology Standards for the Norwegian continental shelf
NPD	- Norwegian Petrolium Directorat
USFOS	- Ultimate Strength of Framed Offshore Structures

Nomenclature

A	- Compression Area
a_1	- Added mass in surge
a_i	- Added mass of installation
a_s	- Added mass of ship
α_0	- Initial angle, snap through problem
α	- Deformed angle, snap through problem
C	- Damping matrix of dynamic equilibrium equation
E	- Young's module
E_k	- Dissipated kinetic collision energy
E_s	- Total strain energy
$E_{s,i}$	- Strain energy, installation
$E_{s,s}$	- Strain energy, ship
ε	- Strain
ε_{eq}	- Equivalent plastic strain
F^n	- Stress convergence vector
H^n	- Hourglass control parameter
h	- Displacement height, ref. fig. 3.3
J	- Mass moment of inertia of installation
K	- Stiffness matrix of dynamic equilibrium equation
k	- Strength coefficient, hard steel
$\mathbf{K}(\mathbf{r})$	- Global stiffness matrix
kg/m^3	- Weight per cubic meter
Km/h	- Kilometer per hour
l	- Bar length, ref. fig. 3.3
M	- Mass matrix of dynamic equilibrium equation
m	- Meters
mm	- Millimeters
m/s	- Meters per second
mt	- Metric tonnes
m_s	- Mass of ship
m_i	- Mass of installation
M_{tot}	- Total ship mass under collision

N	- Newton
n	- Hardening coefficient, hard steel
Nam/h	- Nautical mile per hour
N/mm^2	- Mpa
P^n	- External loads/ body forces
R	- Global force
r	- Displacement
R_i	- Resistance of installation
R_s	- Resistance of ship
$\ddot{r}_{n+1}$	- n+1 time increment of acceleration
$\dot{r}_{n+1}$	- n+1 time increment of velocity
r_{n+1}	- n+1 time increment of displacement
$\ddot{r}_n$	- n time increment of acceleration
$\dot{r}_n$	- n time increment of velocity
r_n	- n time increment of displacement
R_{n+1}	- n+1 time increment of external forces
R_n	- n time increment of external forces
Δr	- Displacement increment, snap through problem
S	- Axial force, positive in compression direction
s	- Seconds
σ	- Stress
σ_{eq}	- Equivalent yield stress
σ_Y	- Yield stress
Δt	- Incremental step size
u^{n+1}	- New displacement, central difference method
$v^{n+\frac{1}{2}}$	- New velocity, central difference method
v_s	- Ship velocity under collision
v_i	- Installation velocity under collision
V_{Col}	- Vessel collision speed
$W_{s,max}$	- Max displacement of vessel under collision
$W_{i,max}$	- Max displacement of installation under collision
z	- Distance from pivot point to point of contact
γ	- Accuracy parameter, Newmark method
β	- Accuracy parameter, Newmark method
α	- Accuracy parameter, HHT- method
x^0	- Old geometry, central difference method
x^{n+1}	- Updated geometry, central difference method

Chapter 1

Introduction

The platform structures in the North Sea are built for harsh environments, a long life span and different accidental loads. One of these accidental loads is ship impact. This could cause severe damages to the subjected structure, and there would be a certain possibility for collapse. During the last ten years there have been a total of 26[NPD, 2009b] collisions between installations and visiting vessels on the Norwegian continental shelf. Six of the collisions had large hazard potential. There is no single reason for why these accidents happen. Several factors are important: bad organizing, human errors, technical errors and inadequate training.

The platform Ekofisk 2/4-W was an unmanned water injection facility on the Ekofisk field, operated by Conoco Phillips. It was a three legged jacket structure, and was installed in 1972. It was mainly constructed as a bridge support, but was converted in 1989 when a water injection module was installed. As a part of the conversion, additional structural members were installed and other improvements done.

Figure 1.1: Ekofisk 2/4W and Big Orange XVIII

The offshore vessel was built for well stimulation at locations in the North Sea. The vessel was designed for high stability and good handling and control. The main dimensions of Big Orange were obtained from Schlumberger[Schlumberger, 2009] and NPD[NPD, 2009b].

Big Orange collided on the 8th of june 2009 with the Ekofisk 2/4W installation. The vessel velocity was 9.3 knots, 4.78 m/s, under the collision. The weight of the vessel was estimated to be 4661 metric tonnes in the moment of collision [NPD, 2009a]. The main dimensions and key values are given in table 1.1.

Property	**Value**	**Unit**
Loa	76	m
Beam	18	m
Draught	7	m
Dead weight	3700	mt
Classification	DNV	–
Weight at time of collision	4661	mt
Velocity at time of collision	9.3	$Knots$

Table 1.1: Main dimensions of BOXVIII

1.1 Scope of work

The scope of work in this master thesis is to make FE models of the Ekofisk installation and the top part of the bow of Big Orange XVIII. The bow is to be analyzed in a collision with a rigid structure with the same shape as the leg/brace connection which was hit in the collision. The force-deformation curves obtained from this analysis should be used to perform collision analyses on the FE model of Ekofisk 2/4-W.

Obtained results will be compared with reported damage on the installation and vessel, and improvements to NORSOK Appendix A may be proposed.

Chapter 2

Collision causes and structural damage to installation and vessel

The collision between the installation and the offshore vessel, which was classified as a major accident [NPD, 2009b], caused severe structural damage to the vessel bow and the platform installation. No personnel on neither the vessel nor the facility was physically hurt under the collision.

2.1 Collision causes and time span

Big Orange XVIII (hereafter reffered to as BOXVIII) was on its way to the Ekofisk installation to perform well stimulation operations. At 0402 in the morning the duty officer activated the autopilot to answer a phone call from Ekofisk 2/4-X. When he returned to the steering position the autopilot was not deactivated. The duty officer recieved an approval to enter the safety zone, in which the autopilot should be turned of.

Because the autopilot onboard BOXVIII was active in the safety zone on 500 meters, the course of the vessel was not like the duty officer had planned.

From 0413 to 0416 there was no control of the offshore vessel. An attempt was made to maneuver the vessel from collision course, but since the autopilot was active, the vessel followed the present course and collided with Ekofisk 2/4-W at 0417 on the 8th of june 2009.

The above information was gathered from the investigation report which was made of NPD after the accident [NPD, 2009a].

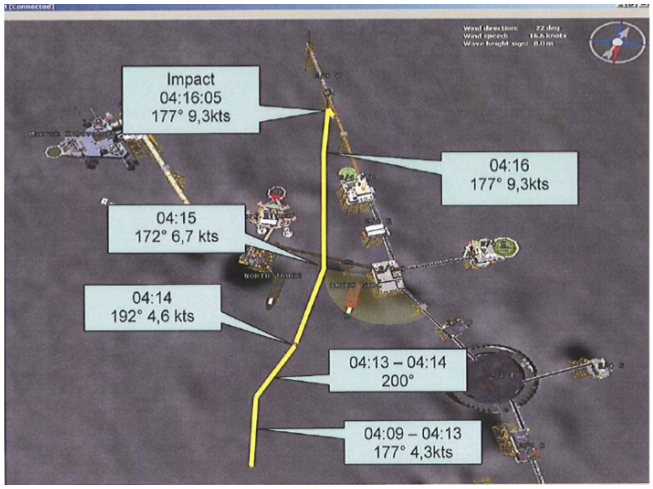

Figure 2.1: Collision time event

2.2 Structural damage

2.2.1 Ekofisk 2/4-W

The Ekofisk installation was partly pushed out of position after the collision with BOXVIII, due to plastic damages to the structure. The maximum displacement under the collision was reported to be approximately two meters[Gjerstad, 2011]. Several braces were teared loose from the main load-bearing structure. The water injection riser for well W05 was severely bent, and some wellheads were dislocated. The conductors in the centre of 2/4W were dented.

Figure 2.2: Undamaged and damaged north face of Ekofisk 2/4W

A local buckling was located on the southern leg near the cross-over to the pile. Cracks were discovered between the northwest and the northeast legs and the deck. The crack on the northwest leg near the topside was approximately half of the circumference. The crack on the northeast leg was approximately two thirds of the circumference. There were also some subsea damages to braces at levels $-2.5m$ and -15m beneath the sea surface.

Figure 2.3: Crack in connections between leg and topside

The bridge on the south side of 2/4W going to the south flare, illustrated in figure 2.4, was pushed into the topside and bearing structure. This caused damage to the bridge itself as well as to the bridge landing system.

Figure 2.4: Bridge landing. Left: south. Right: north

The north bridge landing, which connected the bridge with the rest of the Ekofisk structure, got some structural damage at the mid span under the collision. This was mainly due to interaction with the superstructure of BOXVIII.

The crew which were asleep on the 2/4Q installation, three installations links north from 2/4W illustrated in figure 2.5, woke up under the collision because they felt the platform accelerate and move[Gjerstad, 2011]. This may imply that energy propagated through the north bridge, as well as through the south bridge.

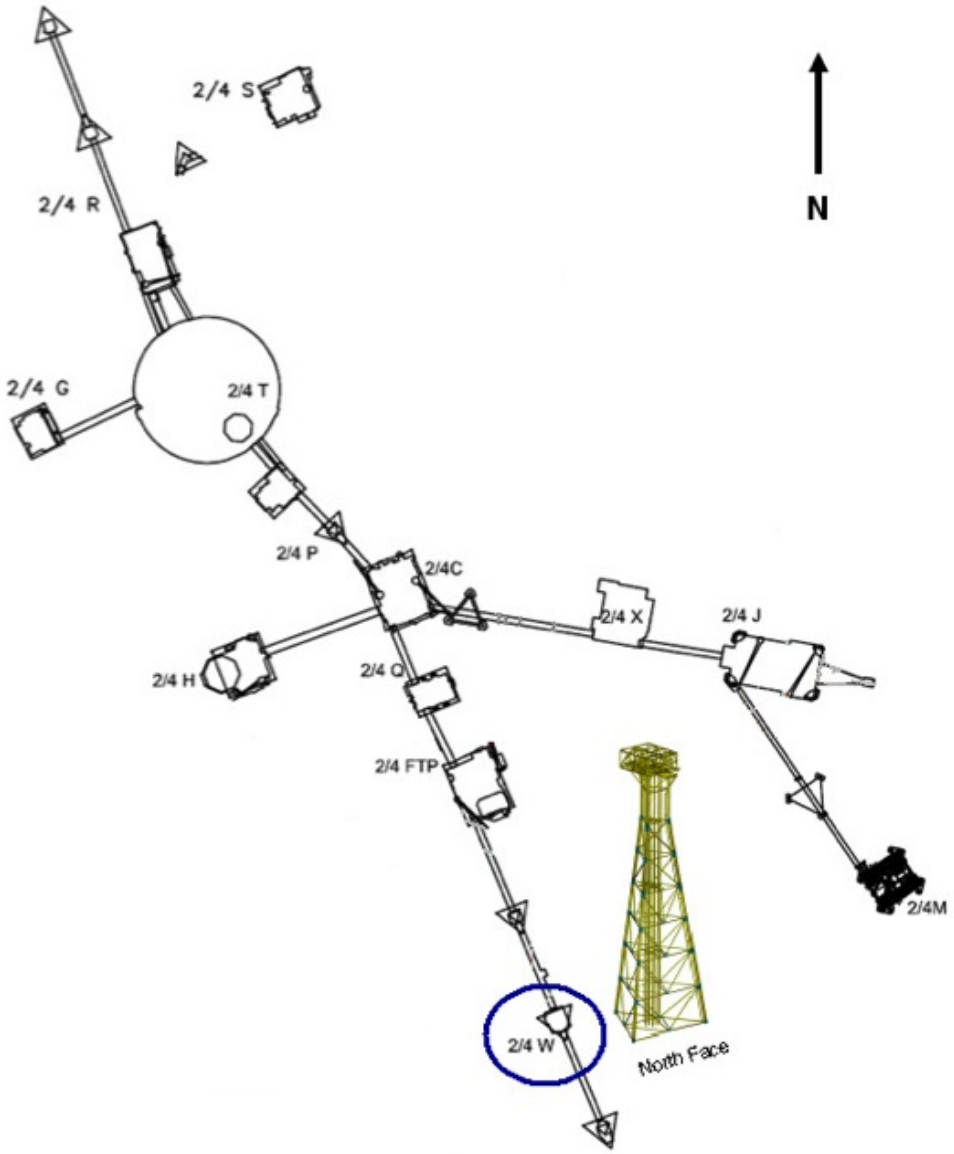

Figure 2.5: Overview of the structures at the Ekofisk field

2.2.2 Big Orange XVIII

The bow of BOXVIII was pushed in approximately three meters when it collided with the north face of 2/4W. The equipment on the vessel which interacted with the north bridge was torn of under the collision. This made the vessel inoperational.

Figure 2.6: The damaged bow of Big Orange

In figure 2.6 and 2.7, marks of the jacket structure can be seen. The vessel collided with two of the jacket main legs. At starboard side in the connection point with the northwest leg and two of the jacket braces, and the northeast jacket leg at port side.

Figure 2.7: Left:Vessel equipment torn off. Right: Bow pushed in, from side

The damages to BOXVIII were not documented in any report. The only documentation of the damages were pictures taken shortly after the accident.

Chapter 3

Design principles for ship collision and accidental loads

There are many different design codes for ship collisions. In this thesis there has been an emphasis on the NORSOK-N004 code, appendix A- accidental loads [NORSOK, 2004].

Ship collisions are characterized by a certain kinetic energy which is governed by the mass and speed of the ship at the time of impact. The mass of the ship includes hydrodynamic added mass. A part of the kinetic energy is dissipated as strain energy in the installation and to the vessel. Another part of the kinetic energy, depending upon the impact conditions, may remain as kinetic energy after the impact. This is often the case if the collision is non-central, which means that the contact force does not go through the COG of the installation. Large plastic strains and structural deformations are usual both to the vessel and installation under ship collision, because of the large amount of dissipated strain energy.

In ship impact scenarios there are both large in-elastic deformations at the collision contact point, as well as global hull bending. Non- linear FE analysis is normally used to determine the structural effects of a ship collision. A brief summery of this method is covered in section 3.2. Alternatively, an energy consideration as well as elastic-plastic methods could be used. When analyzing with the latter method, conservation of momentum and energy is used as the main principles. This is a quasi-static method of approach.

3.1 Strain- energy dissipation

A full analysis of ship collisions is very time consuming as it is a theoretically demanding problem. It is therefore often convenient to split the collision problem into two uncoupled analyses: external and internal collision mechanics. The latter one consideris energy dissipation and deformations, and is documented here.

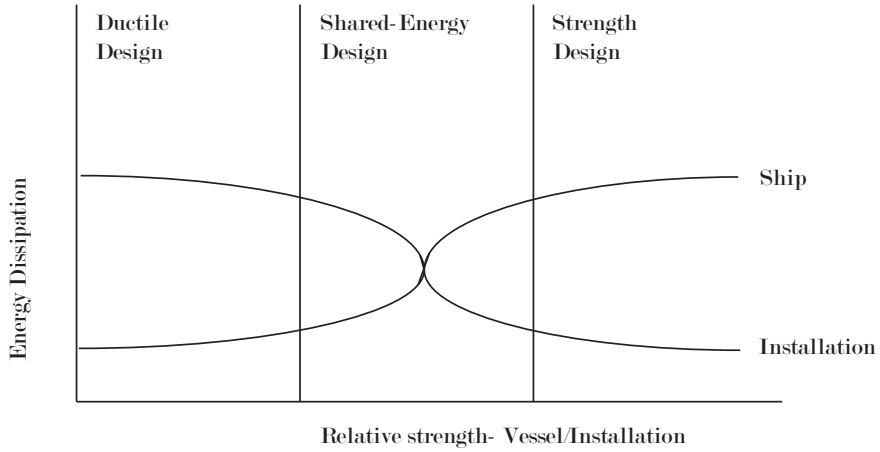

Figure 3.1: Energy dissipation to installation and ship

The distribution of strain energy is divided into three different levels of dissipation, illustrated in figure 3.1:

- Strength design: The installation is strong enough to resist the collision force with minor deformation. The ship is forced to deform and dissipate the major part of the energy.
- Ductility design: The installation undergoes large plastic deformations. The installation dissipates a major part of the collision energy.
- Shared-energy design: Both installation and ship contributes to the energy dissipation.

Because of the large deformation to both BOXVIII and the 2/4-W installation, the collision between the two can be analyzed as a shared-energy design collision. With this design principle, both the magnitude and distribution of the collision force depends upon deformation of both the installation and the ship bow. The strength design or ductility design is favourable in a calculation point of view. When this is the case, the response of the soft (yielding) structure can be calculated with simple considerations of the geometry of the rigid (non-yielding) structure. In most cases, shared-energy design is used.

The part of the collision energy which is dissipated into strain energy can be calculated in three different ways, depending on the type of installation and the purpose

of the analysis. The different strain energy relations are given in equation 3.1 - 3.3.

1 - Compliant installations

$$E_s = \frac{1}{2}(m_s + a_s)v_s^2 \frac{(1 - \frac{v_i}{v_s})^2}{1 + \frac{m_s + a_s}{m_i + a_i}} \tag{3.1}$$

2 - Fixed installations

$$E_s = \frac{1}{2}(m_s + a_s)v_s^2 \tag{3.2}$$

3 - Articulated columns

$$E_s = \frac{1}{2}(m_s + a_s)\frac{(1 - \frac{v_i}{v_s})^2}{1 + \frac{m_s z^2}{J}} \tag{3.3}$$

In the case of the Ekofisk collision, the velocity of the installation was $v_i \simeq 0$ compared to the velocity of BOXVIII. The installation was further assumed to be fixed due to the duration of the impact and because the installation was a jacket structure.

A load-deformation relationship can be made for the structural response of the ship and installation. The strain energy is divided into two separate parts: energy dissipated by the installation and energy dissipated by the ship.

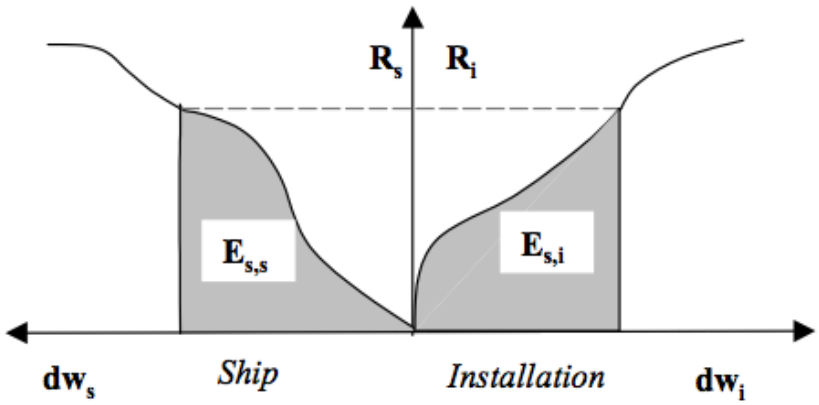

Figure 3.2: Load-deformation relations for ship collisions [NORSOK, 2004]

$$E_s = E_{s,s} + E_{s,i} = \int_0^{Ws.max} R_s dw_s + \int_0^{Wi.max} R_i dw_i \tag{3.4}$$

The load-deformation relations are often established separately from each other by assuming that the other structure is rigid. This principle of two uncoupled analyses is used in this thesis. Because both structures dissipate an amount of energy regardless of the relative strength, this method have some limitations.

The stronger of the ship and platform will often experience less damage, and the softer more damage than what the method described above predicts. The impact force is distributed over a large contact area when the soft structure deforms. The resistance of the strong structure increases accordingly.

3.2 Non-Linear Finite Element Analysis

3.2.1 Material properties

Structural response is based on the following principles: Equilibrium, Kinematic compatibility expressed by strains, and a stress-strain relationship. Non- linear response of a structural problem is further recognized from the following characteristics [Moan, 2003]:

- Non-linear behavior of boundary conditions
- Non-linear material behavior
- Non-linear geometric behavior, e.g large deformations

In an ordinary linear analysis, the main assumption is that the deformations are small, and a linear stress-strain relationship corresponding to Hookes's law is governing.

$$\sigma = E\varepsilon \tag{3.5}$$

When this is the case, strains can be found with linear functions of displacement gradients, and equilibrium is found by referring to the initial structural configuration. These assumption give incorrect results in non-linear analysis. The stiffness matrix will be depending on the displacement when non-linearities are to be accounted for. The stiffness relation will therefore be on the form of equation 3.6.

$$\mathbf{R} = \mathbf{K}(r)\mathbf{r} \tag{3.6}$$

Non-linear material behavior is due to the effects of passing the point of yielding, where there will plastic behavior. Non-linear boundary problems involves contact, for example a collision. This type of non-linearity may occur even if the material is linear and the displacements are small. An example of a typical non-linear

displacement problem is the two-bar snap-through problem, illustrated in figure 3.3.

For the snap-through problem, the axial shortening of r is:

$$\Delta = \frac{l}{cos\alpha_0} - \frac{l}{cos\alpha} \tag{3.7}$$

Hence the strain becomes:

$$\varepsilon = \frac{\Delta}{l/cos\alpha_0} = 1 - \frac{cos\alpha_0}{cos\alpha} \tag{3.8}$$

The compression force:

$$S = EA\varepsilon \tag{3.9}$$

The equilibrium for the deformed truss:

$$\mathbf{R} = 2Ssin\alpha = 2EA\varepsilon = 2EAsin\alpha(1 - \frac{cos\alpha_0}{cos\alpha}) \tag{3.10}$$

Introducing trigonometrical laws:

$$sin\alpha = \frac{h-r}{\sqrt{l^2+(h-r)^2}}, cos\alpha = \frac{l}{\sqrt{l^2+(h-r)^2}}, cos\alpha_0 = \frac{l}{\sqrt{l^2+h^2}} \tag{3.11}$$

Inserting trigonometrical equations in 3.11 into equation 3.10:

$$\mathbf{R} = \frac{2AE}{l}\Big(\frac{h}{r}\Big)\Big(\frac{l}{\sqrt{l^2+(h-r)^2}} - \frac{l}{\sqrt{l^2+h^2}}\Big)r \tag{3.12}$$

Equation 3.12 is on the same form as equation 3.6, a stiffness relation which depends on the deformation. This is a non-linear stiffness relation.

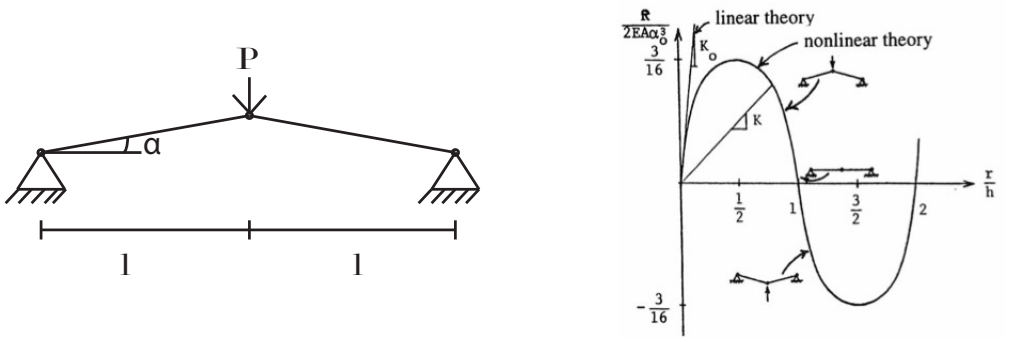

Figure 3.3: Two bar problem before, during and after snap-through

This problem must be solved by non-linear theory because of the 'snap-through'-effects. The two bars will get axial compression when loaded from above, and will at a certain load point snap down, like illustrated in figure 3.3.

3.2.2 Solution techniques

Various techniques for solving non-linear problems exist. The three most common techniques are:

- Incremental procedures, e.g Euler- Cauchy
- Iterative procedures, e.g Newton- Raphson
- Combined procedures, e.g Updated Newton- Raphson

Incremental methods provide the solution of a non-linear problem by a stepwise external loading. Δr , the displacement increment, is calculated for each load step. The incremental stiffness matrix **K** is obtained based on the displacement and the load, like described by equation 3.6.

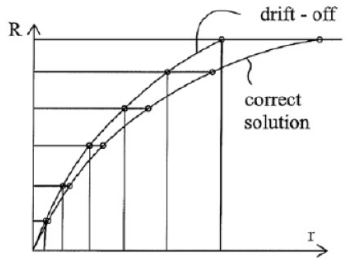

Figure 3.4: Euler-Cauchy increment

This method does not provide exact solution. It has a drift-off deviation, illustrated in figure 3.4.

The most frequently used method of approach is the Newton-Raphson iteration method, illustrated in figure 3.5. This method requires that **K** is established, and that the displacement is solved for each iteration step. The method is more time consuming, but provides more accurate results than pure incremental methods.

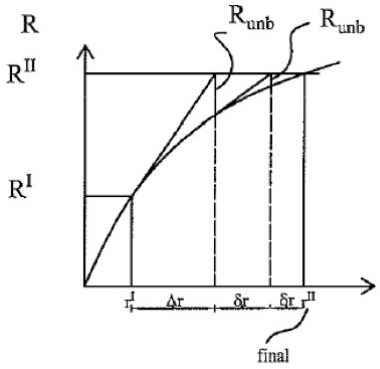

Figure 3.5: Newton-Raphson iteration

The combined method applies external loads in increments, and finds equilibrium in each increment by iteration. The updated Newton-Raphson method is illustrated in figure 3.6.

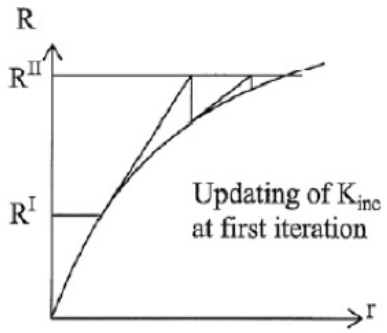

Figure 3.6: Updated Newton-Raphson method

There also exists more advanced solution procedures, like the arch-length techniques. These methods were introduced by Riks and Wempner in 1971 and 1972 [Moan, 2003]. Arch-length methods are used to find solutions beyond the unloading point of a load-displacement curve. The method can find post-collapse nature, and makes it possible to investigate if a structure is ductile or brittle.

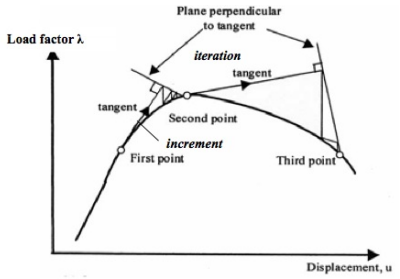

Figure 3.7: Arch-length method

The problems investigated in this thesis is of non-linear nature. The time integration methods which are used to analyze these types of problems are split into two different groups: implicit and explicit methods. In explicit methods, the equation of motion is evaluated at an old time step to calculate the displacement. Implicit methods use the equation of motion at a new time step to obtain the displacement. Implicit methods require higher time cost per cycle, but fewer steps. Explicit methods require many steps, but the time cost is decreased. LS-DYNA uses an explicit solver[dynasupport.com, 2011]. USFOS uses an implicit solver for direct time integration [Søreide et al., 1993].

3.2.3 Direct integration of equation of motion for nonlinear problems in LS-DYNA

The semi-discrete equation of motion to be solved for nonlinear problems using the central difference method in LS-DYNA are [Hallquist, 2006]:

$$Ma^n = P^n - F^n + H^n \tag{3.13}$$

P^n accounts for external loads and body forces, F^n is the stress convergence vector and H^n is the hourglass resistance. When advancing to time t^{n+1} using the central difference integration:

$$a^n = M^{-1}(P^n - F^n + H^n) \tag{3.14}$$

From the acceleration, the velocity and displacement are:

$$v^{n+\frac{1}{2}} = v^{n-\frac{1}{2}} + a^n \Delta t^n \tag{3.15}$$

$$u^{n+1} = u^n + v^{n+\frac{1}{2}} \Delta t^{n+\frac{1}{2}} \tag{3.16}$$

where

$$\Delta t^{n+\frac{1}{2}} = \frac{(\Delta t^n + \Delta t^{n+1})}{2} \tag{3.17}$$

The new geometry are obtained by adding the new displacement increments:

$$x^{n+1} = x^0 + u^{n+1} \tag{3.18}$$

The critical time step for the integration to obtain stability becomes

$$\Delta t \leq \frac{2}{\omega_{max}} \tag{3.19}$$

Where ω_{max} is the largest natural frequency of the structure. This frequency is bound by the highest frequency of any individual element in the finite element mesh.

Another method which can be used in LS-DYNA is the subcycling method, also called the mixed time integration method. This method sort elements based on their time step size into groups whose step size is an even multiple of the smallest element step size. The groups with different time steps are treaded differently to save time. A more thorough explanation of the method are given in the LS-DYNA theory manual.

3.2.4 Non-linear dynamic equilibrium in USFOS

USFOS uses the HHT-α method for time integration when solving the dynamic equilibrium equation[Søreide et al., 1993]. This method takes use of time averaging of the damping, stiffness and load matrix, expressed by the α-parameter. A beneficial feature of the integration method is that it uses artificial damping of higher frequency modes without reducing the grade of accuracy. The equilibrium equation with the integrated α-parameter is illustrated in equation 3.20.

$$M\ddot{r}_{n+1}+(1+\alpha)C\dot{r}_{n+1}-\alpha C\dot{r}_n+(1+\alpha)Kr_{n+1}-\alpha Kr_n = (1+\alpha)R_{n+1}-\alpha R_n \quad (3.20)$$

The incremental solution becomes as in equation 3.21 and 3.22.

$$\dot{r}_{n+1} = \dot{r}_n + \Delta t(\gamma)\ddot{r}_n + \Delta t\gamma\ddot{r}_{n+1} \quad (3.21)$$

$$r_{n+1} = r_n + \Delta t\dot{r}_n + \frac{\gamma t^2}{2}(1-2\beta)\ddot{r}_n + \Delta t^2\beta\ddot{r}_{n+1} \quad (3.22)$$

The parameters γ and β are the parameteris in the Newmark-β method. These parameters determines the stability and accuracy.

To avoid artificial damping, the γ- value is set to 0.5 in the original Newmark-β method where α=0. Different integration methods are applied by changing the value of γ. Some different methods are shown in table 3.1.

Condition	**Method**	**Stability**
γ=0	Central difference scheme	*Conditionally*
γ=1/4	Constant average acceleration	*Unconditionally*
γ=1/6	Linear acceleration	*Conditionally*

Table 3.1: Stability of integration methods

Only the method with constant average acceleration is unconditionally stable. The other methods must have criteria for the accuracy parameters to obtain stability.

During load incrementation, an important concept to avoid large over-prediction of the yield surface is scaling of step length. This is considerably more complex to apply in dynamic analysis than for the static analysis. The natural parameter to scale for dynamic analysis is the time step. However both the different components of the displacement increment given in equation 3.22 as well as the effective stiffness and load are non-linear functions of the time step.

Chapter 4

Finite Element Models

4.1 Ekofisk 2/4-W

Several improvements were done to 2/4W after first installation in 1972. In 1987, the platform deck legs were extended 7 meters due to seafloor subsidence. When the water injection module was installed in 1989, additional structural members were installed. In 1995 the deck legs were grout reinforced. Braces between the deck legs were installed in 2003 du to increased risk for wave-in-deck loads. In 2007, nine sub sea braces were reinforced by grouting, and two conductors were removed. The reinforcements were meant to improve the ability to resist storms, and to meet the updated NORSOK requirements.

The deck clearance on 2/4W was reduced by more than two meters compared with the air gap at the time of installation. This is due to sea floor subsidence. In June 2009 the subsidence was 9.4 meters[DNV, 2006].

A model was created by the candidate in the fall of 2010. This model was based on drawings from 1972 when the structure first was installed. Because of the many improvements described above and the soil subsidence, this model did not represent 2/4W in a correctly manner. An USFOS model of 2/4W was therefore provided by Atle Johansen at DNV[Johansen et al.,], which was made in the time shortly after the accident took place. The model was used for pushover analysis in damaged condition to check the capacity of the damaged structure.

4.1.1 USFOS model

The model of 2/4W included all the improvements done to the structure since the installation in 1972, as well as the grouted members. The secondary members such as risers and conductors were modeled to transfer loads to the jacket, and to not contribute to the structural strength. Eight conductors were led through the centre of the structure and down to the sea bed. These conductors were guided at levels with horizontal braces.

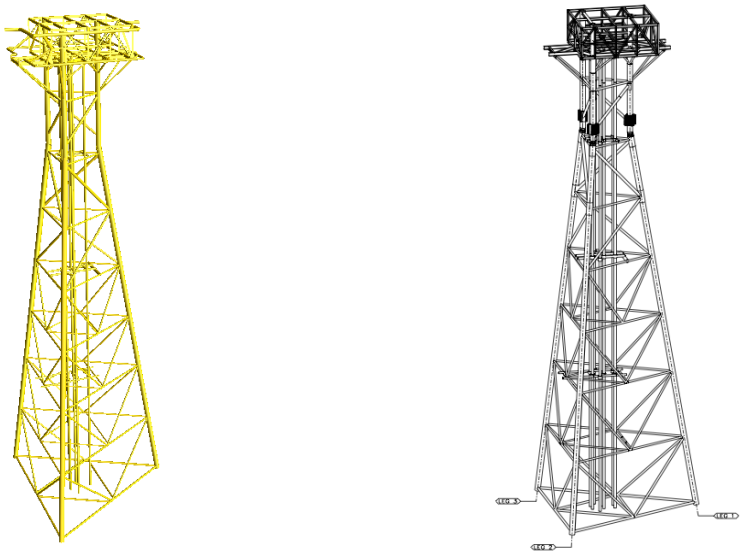

Figure 4.1: USFOS model of 2/4W

The member diameters and thicknesses for the jacket structure are given in table 4.1.

Member	**Diameter [m]**	**Thickness [m]**
Legs over water	1.067	0.030
Diagonal braces over water	0.508	0.025
Horizontal braces over water	0.457	0.019
Legs under water	1.120	0.059
Diagonal braces under water, -7 to -15m	0.559	0.025
Horizontal braces under water, -7 to -15m	0.356	0.013
Diagonal braces under water, -15 to -80m	0.356	0.013
Horizontal braces under water, -15 to -80m	0.356	0.010
Conductors	0.508	0.044

Table 4.1: Member details, 2/4W

The model included soil data from the Ekofisk field, which was provided from NGI[C.J.F.Clausen et al., 2006]. This was added to recreate the boundary conditions for the reaction forces. The soil model was created with the computer program GENSOD[DNV, 2006] by DNV shortly after the accident.

There were large horizontal distances between the piles from the three legs. The distance between the conductors were not large. Group effects were considered for the soil modeling because of the proximity of the piles. Disks at different levels represented the soil capacity along the piles.

The 2/4W installation was connected to Ekofisk 2/4F and a flare support through bridges. The bridges were not included in the USFOS model. They were replaced with nodal masses which represents the live and dead load of from bridges.

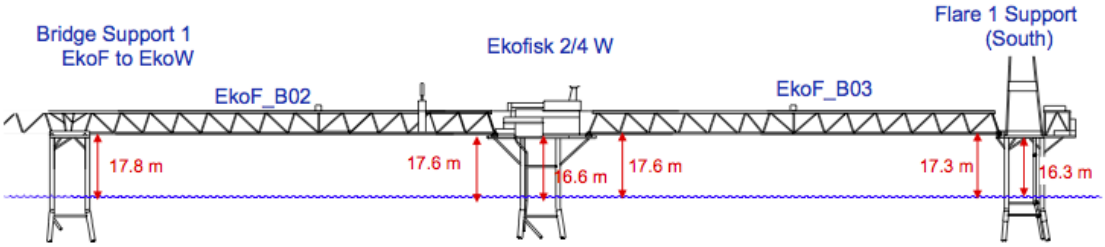

Figure 4.2: Connection to bridges from 2/4W

The topside weight of 2/4W was in june 2006 updated by Weight and Sea AS [Weight.and.Sea.AS, 2006]. The total weight of the topside was estimated to 877 mt, while the weight of the structure including the jacket and the topside was estimated to 2894 mt. The weigh of the topside was, as the bridges, modeled as nodal masses on the deck structure.

Marine growth was given to the members in USFOS based on NORSOK recommendations [NORSOK, 2004]. The added marine growth can be seen in table 4.2. The given water depth refers to MWL. The value refers to added thickness on the structural members.

Water depth	**Value**	**Unit**
Above +2 m	0	mm
+2 m to -40 m	100	mm
Below -40 m	50	mm

Table 4.2: Marine growth, 2/4W

4.1.2 Grouted Members

Grouted members are units, typically hollow and cylindrical, which have been filled with a material such as sand, concrete or gravel to reinforce the members

and increase their structural capacity. Several members of the 2/4W structure were grout reinforced in the time after first installation. These reinforcements were also implemented in the computer model. The grout material details used in the USFOS model of 2/4W can be seen in table 4.3 [DNV, 2006].

Material Property	**Value**	**Unit**
Density	2800	kg/m^3
Young's Module	40000	N/mm^2
Compressive Strength	130	N/mm^2

Table 4.3: Grout information, 2/4W

All of the three legs as well as some of the diagonal braces were reinforced with grout. An overview of the reinforced braces can be seen in figure 4.3.

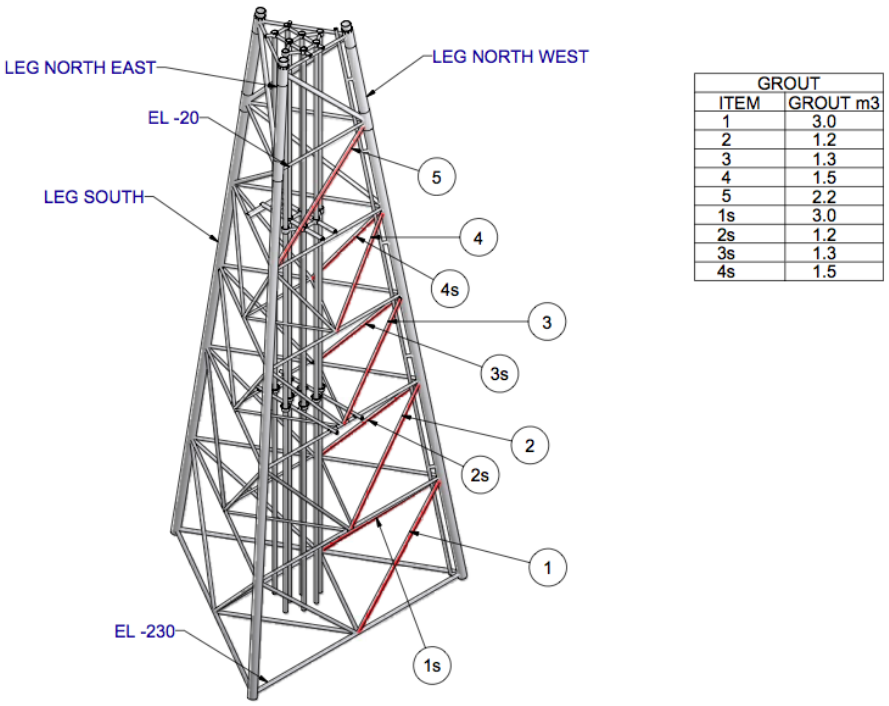

Figure 4.3: Reinforced braces[DNV, 2003]

The braces which were grout reinforced were located at the north side of the structure. This was the same side as the BOXVIII collided with.

The USFOS model file of 2/4W is given in appendix D.

4.2 Big Orange XVIII

The model of BOXVIII was made in MSC.Patran. This is a modeling software from MSC Software [mscsoftware.com, 2011]. The necessary drawings of the relevant ship parts was provided by Ulstein Hatløø[Ulstein, 1983b]. The FE model consisted of frame 97 to 109, i.e the upper part of the vessel bow. The area under the sea surface was not modeled. There was no interaction between this area and the jacket structure.

4.2.1 Bow geometry

The upper bow area which was affected by the collision consisted of four decks, including an upper top deck. All of the decks were supported by horizontal deck stiffeners, and the hull plates were supported by vertical frames. The stiffeners under the decks were both longitudinal and transverse, illustrated in the drawing of deck 02 in figure 4.4.

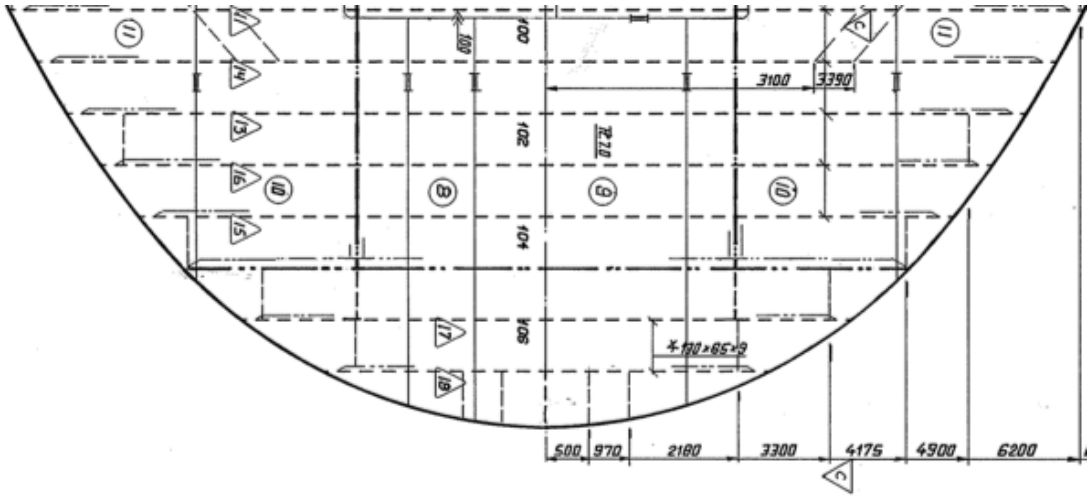

Figure 4.4: Stiffeners and details in deck 02

An overview of the decks can be seen in figure 4.5 and 4.6. The bottom line in figure 4.6 represents deck 01. The next line represents deck 02, also called the forecastle deck, illustrated in figure 4.4. The top line represents the upper top deck surrounded by a steel supporting fence, 1.3 meters high. Deck 00 is not illustrated in the figure, but was located below deck 01.

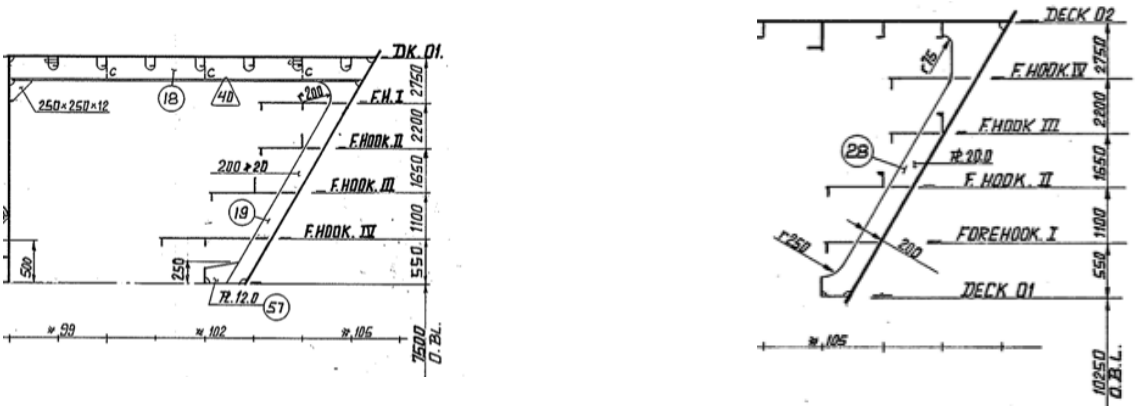

Figure 4.5: Bow stiffeners on Big Orange

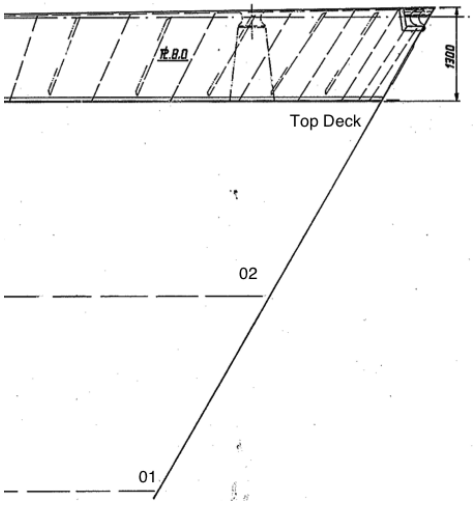

Figure 4.6: Overview of decks

4.2.2 Modeling and simplifications

The vessel bow was deformed approximately three meters back from its original position, ref section 2.2.2. The modeled area was greater than only the damaged part of the bow, to allow for the correct force transfer. Shell elements were used to model the different parts of the vessel.

The four decks were modeled first. This was done by inserting nodal points from the relevant drawings provided by Ulstein Hatlø, illustrated in figure 4.4 and 4.5. After the points were inserted, curves were created between the nodal points, forming the decks. By inserting more nodal points from the drawings, the hull structure of the ship was modeled. After the decks and the hull structure were modeled, the transverse and longitudinal stiffeners were made. The stiffeners were, as the ship hull and deck plates, modeled as shell elements with specific thicknesses.

Several simplifications were done when making the FE model of BOXVIII. Details as top deck bollards, winches and front fence holes illustrated in figure 4.7 was neglected. All the plates which stiffened the side fence were not modeled, only the three front stiffeners and two side stiffeners which had direct contact with the 2/4W leg under the collision.

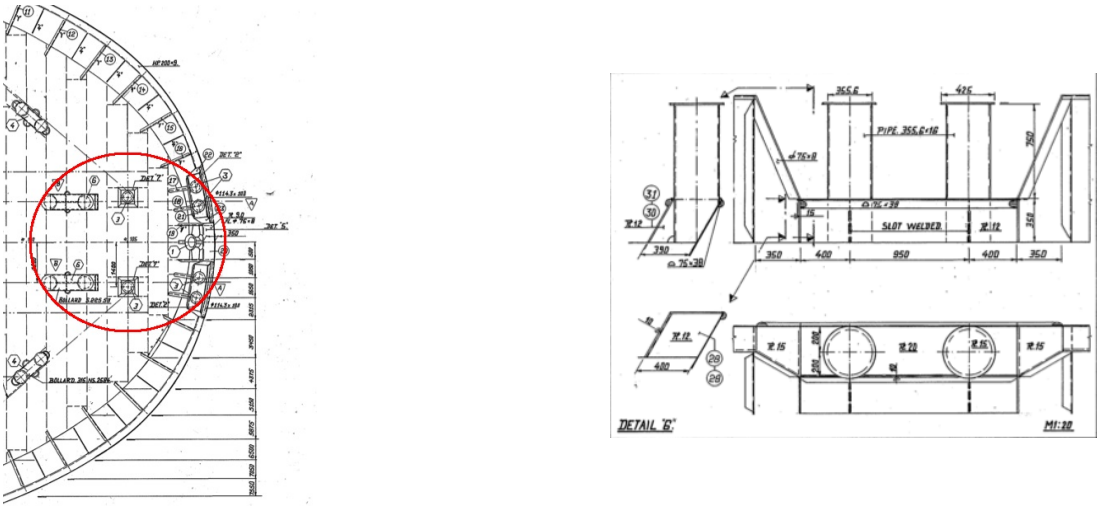

Figure 4.7: Top deck details and bollards

The connection with the deck stiffeners and the transverse frames were also simplified. The two stiffeners were connected together with a welded plate, like the stiffener connection illustrated in figure 4.8. The connection was however modeled as a fully connected shell element.

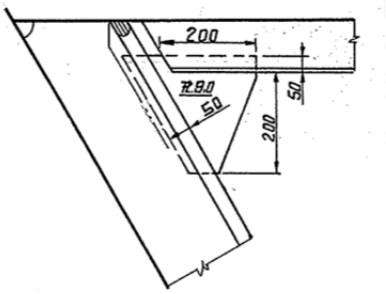

Figure 4.8: Connection point between vertical/horizontal stiffeners

Some parts of the bow consists of curved elements. The model in LS-DYNA was not modeled with any curved elements. This was simplified with tangential lines to make the modeling of the bow easier and faster.

4.2.3 Materials and meshing

The model of the bow was divided into several parts with specific geometrical properties. After discussions with supervisor, hard steel was used as the material for all the elements in the bow model. This steel type was the most frequently used material in vessels constructed at the same time as BOXVIII. The details for the used material can be seen in table 4.4.

Material Property	**Value**	**Unit**
Density, ρ	7850	kg/m^3
Young's Module, E	210E3	N/mm^2
Yield Strength, σ	275	N/mm^2
Poisson's ratio, ν	0.3	–
Hardening exponent, n	0.24	–
Strength Coefficient, k	740	N/mm^2

Table 4.4: Material properties of Big Orange bow in LS-DYNA

The material accounted for elastic-plastic behavior with isotropic hardening, using plain stress theory. The material was provided by Zhenhui Liu[Liu, 2011]. The equivalent stress-strain relationship was represented by a power law formulation which included the plateau strain[Alsos, 2008]. The stress-strain curve is given in figure 4.9.

$$\sigma_{eq} = \begin{cases} \sigma_Y & \text{if } \varepsilon_{eq} \leq \varepsilon_{plat} \\ K(\varepsilon_{eq} + \varepsilon_o)^n & \text{otherwise} \end{cases} \tag{4.1}$$

$$\varepsilon_0 = (\frac{\sigma_Y}{K})^{\frac{1}{n}} - \varepsilon_{plat} \tag{4.2}$$

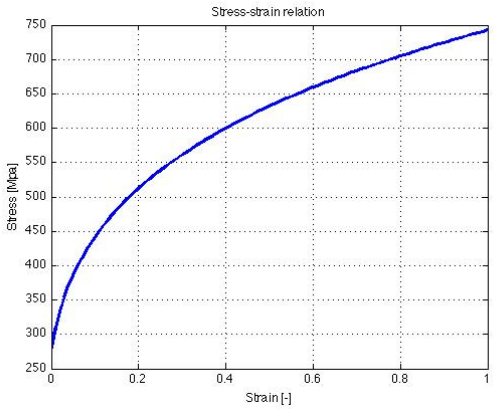

Figure 4.9: Plastic stress-strain relations

The bow consisted of five parts with different shell thicknesses. The values were found from the structural drawings of BOXVIII provided from Ulstein Hatlø [Ulstein, 1983a]. The parts and the respective thicknesses can be seen in table 4.5 and in figure 4.10.

Part/ colur	**Thickness**	**Unit**
Yellow/Hull	11.5	mm
Red/Hull and stiffenersl	15	mm
Green/ Decks	15	mm
Light Green/ Hull and fence	8	mm
Blue/ Deck stiffeners	8	mm

Table 4.5: Thicknesses on hull plates, decks and stiffeners

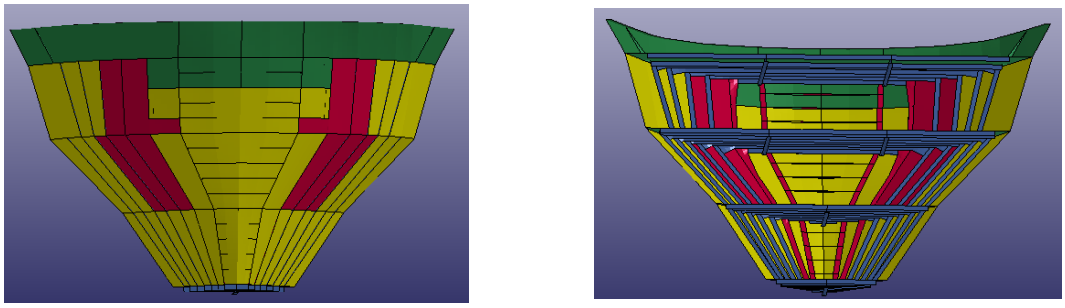

Figure 4.10: Bow parts and thicknesses

In addition to these five parts which the bow consisted of, the model also included the rigid jacket structure. This was modeled as four infinitely rigid cylinders, which modeled the two jacket legs, the diagonal brace and the horizontal brace which the bow interacted with under the collision. The two braces were modeled with a diameter on $450mm$, and the jacket legs were modeled with a diameter on 1067 mm (42 inches)[DNV, 2003]. The clamps which are illustrated in figure 4.11 was not modeled. The horizontal distance between the two jacket legs was 9906 mm[DNV, 2003].

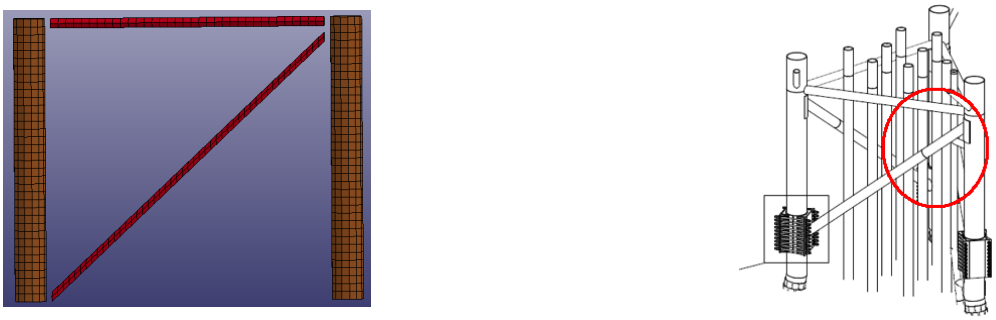

Figure 4.11: Jacket model in LS-DYNA

The material used for the jacket structure in LS-DYNA was normal steel. Material values are given in table 4.6. When using this material type no history are stored for the rigid elements. Computation time was therefore saved and the material did not require many input parameters because of the rigid nature.

Material Property	**Value**	**Unit**
Density, ρ	7850	kg/m^3
Young's Module, E	210E3	N/mm^2

Table 4.6: Material properties, jacket legs and braces in LS-DYNA

The risers between the legs were neglected in the model. It was assumed that they did not contribute much to the global deformation of the vessel bow.

The meshing of the model was done in MSC.Patran. The model consisted of quadratic Q4 shell elements. These elements give more accurate approximations then triangular elements[Logan, 2007]. The first mesh size was made with elements of 450mm length. After discussions with Zhenhui Liu, the meshing standard at the Institute of Marine Technology was settled to be $120mm$ element size.

4.3 Collision modeling

The structure which the bow collided with was at an early phase modeled as one single rigid cylinder which interacted with the starboard side of the vessel. After discussions with Atle Johansen at DNV [Johansen et al.,] it became clear that the bow collided with two of the vertical legs as well as a diagonal brace and a horizontal brace between the two legs. The vessel collided first with the starboard side into the north-west leg, and after a delay it collided with the port side into the north-east leg. The vessel also interacted with the risers behind the two legs, but this interaction was neglected because the two legs and the diagonal brace accounted for almost all of the deformation. The structure which the bow collides with can be seen in figure 4.11.

The parts which was included in the bow model was fixed at certain points in the collision model, while the two parts which includes the legs and braces were moving in a constant speed against the bow until it reached a certain prescribed displacement. By modeling the collision this way only one parameter, the prescribed displacement, could be changed until the desired bow deformation was obtained.

4.3.1 Boundary conditions

The boundary conditions for the model were made to imitate the rest of the vessel behind the bow. After some analysis tests and discussions with supervisor, the boundaries were assumed fixed in translation directions, but free to move in rotational directions. These conditions were applied at locations which can be seen in figure 4.12 and table 4.7.

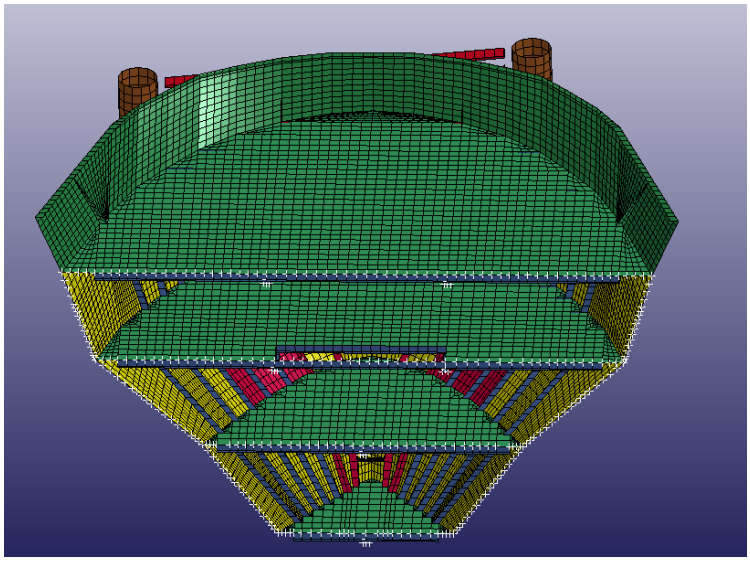

Figure 4.12: Boundary conditions for bow model of Big Orange

The notation 1 and 0 in the table below means fixed and free boundary respectively.

Part	**x, y, z, Rx, Ry, Rz**
Deck structures	1, 1, 1, 0, 0, 0
Longitudinal stiffeners	1, 1, 1, 0, 0, 0
Hull Structure	1, 1, 1, 0, 0, 0

Table 4.7: Boundary, bow model

Alternatively the collision could be modeled by giving the bow an initial speed in the collision direction into the fixed jacket structure. This would however be more difficult, because the mass of the vessel behind the bow and the boundary conditions would have to be modeled correctly.

4.3.2 Contact criteria

If a collision analysis in LS-DYNA consists of a great deal of physical material contact, the user has to implement input commands to control which elements that interacts with each other, and how they interact. One way to do this, is to give all of the involved element the possibility to interact each other. This is however tedious, because the program has to calculate displacements for elements which is unaffected by the collision.

To save analysis time, the bow elements were divided into segments. These segments were again coupled to the different jacket structures which they were to interact with. By doing this, LS-DYNA only calculated the new displacements for elements which actually were involved in a certain interaction.

This is a version of the master-slave technique, where the bow model was the slave and the jacket structure was the master. The friction coefficient for the contact was defined as 0.3[Liu, 2011].

The three segments are described in table 4.8 and figure 4.13.

Ship part	**Jacket part**	**Number**
Starboard ship side	North-west Leg	1
Front side	Diagonal and horizontal brace	2
Port ship side	North-east Leg	3

Table 4.8: Bow segments in LS-DYNA

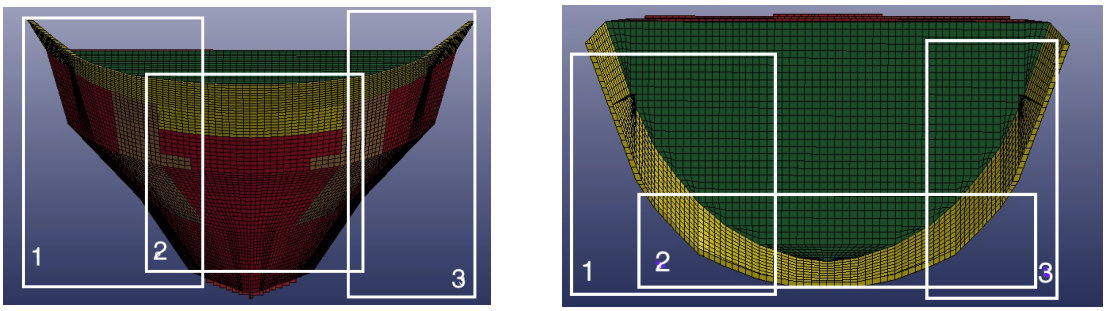

Figure 4.13: Overview of bow segments

If this method is to be used, it is important to gather all involved elements in the respective segments. If elements which are involved in the collision are neglected or missed, some errors could occur. In the modeling of BOXVIII, the segments were chosen conservatively to ensure that all of the involved elements were applied in the analysis.

Chapter 5

Analyses of Big Orange in LS-DYNA

The analyses executed in LS-DYNA were the crushing analyses between the BOXVIII bow and the rigid jacket structure described in section 4.3. The analyses were performed to obtain data, used for modeling the deformation of the bow in the collision analyses in USFOS.

Several analyses were executed with different input parameters, to get the best possible results compared to the reported damage. The mesh was also refined several times, to increase the accuracy of the results.

5.1 LS-DYNA input parameters

The input file for the LS-DYNA analysis consisted of several keywords that controlled the analysis. Some of the input controlled the model geometry. These were automatically created by MSC.Patran. Other inputs such as boundary conditions, material properties, termination time, output control, displacement length and contact criteria were entered manually. The complete input files can be found in appendix D.

Some parameters were the same for every analysis, such as material properties, boundaries and contact criteria. Parameters such as output control and described displacement were however changed many times to tune the output to better imitate the real damage.

The termination time was set to $1.0s$ for all of the analyses, which meant that the dynamic impact analysis had a duration of one second. The cylindrical jacket struc-

ture in the model had a prescribed displacement. The displacement was however not the same for every part. This was to account for disconnection of braces, which happened to both the horizontal and diagonal brace under the collision.

The analysis was executed several times before a satisfying result was obtained, and the damage could be compared to the documented damage. The different prescribed displacements which were used in the final input file can be seen in table 5.1.

Part	**Displacement**	**Unit**
Jacket legs	-5600	mm
Horizontal brace	-1200	mm
Diagonal brace	-4000	mm

Table 5.1: Prescribed displacements of jacket structure

5.2 Results of collision analysis against rigid structure

The first analysis had a mesh size of $450mm$. The duration of the analysis was approximately one hour. The deformed vessel bow is illustrated in figure 5.1.

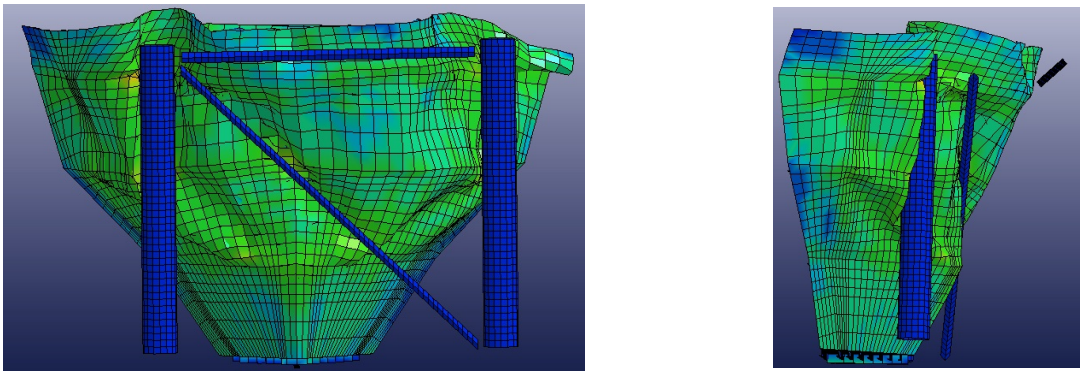

Figure 5.1: The deformed vessel bow from front and from starboard side. $450mm$ mesh

The ship hull plating on the starboard side had started to fold under the compression force from the northwest jacket leg. The diagonal brace left a mark in the BOXVIII bow which was similar to the document damage from the collision. The mark after the northeast leg at the port side of the vessel was also consistent with the reported damage. The load-deformation values from LS-DYNA were post-processed in Matlab to calculate the dissipated energy. The load-deformation curves from Matlab are given in figure 5.2. The Matlab code is given in appendix C.

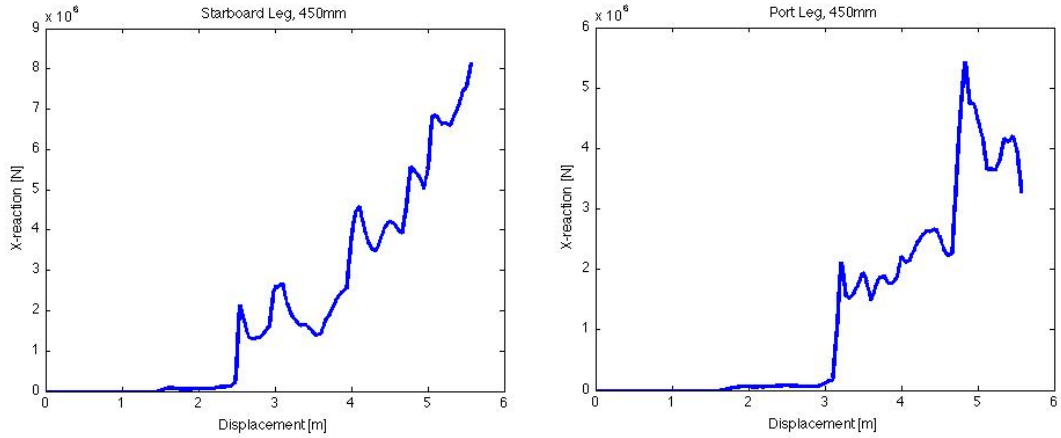

Figure 5.2: Load-deformation curves from Matlab with 450mm mesh size. Left: Starboard leg. Right: Port leg

The maximum force on starboard side was $8MN$ at 3.0 m deformation after first contact. The absorbed energy in vessel from starboard side contact was $11.2MJ$. The maximum force on port side was $5.5MN$ at $2.0m$ deformation after first contact. The absorbed energy from port side contact was $6.9MJ$. The resultant force at maximum deformation at $3.0m$ was $11.5MN$, and the total absorbed energy including the braces was $23.3MJ$. The results are given in table 5.2.

Result	**Value**	**Unit**
Max force x-dir, starboard side	8.0	MN
Max force x-dir, port side	5.5	MN
Resultant force x-direction at max deformation	11.5	MN
Absorbed energy, starboard side	11.2	MJ
Absorbed energy, port side	6.9	MJ
Absorbed energy, braces	5.2	MJ
Total absorbed energy	23.3	MJ

Table 5.2: Results LS-DYNA, 450mm mesh

The model was after the first analysis refined to a finer mesh with 250mm element size. This was done to check convergence of the results. If the results for the 250mm analysis were similar to the 450mm mesh analysis, no further meshing would be done.

The duration of the analysis was approximately 5 hours. The deformed vessel bow is illustrated in figure 5.3.

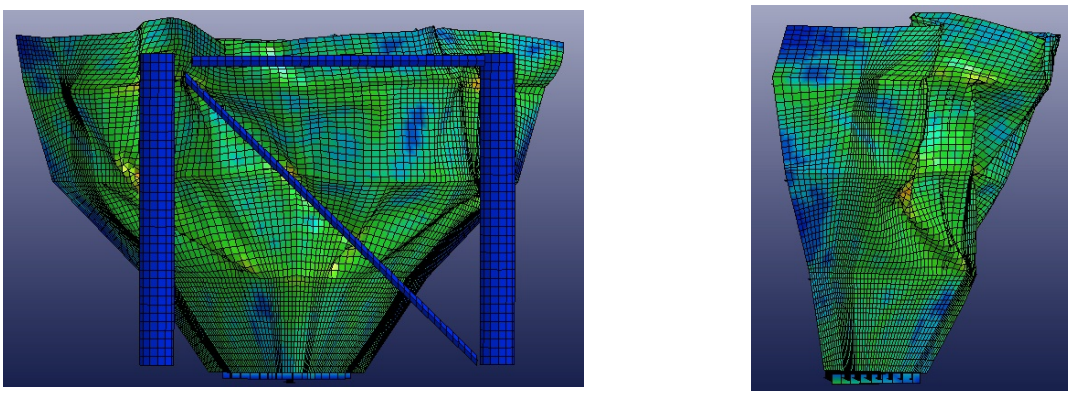

Figure 5.3: The deformed vessel bow from front and from starboard side. 250mm mesh

After the model was refined, the folding mechanism was enhanced and became more similar to the documented deformation. As a result of the refinement, the deformation force in the collision direction became lower for both starboard and port side of the vessel. The curves did however show the same characteristics for higher and lower force peaks. The load-deformation curves are illustrated in figure 5.4.

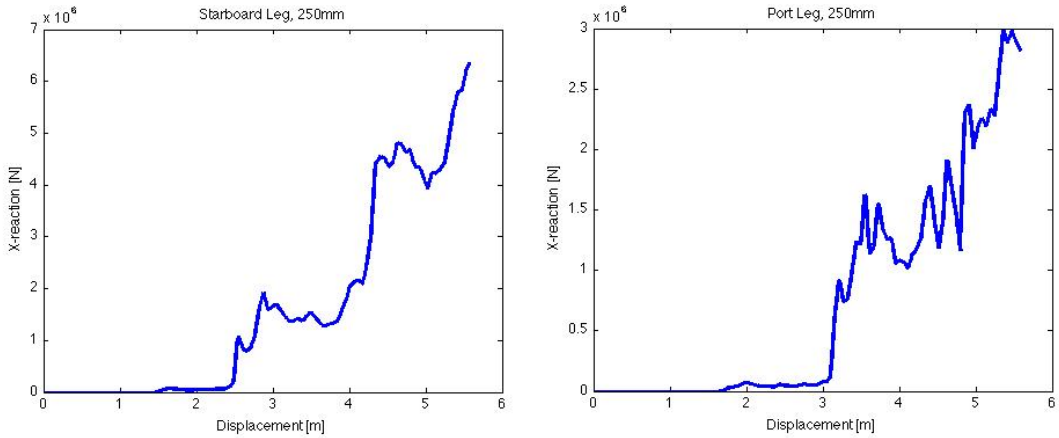

Figure 5.4: Load-deformation curves from Matlab with 250mm mesh size. Left: Starboard leg. Right: Port leg

The results of the 250mm mesh analysis can be seen in table 5.3.

Result	**Value**	**Unit**
Max force x-dir, starboard side	6.5	MN
Max force x-dir, port side	3.0	MN
Resultant force x-direction at max deformation	10.0	MN
Absorbed energy, starb.side	8.9	MJ
Absorbed energy, port side	4.0	MJ
Absorbed energy, braces	4.015	MJ
Total absorbed energy	16.915	MJ

Table 5.3: Results LS-DYNA, 250mm mesh

Compared to the first analysis, the analysis with 250mm mesh absorbed less energy. The difference was:

$$\delta E = E_{T,450} - E_{T,250} = 23.3MJ - 16.915MJ = 6.385MJ \tag{5.1}$$

The energy balance was not similar but gave a difference in absorbed energy. The mesh was refinement to an element size of 200mm. With this element size, the model consisted of 24187 elements. The duration of this analysis was approximately 30 hours. The deformed bow with 200mm mesh is illustrated in figure 5.5.

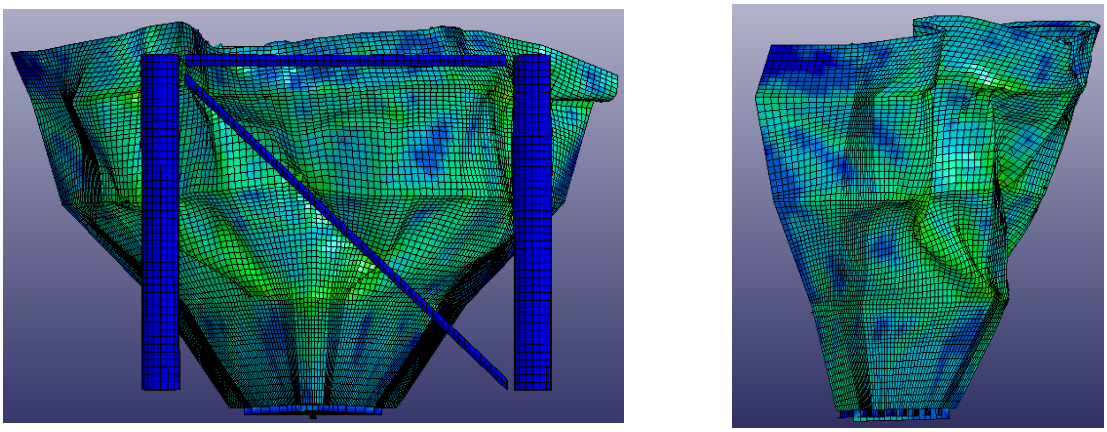

Figure 5.5: The deformed vessel bow from front and from starboard side .200 mm mesh

The results of this analysis was similar to the results from the 250mm mesh analysis in forms of absorbed energy, folding mechanisms and force-deformation characteristics. The load-deformation curves post processed in Matlab was for 200mm mesh similar to the 250mm mesh analysis and are illustrated in figure 5.6.

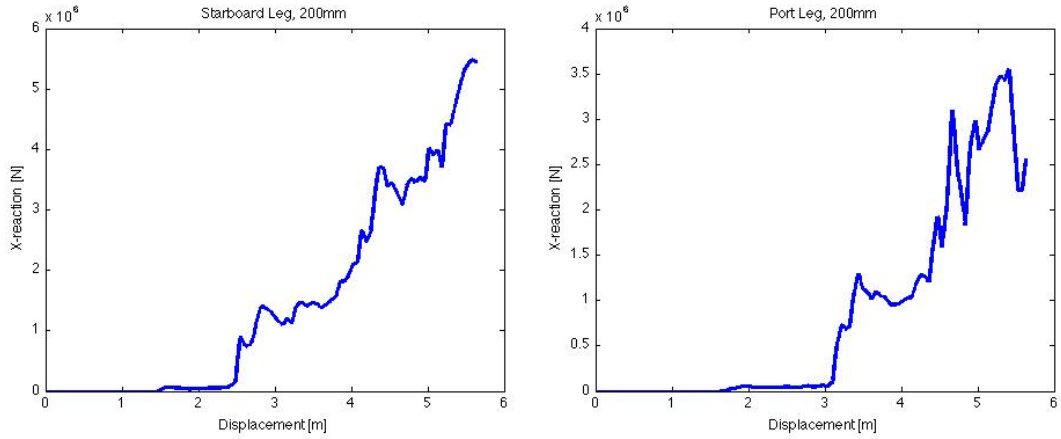

Figure 5.6: Load-deformation curves from Matlab with 200mm mesh size. Left: Starboard leg. Right: Port leg

Because of the similarity of the results, further refinement of FE-mesh was not performed. This was considered the be the most accurate LS-DYNA analysis.

Had the results deviated from the 250mm mesh analysis, the next refinement of mesh would have been to 120mm mesh size.

The results of the 200mm mesh analysis can be seen in table 5.4. The resulting force in collision direction was somewhat lower than for the 250mm analysis. The absorbed energy increased for the port leg and decreases for the starboard leg, although not significantly. The energy inflicted by the two braces was unchanged.

Result	**Value**	**Unit**
Max force x-dir, starboard side	5.5	MN
Max force x-dir, port side	3.6	MN
Resultant force x-direction at max deformation	9.1	MN
Absorbed energy, starb.side	8.1	MJ
Absorbed energy, port side	4.6	MJ
Absorbed energy, braces	4.08	MJ
Total absorbed energy	16.78	MJ

Table 5.4: Results LS-DYNA, 200mm mesh

The total difference in absorbed energy for the last refinement was:

$$\delta E = E_{T,250} - E_{T,200} = 16.915MJ - 16.78MJ = 0.135MJ \tag{5.2}$$

The time duration for each analysis is given in in table 5.5.

Element size	Analysis time	Number
450 mm	60 minutes	1
250mm	300 minnutes	2
200 mm	1825 minutes	3

Table 5.5: Time duration for mesh refinements

The load-deformation curves were to be used in USFOS as non-linear springs. The curves were based on the curves in figure 5.6, but were simplified with fewer points. The signs on the reaction force were reversed to comply with the input preference for USFOS. The zero displacement-point was moved to the point where first contact was made, i.e when the jacket structure collided with the bow.

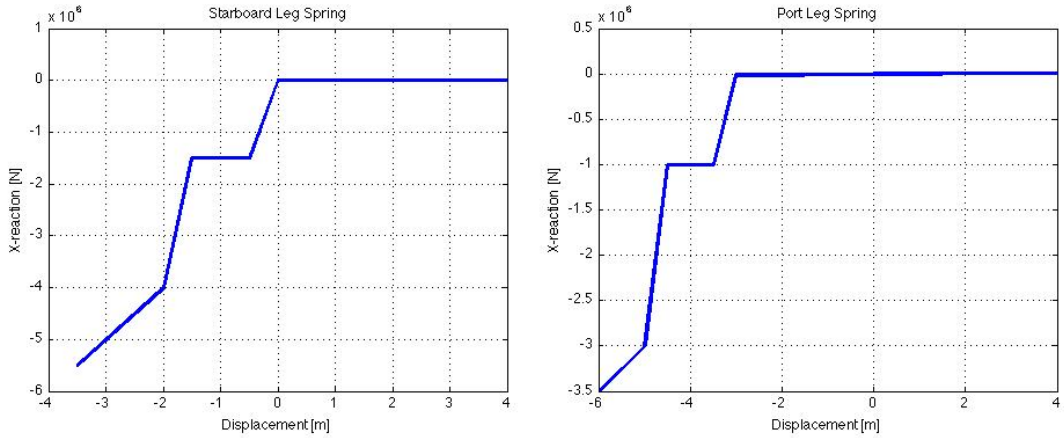

Figure 5.7: Load-deformation curves implemented in USFOS

As can be seen in figure 5.7, the port spring was modeled with a three meter delay. This was done do imitate the contact delay for the port leg with respect to the starboard leg. The values from figure 5.7 can be seen in table 5.6.

Force	Displacement
1.0e4 kN	0.01 m
-1.0e4 kN	-0.01 m
-1.5e6 kN	-0.5 m
-1.5e6 kN	-1.5 m
-4.0e6 kN	-2.0 m
-5.5e6 kN	-3.5 m

Force	Displacement
1.0e4 kN	3.5 m
-1.0e4 kN	-3.5 m
-1.0e6 kN	-4.0 m
-1.0e6 kN	-5.0 m
-3,0e6 kN	-5.5 m
-3.5e6 kN	-6.5 m

Table 5.6: Spring properties, vessel bow. Left: starboard side. Right: port side

Chapter 6

Analyses of Ekofisk 2/4W in USFOS

The USFOS model of 2/4W was analyzed in several different scenarios:

- Preliminary pushover analyses
- Static and dynamic collision analyses
- Pushover analyses in damaged condition
- Collapse analysies

The pushover analyses in damaged conditions were to be applied after the static collision analysis. The collapse analyses were executed to investigate the remaining capacity of the structure and and to check the margins the structure had against total collapse.

6.1 Pushover analysis for environmental loads, undamaged condition

Before the collision analyses with integrated load-deformation curves from LS-DYNA were performed, pushover analyses in undamaged condition were applied to the jacket model.

A pushover analysis is an analysis which applies a constant vertical load and an increasing horizontal load to a structure[Amdahl and Skallerud, 2002]. The vertical load represents live and dead load on the structure. The horizontal load represents environmental loads. The load is applied in USFOS as a wave with specific period

and height. USFOS identifies the worst wave phase and uses this in the static pushover analysis. The worst phase is identified according to either max base shear or overturning moment. The analysis is carried out until failure, or as long as the user wants it to last. This type of analysis identifies weaknesses and shows which elements in the structure which would fail first.

Two separate pushover analyses were executed in undamaged condition, with a 180 degrees difference in wave propagation direction. The environmental parameters for the first pushover analysis can be seen in table 6.1 [DNV, 2003].

Input	**Value**	**Unit**
Wave height	24.05	m
Wave period	14.14	s
Current speed	0.69	m/s
Water depth	81.10	m
Wave theory	Stokes 5th order theory	$-$
Direction of wave	North, 0	*Degrees*

Table 6.1: Environmental conditions for pushover analysis, north bound waves

The first pushover analysis had north propagating waves. This was opposite of the collision direction which was from north. The load-displacement curve for the pushover analysis can be seen in the figure 6.1.

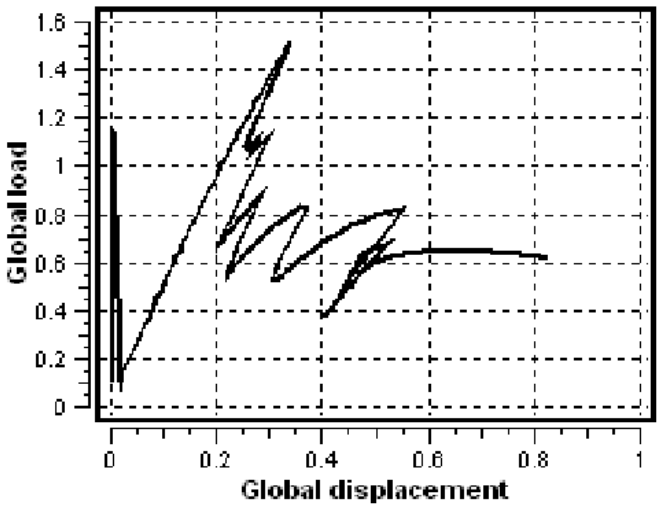

Figure 6.1: Load-displacement, pushover analysis in undamaged condition, north bound waves

The global load increased until a member failed. When that happened, the global load level dropped. The load level then increased again until a second member

failed. This stepwise increase and drop in the load level as braces fails is illustrated in figure 6.1. This is a typically load-displacement characteristic for this type of structure [Amdahl and Skallerud, 2002]. The structural response is illustrated in figure 6.2. The fringe range illustrates plastic utilization.

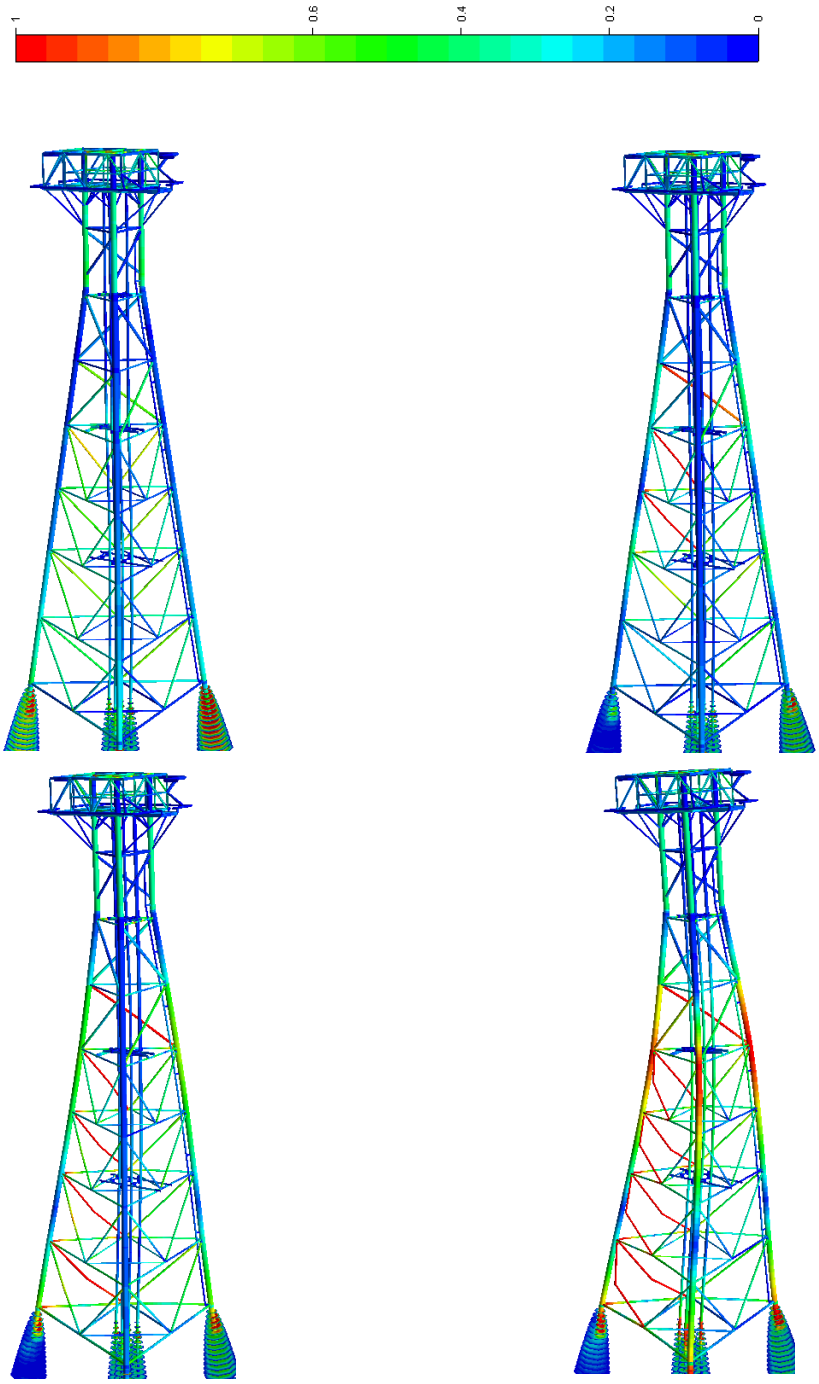

Figure 6.2: Structural response pushover analysis, waves north bound. Top left: initial load peak. Bottom right: End of analysis.

At the first load peak the first member failed. This was a brace in the second submerged level (-15m) and the global deformations were small. After this first failing member, several braces in the second to sixth submerged levels started to fail. At the end of the analysis the legs started to fail and the jacket got global bending.

The second pushover analysis had south propagating waves, which was the same as the collision direction. The other environmental conditions were similar to the first analysis.

Input	**Value**	**Unit**
Wave height	24.05	m
Wave period	14.14	s
Current speed	0.69	m/s
Water depth	81.10	m
Wave theory	Stokes 5th order theory	$-$
Direction of wave	South,180	$Degrees$

Table 6.2: Environmental conditions for pushover analysis, south bound waves

The load-displacement curve is illustrated in figure 6.3. The curve showed the same characteristics as the first pushover analysis, with repeating increases and drops in the load level. Both the load level and the global displacements before first load drop were somewhat higher than for the first pushover analysis.

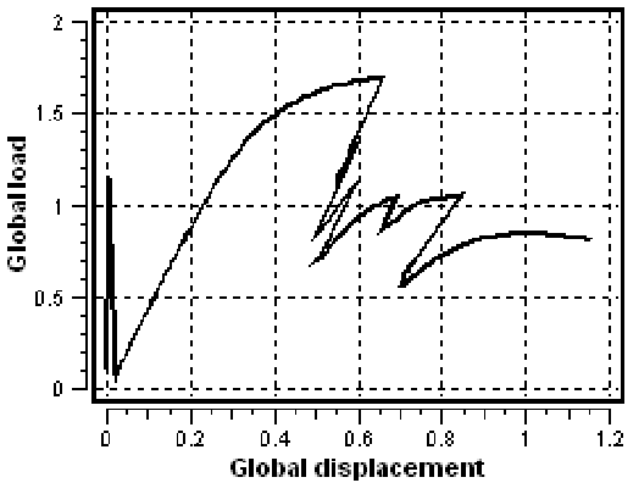

Figure 6.3: Load- displacement, pushover analysis in undamaged condition, south bound waves

The structural response is illustrated in figure 6.4. The fringe level represents plastic utilization.

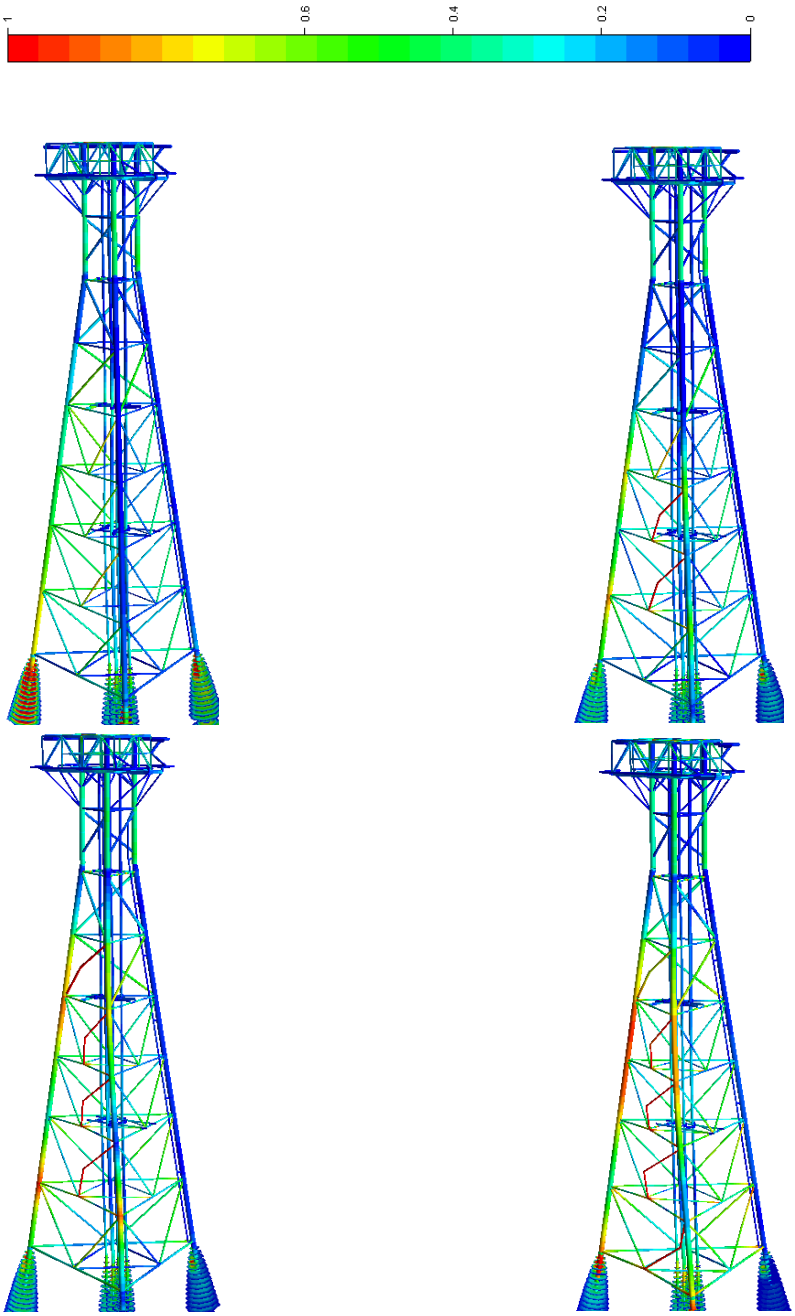

Figure 6.4: Structural response pushover analysis, waves south bound. Top left: Initial load. Bottom right: End of analysis.

The response was less severe for this second pushover analysis. Fewer braces yielded in the middle of the structure, but the legs still started to fail at the end of the analysis. The model showed failing characteristics which were to be expected for this type of structure, and it was assumed that the response of the model represented the 2/4W installations structural behavior in a good way.

6.2 Collision analysis

Before the collision analyses in USFOS were executed, there were many uncertainties considering the exact collision event and at which point on Ekofisk 2/4-W the vessel collided. Because of these uncertainties, many different analyses were performed. As discussed in section 4.3, the preliminary collision model was modeled to represent collision with only one of the jacket legs. Using this model, the jacket failed for both the static and dynamic analysis under less energy than for the real collision. This is discussed in detail in section 6.4.

6.2.1 USFOS input parameters

The first collision analysis which was executed in USFOS was the static collision analysis. The easiest way to perform this types of analysis in USFOS is to use an integrated input command for static ship collisions, and give the dissipated energy as input. The dissipated collision energy was calculated on the following way, assuming the structure to be a fixed installation under the collision[NORSOK, 2004]:

$$E_k = \frac{1}{2}(M_{tot} + a_1)V_{Col}^2 \tag{6.1}$$

The added mass was accounted for[Moan, 2004]:

$$a_1 = M_{tot} \cdot 10\% \tag{6.2}$$

The vessel speed under the collision:

$$V_{Col} = 9.300\frac{Nam}{h} \cdot 1.825\frac{Km}{Nam} = \frac{17.224\frac{Km}{h}}{3.600\frac{Km/h}{m/s}} = 4.784m/s \tag{6.3}$$

Using the parameters in table 1.1, the total dissipated energy was calculated:

$$E_k = \frac{1}{2} \cdot (4661mt + 4661mt \cdot 0.1) \cdot 4.784^2 m/s = 58.7MJ \tag{6.4}$$

This would however not give a very accurate result, because USFOS would assume that the vessel bow was infinitely rigid under the collision. This was not the situation in the real collision, and the collision model was therefore altered.

The collision model was made more accurate by inserting the results from chapter 5. The results were implemented as nonlinear springs at the collision points, as illustrated in figure 6.5. The springs had the same force-deformation characteristics as the results from the LS-DYNA analysis, and represented the bow which deformed gradually as the collision force was increased.

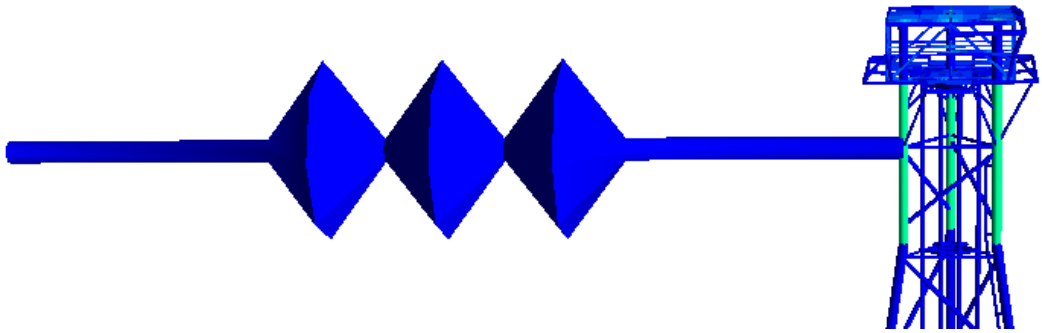

Figure 6.5: Non-linear spring modeled in USFOS

For the static analysis, a horizontal force was applied at the end of the non-linear springs. The force represented the collision force, gradually increasing.

The difficulty with this type of modeling when static analysis is applied is that it is not that easy to have control on the dissipated ship collision energy, because only a horizontal force is applied. The energy had to be calculated after each analysis and cross-checked to investigate if it was similar to the energy calculated in equation 6.4. This was done by integrating the area under the force- deformation curves obtained after each USFOS analysis. For both the dynamic and the static analyses, an energy balance was made where the energy which dissipated into the system was accounted for.

$$E_k = \int_A dA \tag{6.5}$$

This method was the same as described in section 3.1. The integration was done by using the trapeze method in Matlab, which is a numerical integration method [wikipedia.org, 2011]:

$$\int_a^b f(x)dx \simeq \frac{b-a}{2N}[f(x_0) + 2f(x_1) + 2f(x_2) + ... + 2f(x)_{N-1} + f(x_N)] \tag{6.6}$$

For the dynamic analyses, the energy control was easier because the input parameters to the analysis was the vessel mass and speed. The collision was modeled by creating a node with the same mass as the vessel and added mass, and giving it an initial velocity in the direction of the non-linear springs which was connected to the jacket structure. As a check, the load-deformation curves was also here integrated in Matlab to check if the collision energy was similar to equation 6.4.

The collision direction was decided based on the GPS illustration and investigation report provided by NPD [NPD, 2009a]. As described in section 2.1, the vessel collided with the north face of the structure. This was also consistent with the damages on the topside of BOXVIII and the north-going bridge from 2/4W.

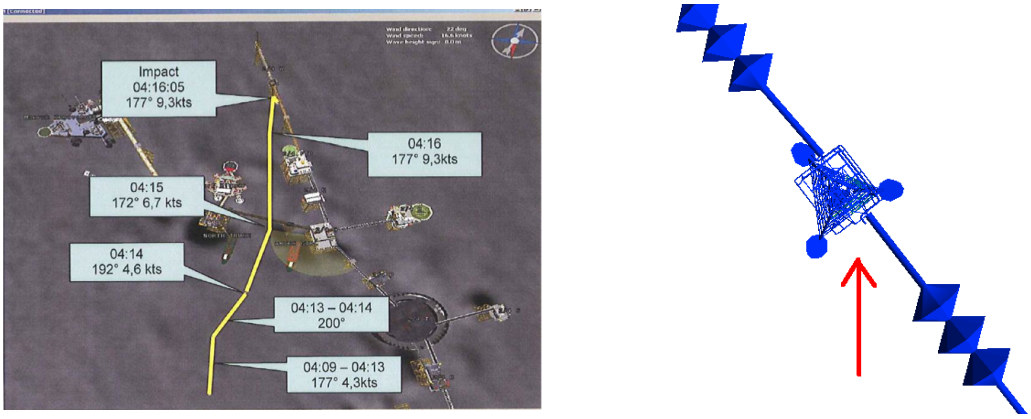

Figure 6.6: Direction of collision

The point of collision was determined after the illustrations of the damaged jacket structure and the marks in the vessel bow. The two north-facing legs were involved, as well as two of the braces near the collision point. No collision forces were applied to the two braces in USFOS. It was assumed that most of the structural response of the jacket was because of forces to the jacket legs. The braces were included in LS-DYNA mainly to get the correct structural deformation pattern.

Figure 6.7: Point of collision

Two non-linear springs were attached to the two points illustrated in figure 6.7, with the characteristics described in figure 5.7 and table 5.6. These two springs ended in a point located $1000m$ from the jacket structure in the direction illustrated in figure 6.6. The reason for this large horizontal distance was to minimize other horizontal force components than in the collision direction. The vertical location of the point was the same as the collision point on the structure. At this point, the collision force was applied.

6.2.2 Static collision analysis

The static collision analysis was as described in section 6.2 modeled as an increasing vertical load applied to a nodal point. This nodal point was linked to the two collision points through two non-linear springs. The applied collision force was on 1MN. The maximal load factor for this force was 1.1. The load-displacement curve for the static collision analysis is illustrated in figure 6.8.

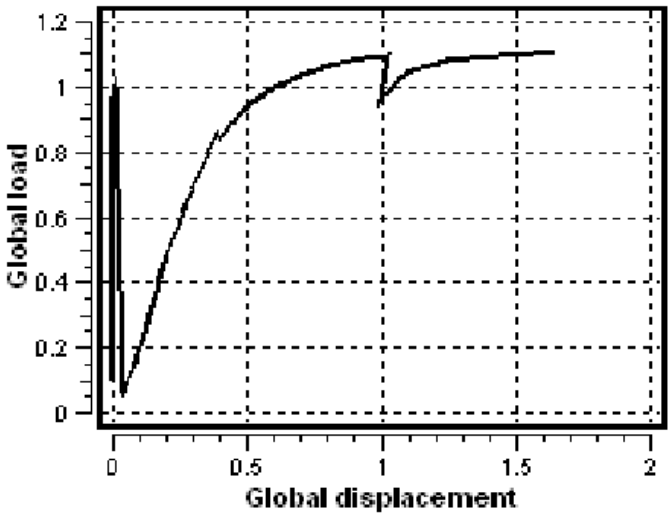

Figure 6.8: Load-displacement curve, static collision analysis

The curve showed an increasing load level and a drop at 1.0 m displacement. The drop indicated a point where braces failed, and the load was re-distributed.

Not many input parameters were necessary for the static collision analysis. The input can be seen in table 6.3.

Condition	**Displacement**	**Unit**
Collision force:	1.0	MN
Minimum collision force increment:	0.0001	–
Initial deformations:	Global shear direction	–
Max analysis step:	1000	–

Table 6.3: Input parameters, static collision analysis

When the load level reached 1.1, the pile and supporting foundation on the south leg started to fail and the entire jacket structure was pushed down in the foundation. Because of this, the load level did not increase further, but the structure got large global displacement on further load steps. The structural response is illustrated in figure 6.9. The fringe range represents plastic utilization.

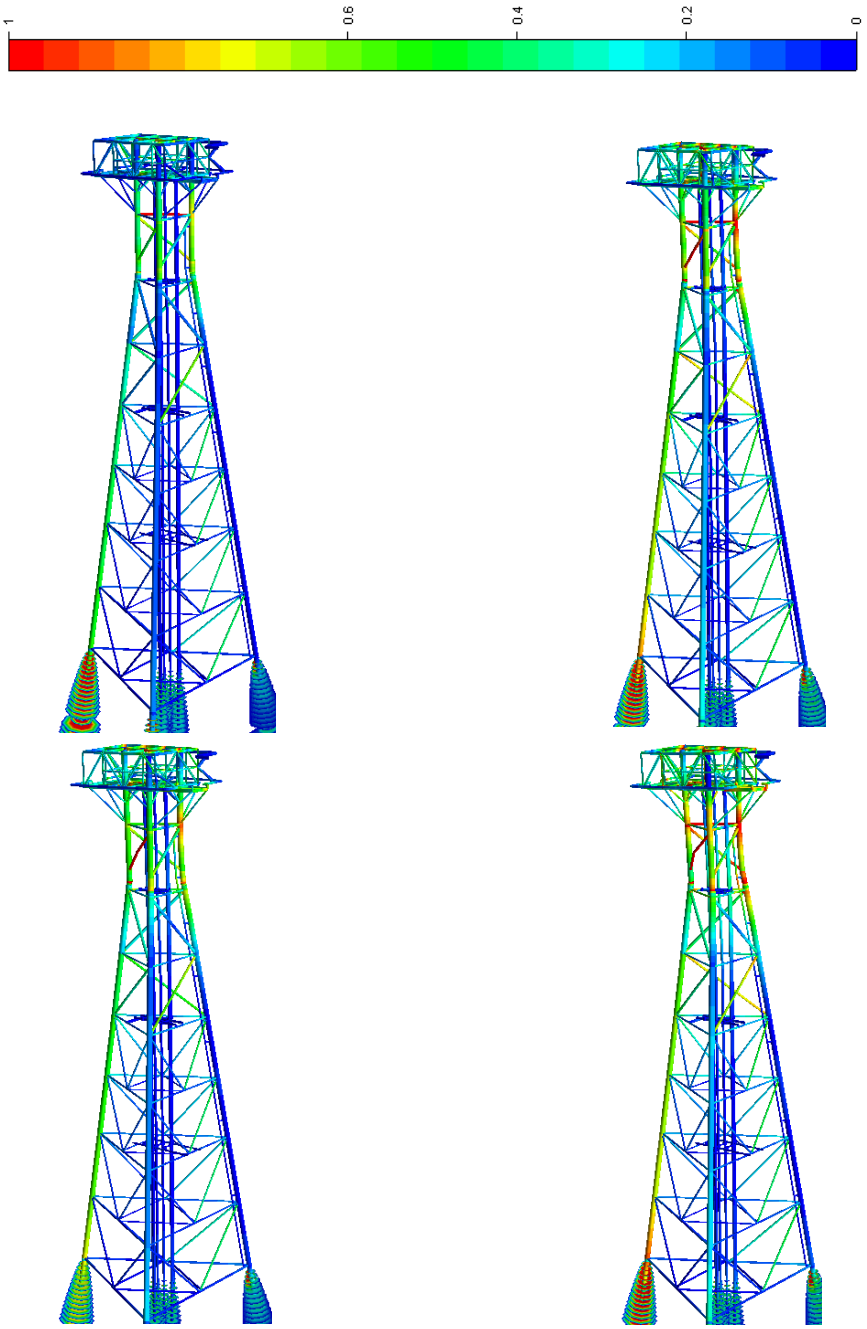

Figure 6.9: Structural response, static collision. Top left: 0.4m disp. Top right: 1.0m disp,peak. Bottom left: Load drop. Bottom right: 1.6m disp

One horizontal and one diagonal brace near the two collision points yielded under the collision, as well as one brace in the second submerged level (-15m). Other braces in the second underwater level was close to maximum plastic utilization capacity near the end of the braces. At the south leg near the cross over to the pile, there were large compression forces. Both the end of the leg and the soil yielded

under the compression. The maximum global displacement of the structure was $1.6m$.

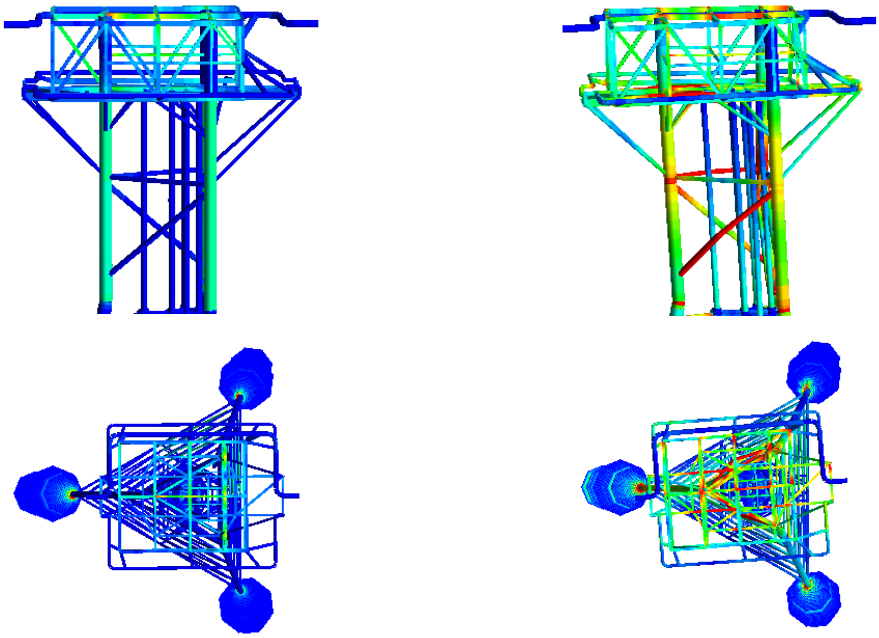

Figure 6.10: Topside deformation, static collision analysis

The topside got a certain counter-clockwise rotation as well as a tilt in south direction, illustrated in figure 6.10.

The energy dissipated into the jacket and into the two springs which modeled the vessel bow. The collision energy was calculated by integrating the area under the load-deformation curves for the jacket and the two springs, using the method described in section 6.2. The energy balance and the analysis results can be seen in table 6.4.

Result	**Value**	**Unit**
Maximum load factor:	1.1	–
Maximum global displacement:	1.6	m
Energy absorbed by 2/4W	14.25	MJ
Energy absorbed by port spring	27.76	MJ
Energy absorbed by starboard spring	16.61	MJ
Total dissipated energy	58.62	MJ

Table 6.4: Analysis results, static collision

The total dissipated energy on $58.62MJ$ was 0.14% less than the energy calculated in section 6.2.

6.2.3 Dynamic collision analysis

The dynamic collision analyses were modeled in the same way as the static collision analysis, with the vessel bow modeled as two non-linear springs at the collision point. The input parameters for the dynamic analysis can be seen in table 6.5.

Input	Value	Unit
Total collision time	6.0	s
Time increment	0.001	s
Mass of colliding mass	5127.1	mt
Initial speed of mass	-4.784	m/s

Table 6.5: Input parameters, dynamic collision analysis

The structural response of the jacket was more similar to the real structural damage than for the static collision analysis. The jacket managed to absorb all of the imposed energy through the non-linear springs. After $4.0s$ the jacket started to unload. The maximal displacement before unloading was 2.1 meters. The time-displacement curve can be seen in figure 6.11.

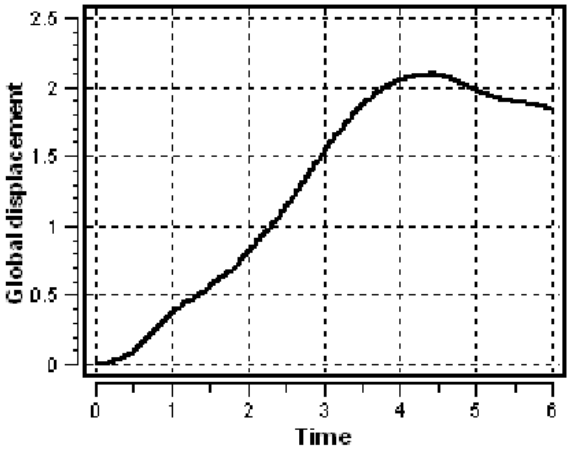

Figure 6.11: Time-displacement curve, dynamic collision analysis

Because of plastic yielding in several members both above and below water, the structural deformation was permanent and the global displacement did not return to zero. The structural response can be seen in figure 6.12.

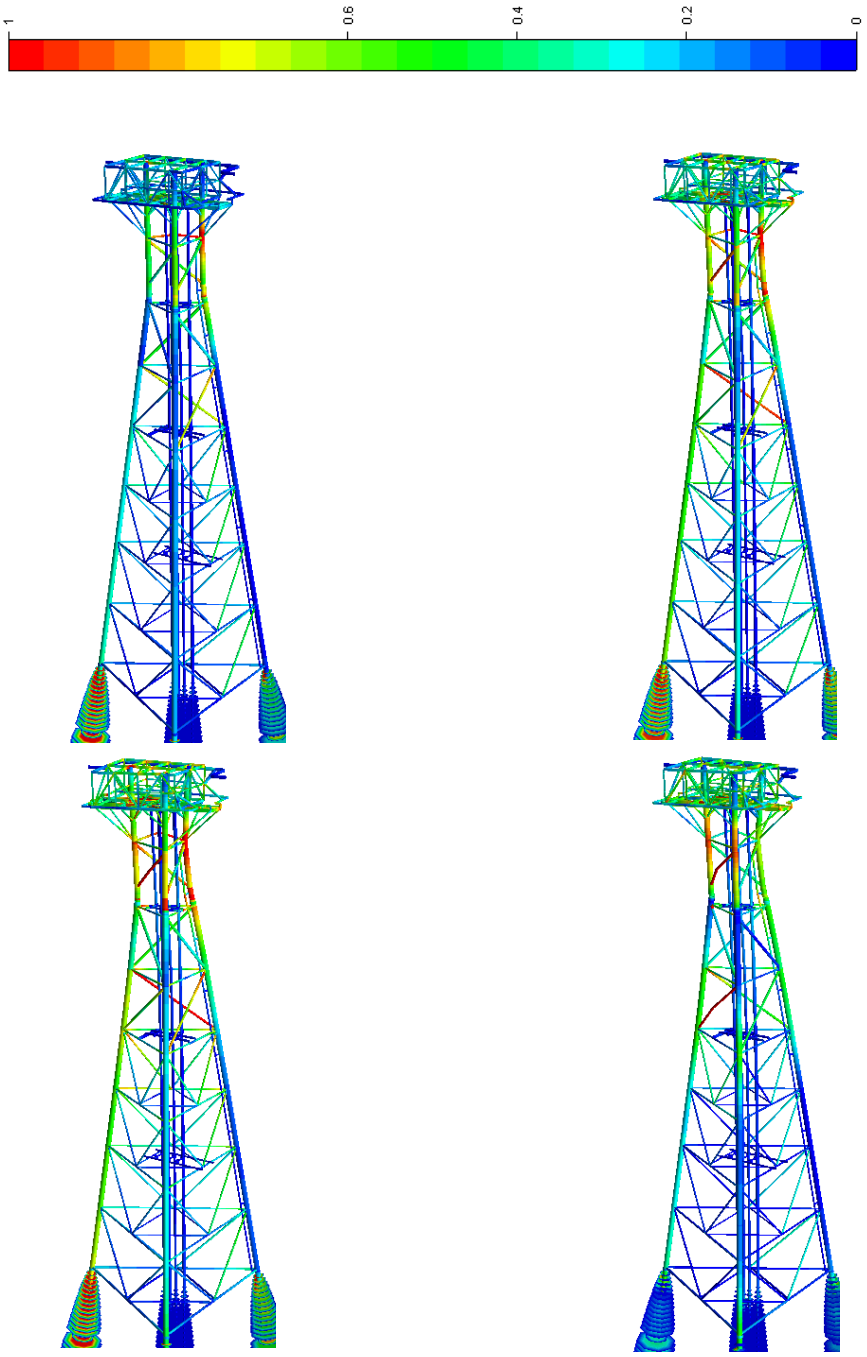

Figure 6.12: Dynamic collision analysis. Top left: t=1.0s. Top right: t=2.0s. Bottom left: t=3.0s. Bottom right: t=5.0s

The horizontal brace in the point of collision was the first member to yield, followed by diagonal braces both on the surface level and in the second submerged level (-15m). Being the point of collision, the north-west leg sustained severe bending. The south leg also got plastic deformation, but not as severe as the north-west leg. The compression force in the south leg, near the cross over to the pile, induced

yielding in the leg at the crossover to the pile (-2m). The foundation supporting the south pile yielded under the collision, but did not fail in the same way as in the static analysis.

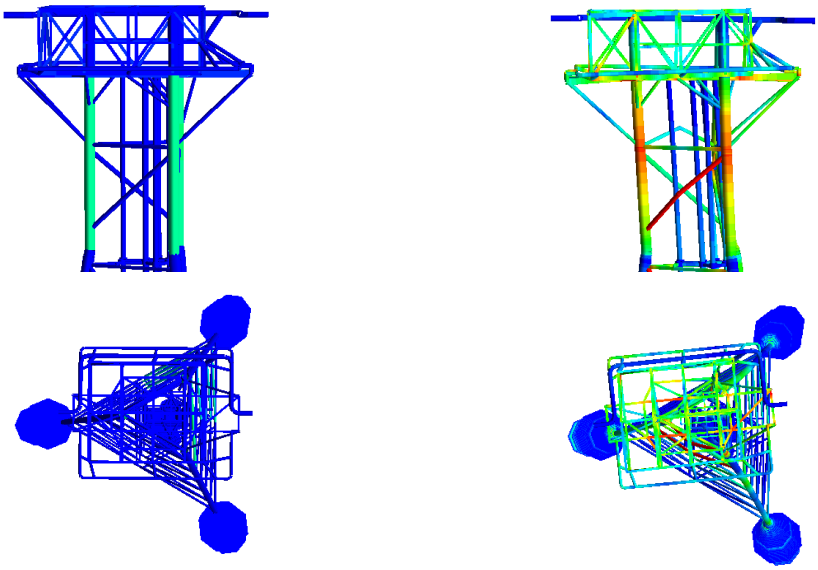

Figure 6.13: Topside deformation, dynamic analysis

Figure 6.13 shows the topside structure before and after the collision. The structure got permanent structural deformation, and the north side of the topside tilted some degrees down towards the collision point.

The direction of the tilt was different from the static analysis, where the topside tilted south. This was because that for the static case, the jacket did not unload, but was terminated with an ongoing load. For the dynamic case momentum was important because of the weight of the topside, and there is unloading from the structure. The topside also got a certain counter-clockwise rotation, illustrated in figure 6.13. The energy balance and the analysis results are given in table 6.6.

Result	**Value**	**Unit**
Maximum displacement	2.1	m
Time at maximum displacement	4.1	s
Total analysis time	565	s
Energy absorbed by 2/4W	20.46	MJ
Energy absorbed by port spring	27.29	MJ
Energy absorbed by starboard spring	10.27	MJ
Total absorbed energy	58.02	MJ

Table 6.6: Analysis results, dynamic collision

The installation absorbed more energy for the dynamic analysis than for the static analysis. The total energy absorption for the system including the energy that dissipated into the two springs was $58.02MJ$. This was 1.2% less than the energy calculated in section 6.2. This was a bigger difference that for the static analysis, but it was still close to the theoretical result.

After discussions with Jørgen Amdahl[Amdahl, 2011] and Vidar-Andre Gjerstad [Gjerstad, 2011], it was evaluated whether or not if the two bridges on the north and south side of Ekofisk 2/4W absorbed energy under the collision. Damage to the south side of the topside because of compression of the bridge and vibration in structural links north of 2/4W, discussed in section 2.2.1, implied that there were some force transfer through the bridges.

A collision model with interfering bridges was made to test these indications. The bridges were for simplicity modeled as non-linear springs with a one meter delay. The delay was applied because of the gliding support mechanism of the two bridges. The spring properties which were used to model the interaction can be seen in table 6.2.3. The two bridges were modeled with the same properties.

Force	**Displacement**
1.0e4 kN	1.0 m
-1.0e4 kN	-1.0 m
-2.0e6 kN	-1.5 m
-5.0e6 kN	-2.5 m
-5.0e6 kN	-4.5 m

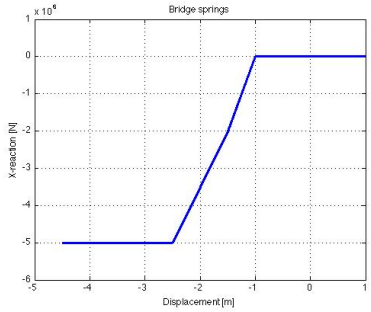

The structure managed to absorb all the energy for this configuration as well. The time-displacement curve for the configuration with both bridges interaction with 2/4W can be seen in figure 6.14. The structural response with bridge support can be seen in figure 6.15.

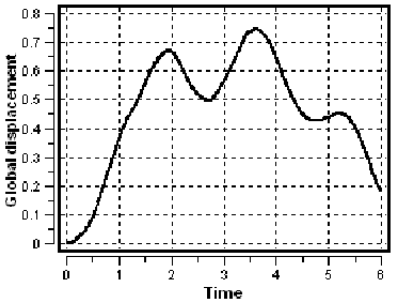

Figure 6.14: Time-displacement curve, dynamic collision analysis with two bridge supports

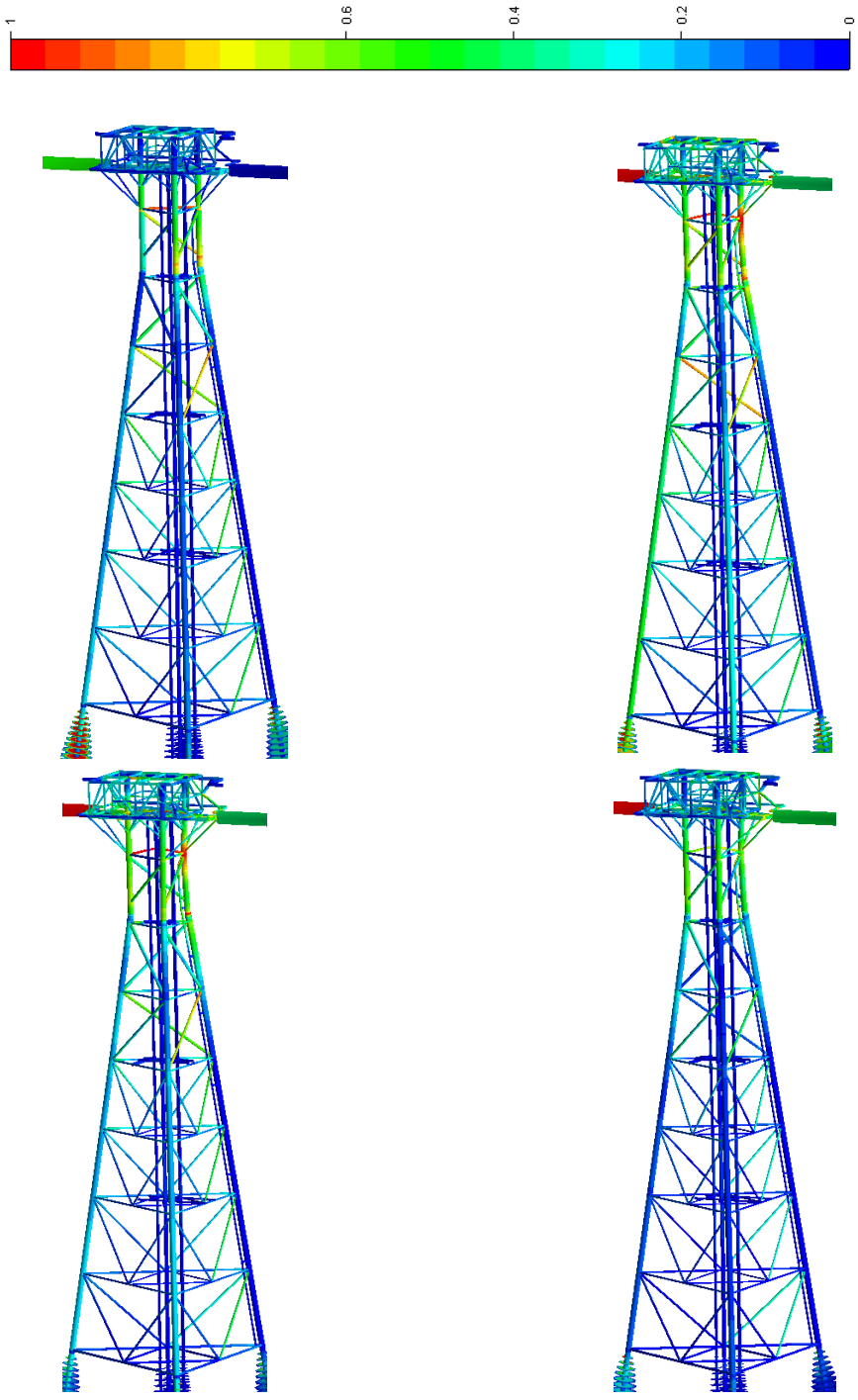

Figure 6.15: Dynamic collision analysis, bridge supported Top left: t=1.0s. Top right: t=2.0s. Bottom left: t=3.0s. Bottom right: t=5.0s

With the two bridges, the system became stiffer than the unsupported configuration. The maximum displacement with the two bridges interacting with the topside after one meter delay was after $3.7s$ only $0.75m$, 36% of the maximum displacement

without any support. The displacement after maximum was also decreasing more rapidly than for the unsupported model.

As discussed in section 2.2.1, the structure retracted to one meter deformation after the maximum displacement. The damage survey by Conoco Philips[Gjerstad, 2009] also described a counter-clockwise rotation under the collision. This rotation was not as intense as it was for the unsupported model.

The response was similar to the analysis without bridge support, but the global displacement was not as severe as for the unsupported model. The horizontal braces near the collision points buckled at the same point as for the unsupported model. Braces in the second submerged level (-15m) were close to full plastic utilization at the same time. The northwest leg had the same bending characteristics at the collision point as for the unsupported model, but the two other legs had less bending and yielding.

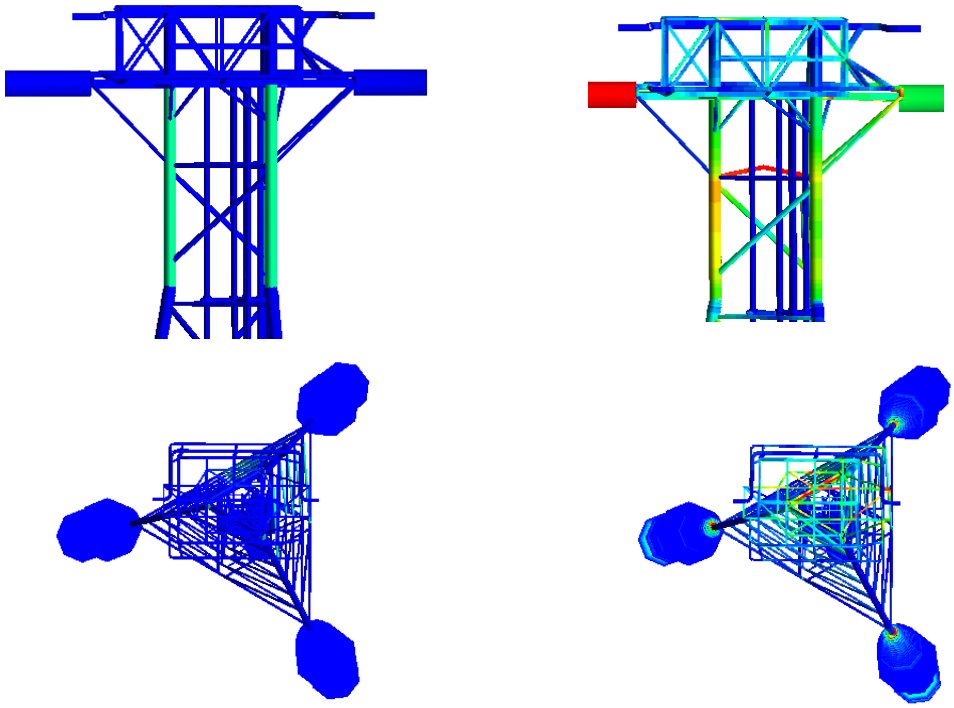

Figure 6.16: Topside deformation, bridge supported

The topside rotated less and tilted fewer degrees downwards than for the unsupported case. The energy balance and analysis results is given in table 6.7.

Result	**Value**	**Unit**
Maximum displacement	0.75	m
Time at maximum displacement	3.6	s
Total analysis time	487	s
Energy absorbed by 2/4W	5.20	MJ
Energy absorbed by port spring	39.38	MJ
Energy absorbed by starboard spring	12.55	MJ
Energy absorbed by bridges	0.8	MJ
Total absorbed energy	57.93	MJ

Table 6.7: Analysis results, dynamic collision with bridge supports

The total absorbed energy on 57.93 MJ was 1.3% lower than the energy calculated in section 6.2.

It is interesting to note that only 1.4% of the energy dissipated into the two bridges. The supports still made the system stiffer, and less deformation was induced. The port spring absorbed 41.2% more energy than for the unsupported model. The starboard spring absorbed 22.2% more energy. Only the jacket structure absorbed less energy compared to the unsupported model. This was consistent with the lower structural damage to the installation.

Because of the low deformations and the low degree of failing members compared to the reported damage, this model was not used in the collapse analyses. The unsupported model had damages that was comparable with the reported damages, and was used in the collapse analysis.

The load-displacement curves which was used to find the absorbed energy can be found in appendix B.2. Velocity and acceleration curves for the dynamic analyses can be found in appendix B.3 and B.4 respectively.

6.3 Pushover analyses for environmental loads, damaged condition

After the static ship collision analysis, pushover analyses in damaged condition was executed to check the remaining capacity of the structure. The structure was analyzed in both south and north bound waves.

The first analysis was with north bound waves, opposite of the collision direction. The environmental parameters was the same as the analysis in undamaged condition, given in table 6.1.

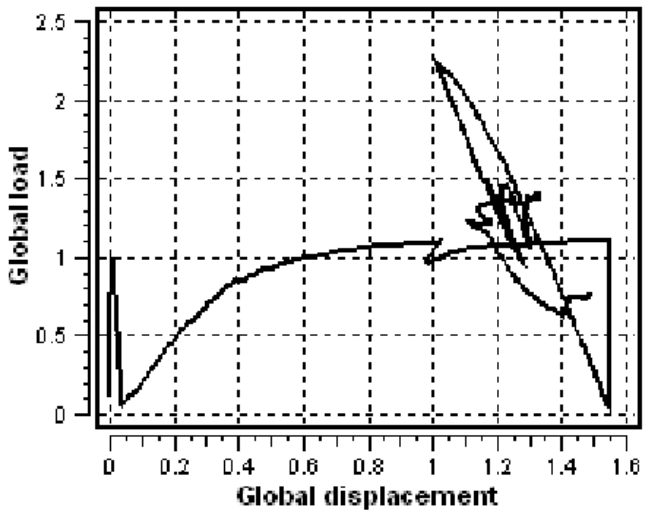

Figure 6.17: Force-displacement curve for pushover analysis in damaged condition. North bound waves

After the collision force had ended, the load dropped to zero and the pushover force was applied to the jacket. The load increased until the first member failed, where the load dropped.

The first member to fail was a diagonal brace in the fifth submerged level -($65m$). After the first member failed, several diagonal braces failed rapidly. The load-deformation curve in figure 6.17 illustrates this with many small local load maximums and minimums.

After several members had failed, the legs started to fail and the global load decreased. The structural response of the jacket is illustrated in figure 6.18.

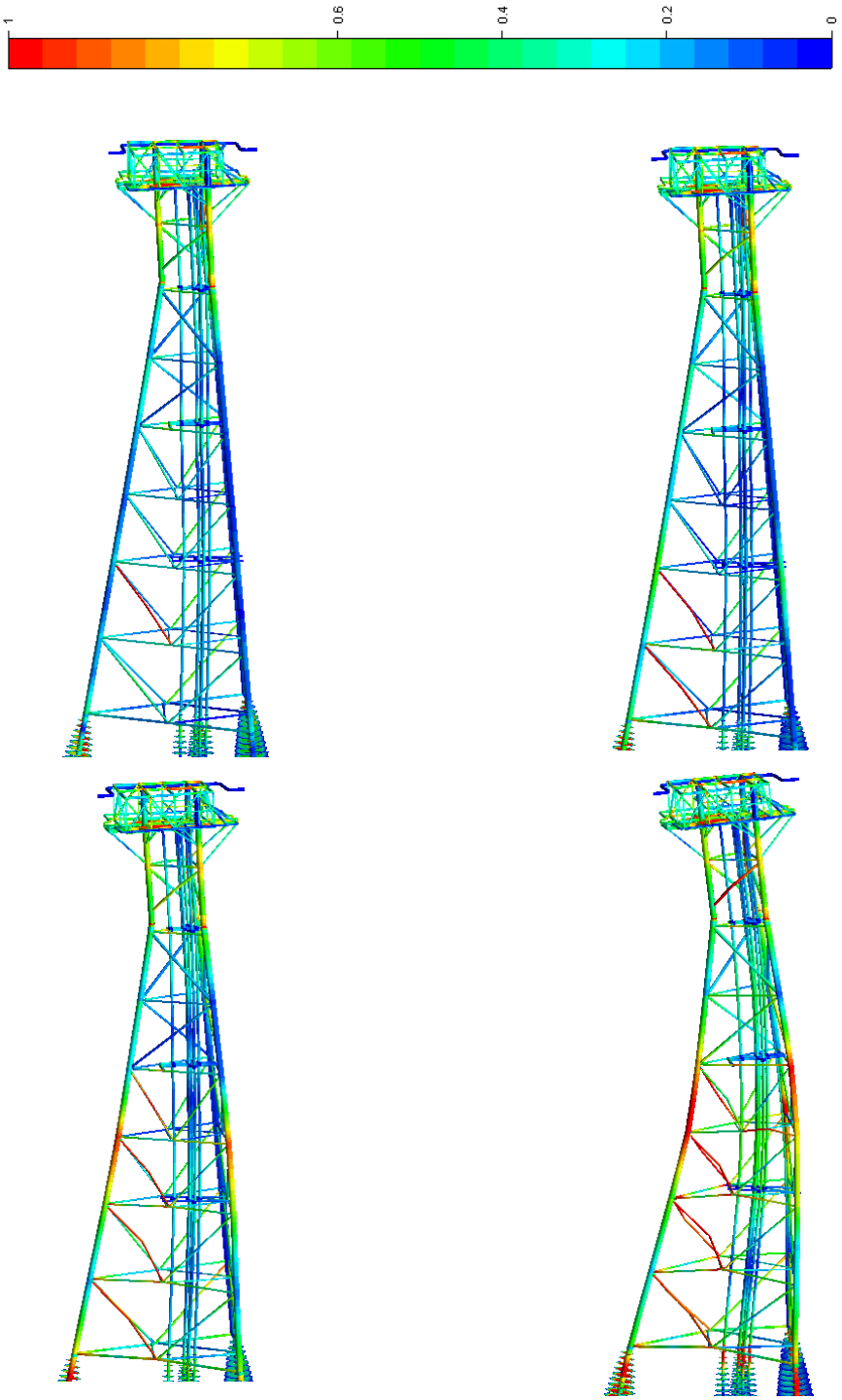

Figure 6.18: Pushover analysis, damaged condition. North bound waves.

The next pushover analysis was executed with south propagating waves. This was the same direction as the ship collision force. The load-displacement curve can be seen in figure 6.19.

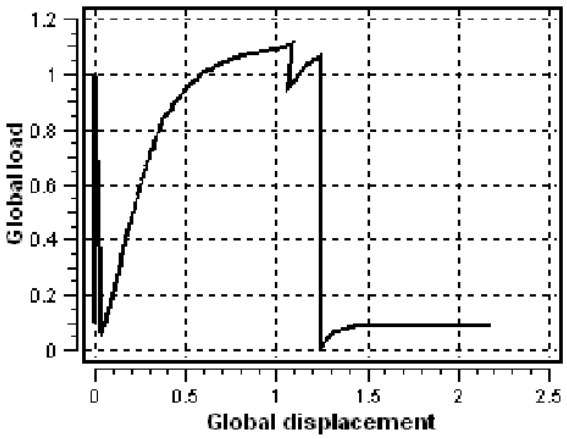

Figure 6.19: Force-displacement curve for pushover analysis in damaged condition. South bound waves

The response with south bound waves was significantly different from the results with north bound waves. Instead of an increase of global load and failing braces, the structure only got an increasing global displacement. The reason for this was yielding and failing in the foundation around the south pile. This point was already heavily loaded from the static ship collision analysis, illustrated in figure 6.9. Because of this, the structure only tilted down towards the south pile when the pushover force was initiated.

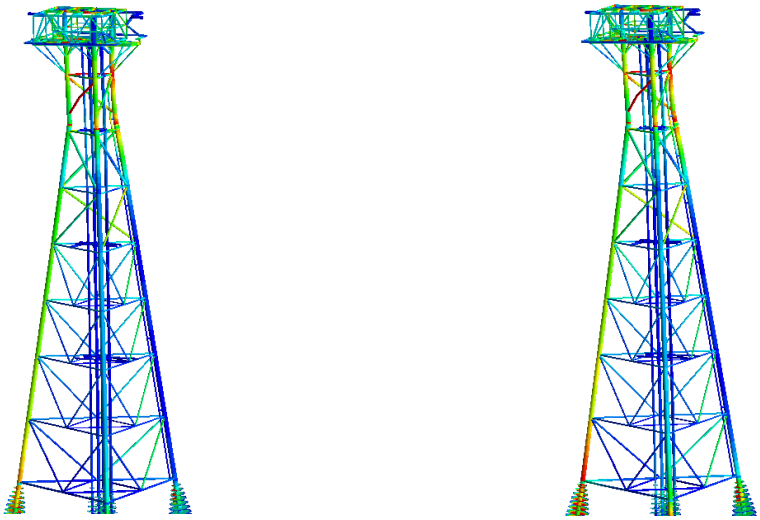

Figure 6.20: Pushover analysis, damaged condition. South bound waves.

6.4 Collapse analysis

After the collision analyses and the pushover analyses were executed, dynamic collapse analyses were performed on 2/4W. This was done in different ways. The first collapse analyses were performed by increasing the collision energy. After this, the collision characteristics were changed.

Based on equation 6.1 in section 6.2, the two parameters which could be changed to increase the energy was the vessel speed and mass. The collision energy was first increased by 5%. The new collision energy would, by following equation 6.1, be $61.635MJ$.

$$58.7MJ + 58.7MJ \cdot 0.05 = 61.635MJ \tag{6.7}$$

$$61.635e6J = \frac{1}{2}(4.661e6kg + 0.1 \cdot 4.661e6kg)V_{col}^2 \tag{6.8}$$

$$V_{col}^2 = \frac{61.635e6J}{\frac{1}{2}(5.1271e6kg)} \tag{6.9}$$

$$V_{col} = \sqrt{24.04} = 4.903m/s \tag{6.10}$$

By solving equation 6.8 the new velocity the ship had to have to increase the collision energy to 61.635 MJ was found to be $4.903m/s$.

$$61.635e6J = \frac{1}{2}(m + 0.1 \cdot m)4.784^2 m/s \tag{6.11}$$

$$\frac{2 \cdot 61.635e6J}{4.784^2} = 1.1 \cdot m \tag{6.12}$$

By solving equation 6.12 for m, the new mass the ship had to have to increase the collision energy to 61.635 was found to be $4.8965e6kg$. Values for increased energy is given in table 6.8. The mass includes 10% added mass, and was the value used in USFOS. Other input parameters in USFOS were the same as in section 6.2.3.

Energy increase	**Velocity**	**Mass+added mass**
0% energy increase, 58.700 MJ	4.784 m/s	5.1271e6 kg
5% energy increase, 61.635 MJ	4.903 m/s	5.3862e6 kg
7% energy increase, 62.809 MJ	4.950 m/s	5.4887e6 kg
10% energy increase, 64.570 MJ	5.019 m/s	5.6426e6 kg
15% energy increase, 67.505 MJ	5.132 m/s	5.8991e6 kg

Table 6.8: Increased energy, velocity and mass

The time-displacement for 5% increase of energy can be seen in figure 6.21 The left curve is with increased velocity, and the right curve is with increased mass.

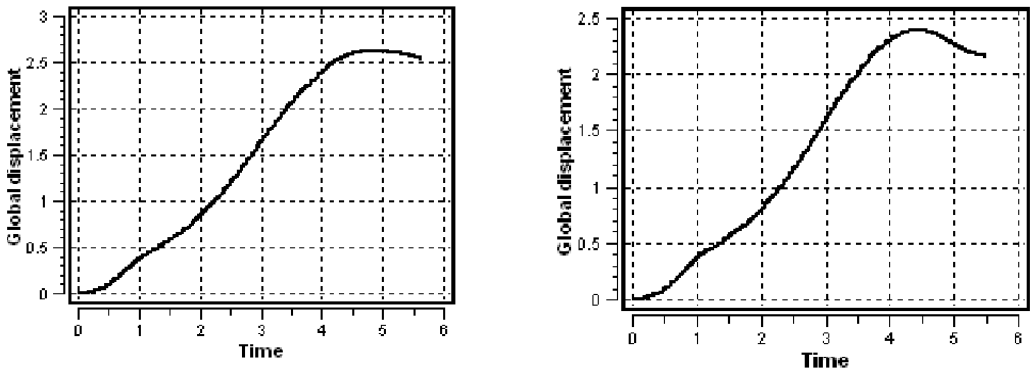

Figure 6.21: Time-displacement curves collapse analysis. 5% energy increase.

The pattern of the curves were similar to the original time-displacement curve given in figure 6.11, but the deformations were larger because of the increase in collision energy. The two different analyses also got a somewhat different response, but had the the maximum deformation after the same time. The maximal response for the two collapse analyses are given in figure 6.22. The left figure is with increased velocity, and the right curve is with increased mass.

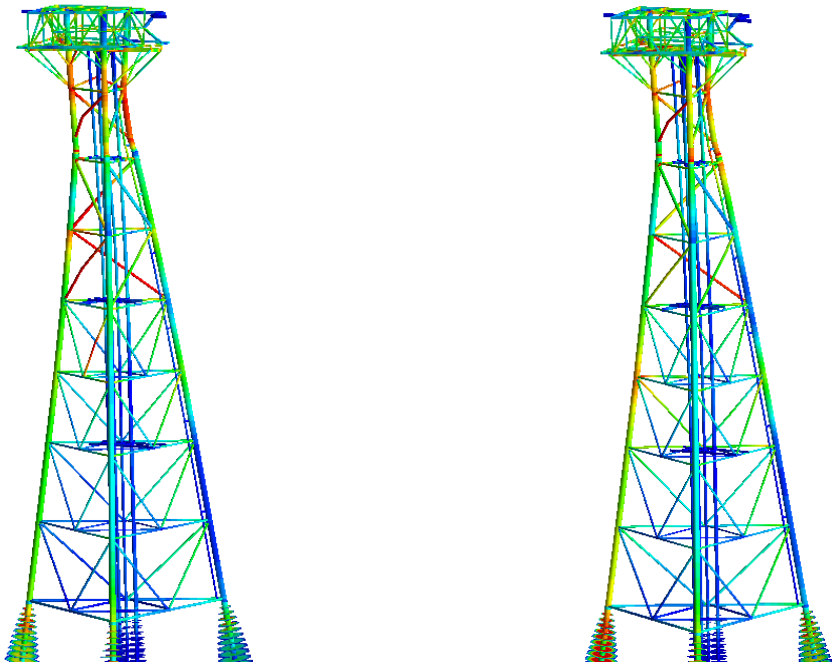

Figure 6.22: Structural response, 5% energy increase.

The response was similar to the dynamic analysis in section 6.2.3, but with more severe deformation and a larger number of members failing. The structural response was also more severe in the model with increased velocity than for the model with increased mass.

Based on the structural response, the damages inflicted with a 5% energy increase was not enough to make the structure collapse. The energy was increased 7% compared to the the original collision energy. The time-displacement curves can be seen in figure 6.23 and the maximal response in figure 6.24.

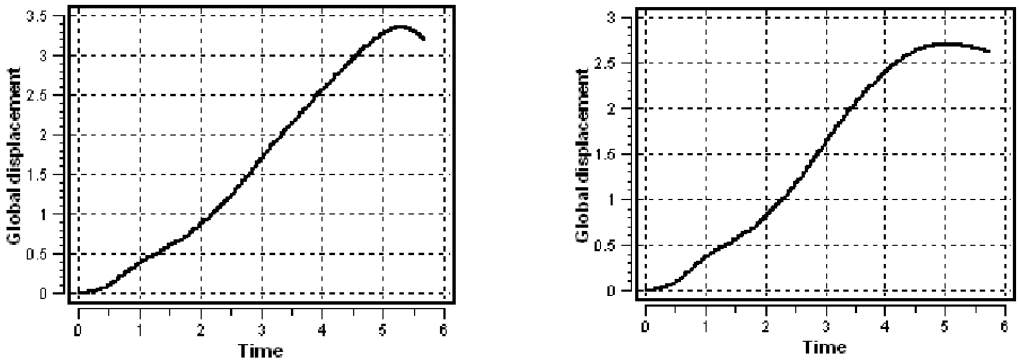

Figure 6.23: Time-displacement curves collapse analysis. 7% energy increase.

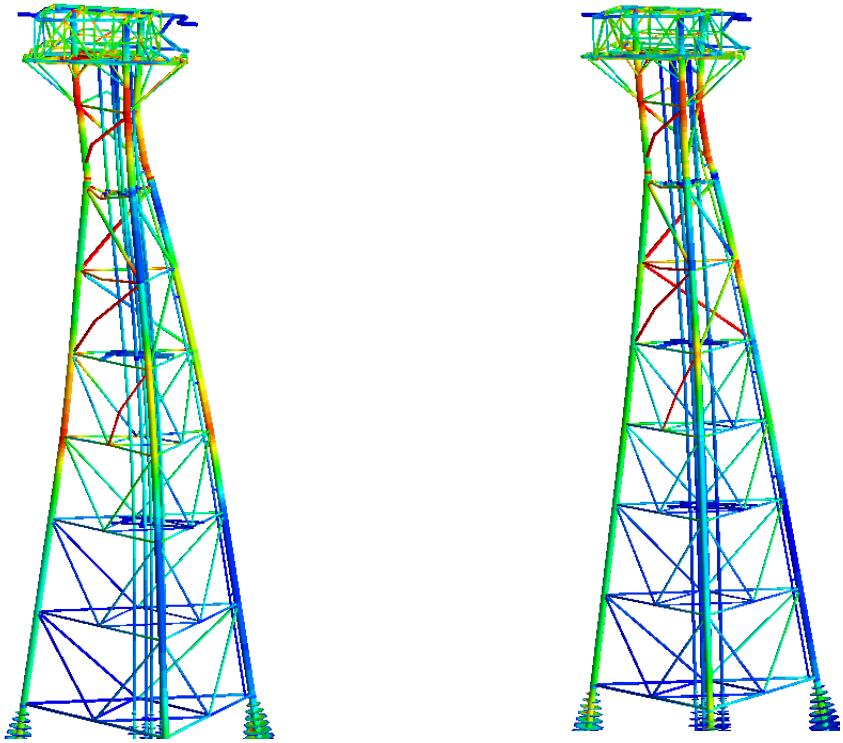

Figure 6.24: Structural response, 7% energy increase.

The trend was the same for this analysis with the increased velocity giving the most severe response, and the maximum deformation after the same time. The structures did not have much capacity left after the impact was over, but still managed to endure the collision with a 7% increase in energy.

The next collapse analysis had a 10% increase in the collision energy. Only the velocity was changed for this energy increase. USFOS had problems calculating the response with increased mass. The time-deformation curve is given in figure 6.25 and the structural response is illustrated in figure 6.26.

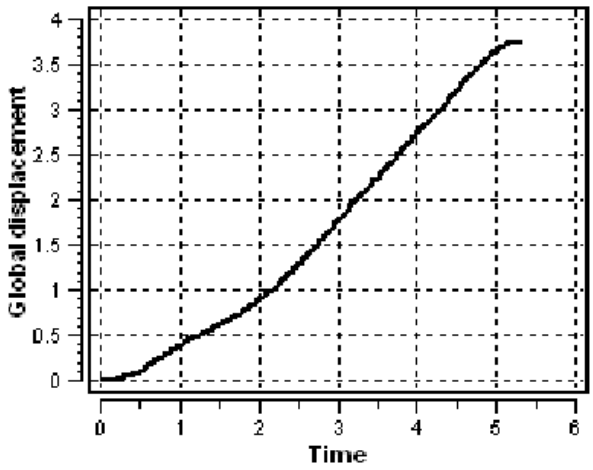

Figure 6.25: Time-displacement curve collapse analysis. 10% energy increase

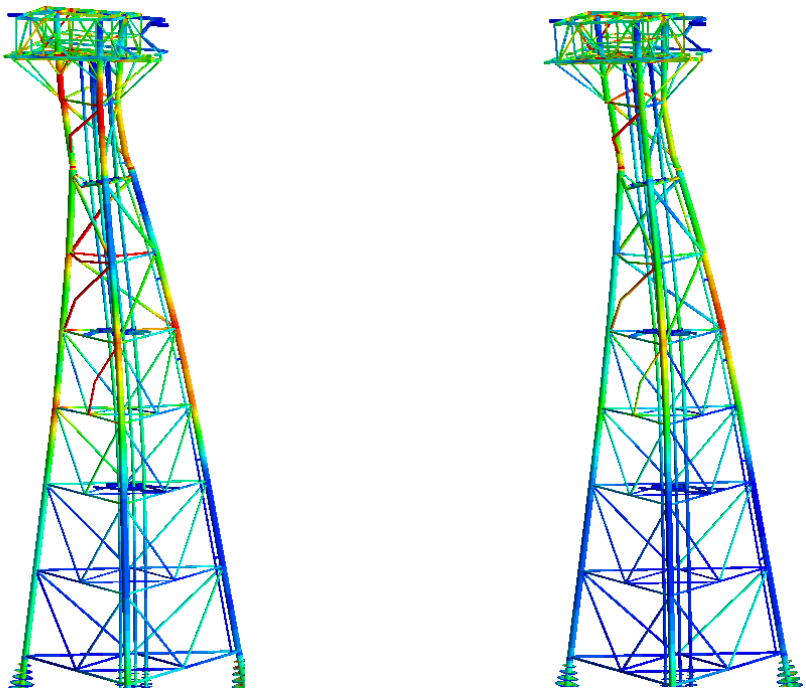

Figure 6.26: Structural response, 10% energy increase. Left: 4.5s. Right: 5.3s

The structural response of the installation was at a peak after 5.3s with severe deformations to the jacket and bearing structure above water. Several braces in

the submerged levels were deformed, and the jacket legs both over and under water were at max plastic utilization. In the right illustration in figure 6.26, the system had started to unload. When this happened, the topside started to tilt and break of towards south. This was different from the collision analyses in section 6.2.3 where the topside tilted towards north after the collision.

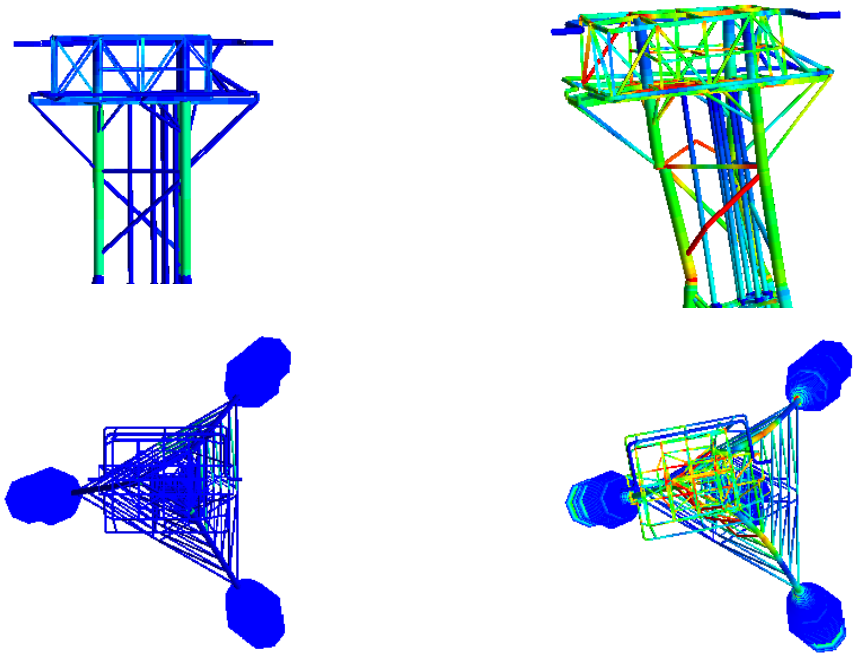

Figure 6.27: Topside deformation, 10% energy increase

The installation could have collapsed after this collision based on the structural response. Because of numerical difficulties in USFOS the post-collapse area for the analyses was problematic to investigate. The results of the collapse analysis are given in table 6.9.

Result	**Value**	**Unit**
Max displacement	3.7	m
Time at max displacement	5.3	s
Collision energy	64.57	MJ

Table 6.9: Collapse analysis, results

The collision speed on 5.019 m/s is equal to 9.76 knots. Compared to the actual collision speed on 9.3 knots, the velocity was increased with 0.46 knots, an increase on 5%.

In the last collapse analyses, the speed and mass of the vessel were unchanged. The collision was however configured in such a way that the vessel only interact with one of the jacket legs. Two different analyses were performed. One had the same direction as the dynamic analysis, and one had a direction from southwest.

For simplicity the same load-deformation characteristics for the starboard side bow was used for both of the analyses.

The time-deformation curves for both the south and north collision with one leg can be seen in figure 6.28. The left curve is the collision from south hitting the south leg. The right curve is the collision from north hitting the northeast leg, ref.figure 2.5.

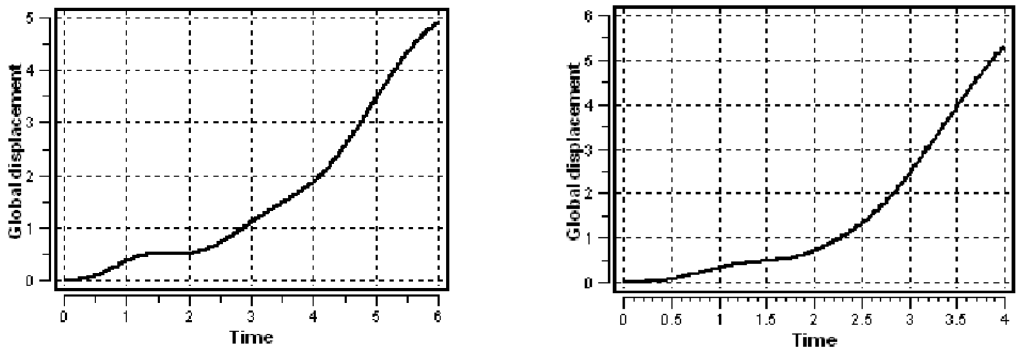

Figure 6.28: Time-displacement curves, one leg collapse analyses

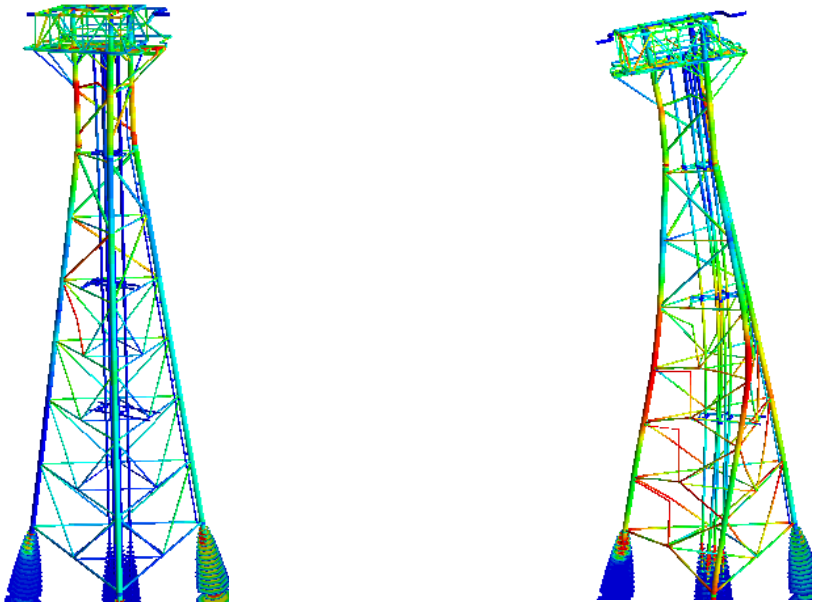

Figure 6.29: Structural response, collapse analysis impact from south

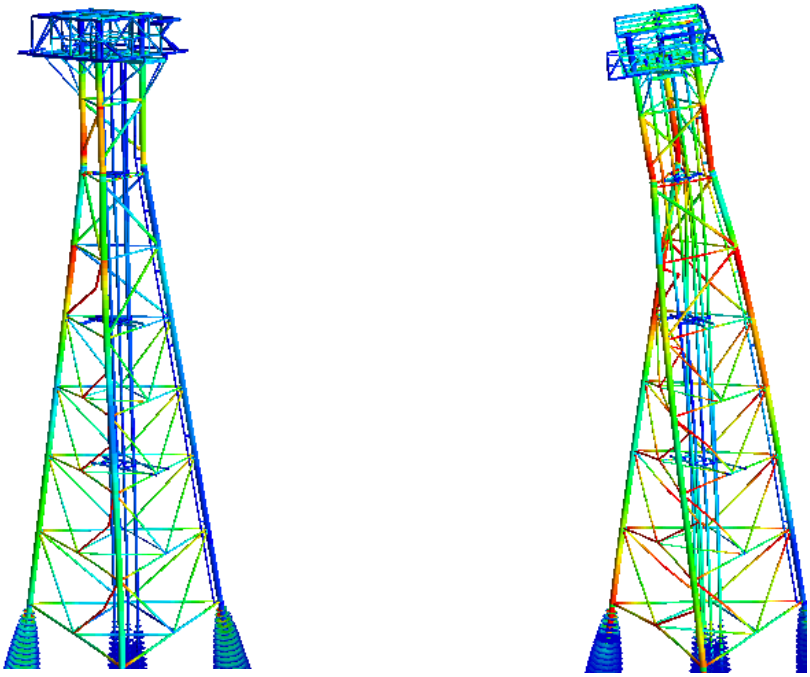

Figure 6.30: Structural response, collapse analysis impact from north

The collision from southwest resulted in large structural deformations to the installation. When hitting only one leg, large counter-clockwise rotations were induced to the system. Several braces failed and at the end of the analysis the south and northeast leg fractured.

The structural response from collision with one leg from north is given in figure 6.30. This analysis also gave large deformations and clockwise rotation. The structure rotated clockwise when the force interacted with the northeast leg. Several braces and two of the legs fractured under the collision force.

Both the analyses of one leg impact gave structural response that would have resulted in the structure collapsing.

More detailed structural response of the final collapse analysis with increased energy can be seen in appendix B.1. Force-deformation curves post processed in Matlab can be seen in appendix B.2. Velocities and accelerations can be seen in appendix B.3 and B.4.

Chapter 7

Discussion of results

7.1 Comparison to reported damage

The analyses results obtained in chapter five and six were compared to the reported damages after the collision. For the crushing analyses in LS-DYNA, only the results from the last analysis with 200mm mesh were compared with the damage to BOXVIII. For the collision analyses in USFOS, only the results from the unsupported dynamic analysis were compared to the reported damage. These were found to be the analyses giving the most accurate results.

7.1.1 Crushing analysis in LS-DYNA

The collision analyses in LS-DYNA were done with three different mesh sizes. The model mesh was refined until the absorbed energy converged sufficiently. The model which gave the best results had a 200mm mesh.

The damages to BOXVIII were not extensively documented after the accident. The vessel was in dock to repair the damages few days after the incident[Johansen et al.,]. The results from the LS-DYNA analyses were because of this compared to pictures taken shortly after the accident.

The marks in the vessel bow was used to decide the point of impact. As can be seen in figure 7.1, the deformations in the bow were similar to the obtained damages from the analysis. There were not much documentation from the port side of the vessel besides from the illustration in figure 7.2, with a mark from the north-east leg.

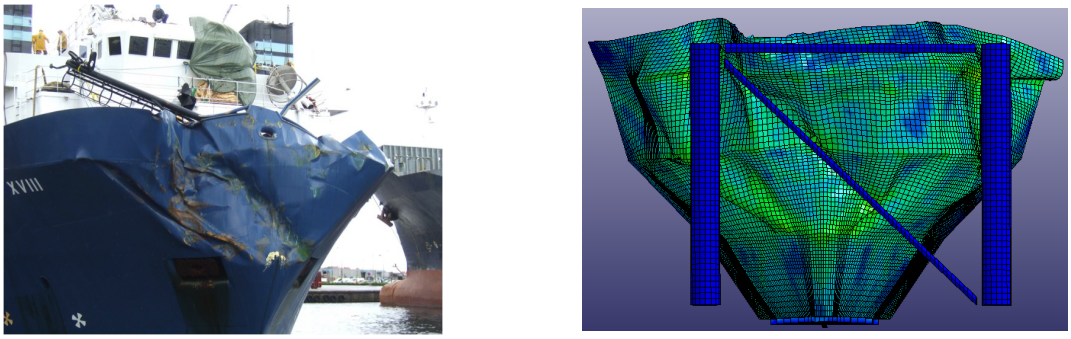

Figure 7.1: Comparison of bow damage, front

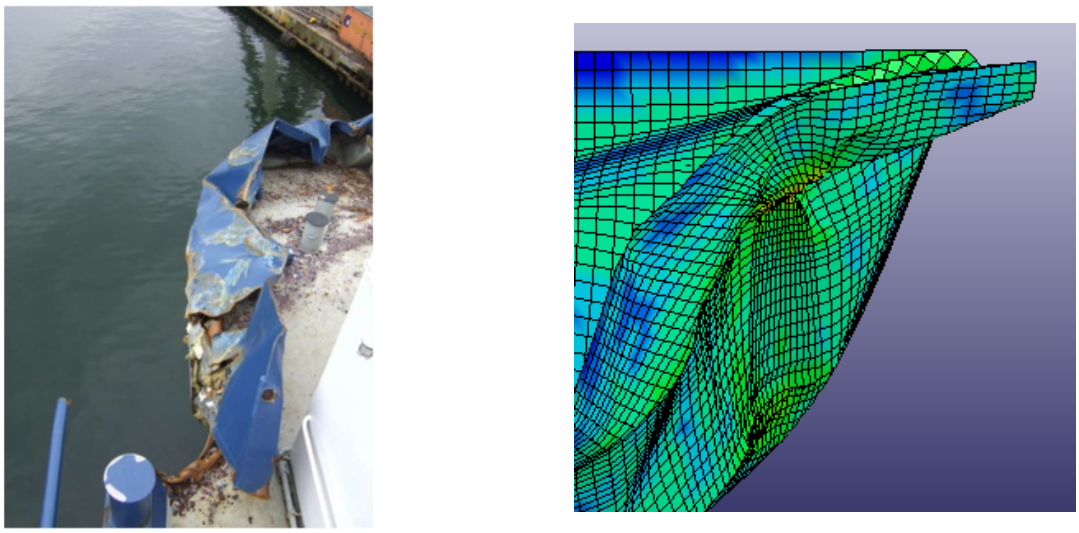

Figure 7.2: Comparison of bow damage, port side

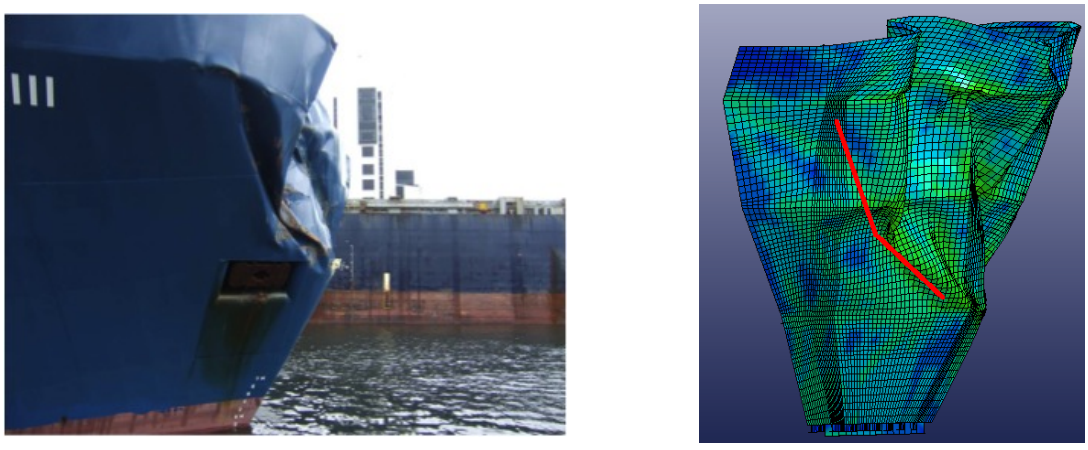

Figure 7.3: Comparison of bow damage, starboard side

The bow got folding on the starboard side under the collision because of the forces from the north-west leg, illustrated in figure 7.3. The results from LS-DYNA

gave folding in almost the exact same place, and with the same characteristics. This gave reason to believe that the obtained results from LS-DYNA were close to the actual damage. This would also mean that the non-linear springs in USFOS had a reasonable load-displacement relation. More detailed illustrations of the deformations obtained from the LD-DYNA analyses are given in appendix A.

7.1.2 Collision analyses in USFOS

The damages to Ekofisk 2/4W was thoroughly documented after the accident, both with pictures and written documentation. This made it easier to compare the obtained results with the actual damage.

Figure 7.4 illustrates damages to the jacket structure under and above water, and was a part of the report from the damage survey done by Subsea7 between the 11th of June and 12th of September 2009 [Subsea7, 2009]. The figure includes the grouted members and all of the anomalies after the collision.

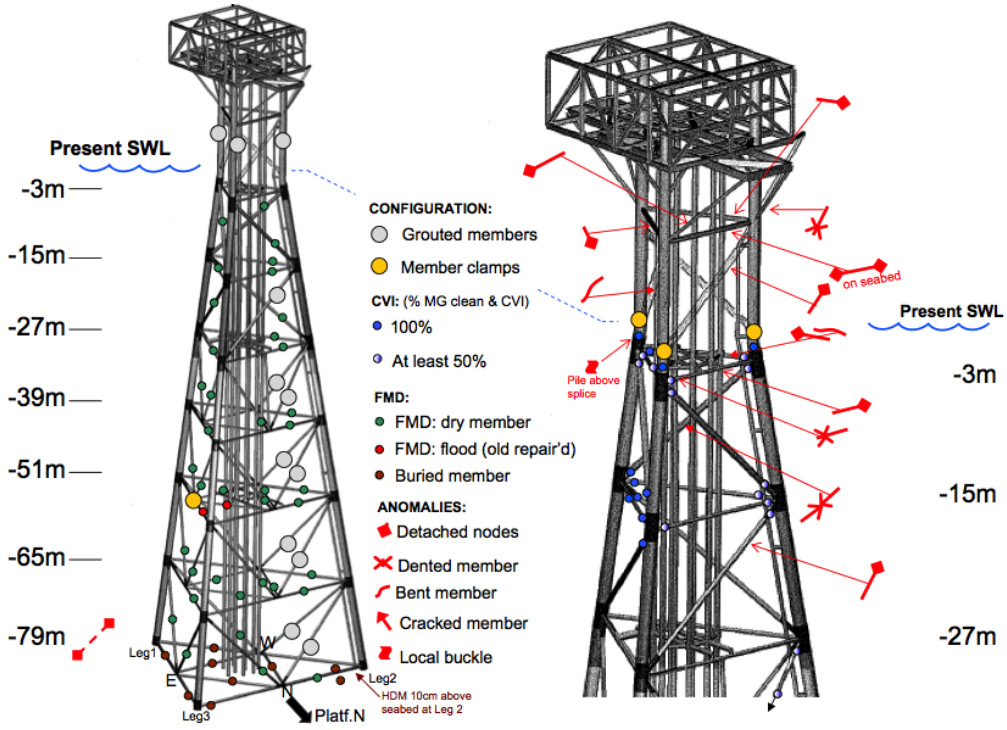

Figure 7.4: Damage survey [Subsea7, 2009]

The damages to the topside structure were documented by Conoco Philips. The damages were described in a separate report made shortly after the accident [Gjerstad, 2009].

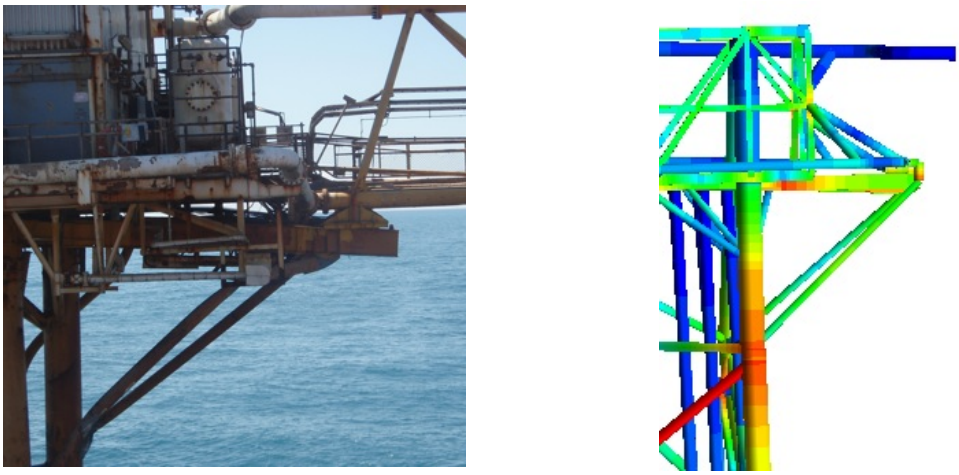

Figure 7.5: Comparison, bridge support 2/4W

Figure 7.6: Comparison, braces above water

After the collision, the topside and bridge support got a permanent tilt down to the north face of the structure. As can be seen in figure 7.5, the dynamic analysis gave the same tilt on the north face but not as intense as the reported damage. Reasons for this could be that the braces supporting the bridge support was torn of by the deck equipment on BOXVIII. This deck equipment was not modeled in USFOS, hence the supporting braces was not damaged or torn of in the analysis.

Other braces were also teared loose in the real collision. In the USFOS analyses, no braces were teared off because of the program features. It is possible to model tear-off in USFOS after a specific time, but not as a result of inflicted damages.

Figure 7.6 shows the damages to the braces and legs above water. Both the north and east facing horizontal brace got detached from the legs. The east facing brace was dented and bent. The north facing brace was found at the sea bed under the damage survey. The east diagonal brace was deformed, while the west diagonal brace was undamaged.

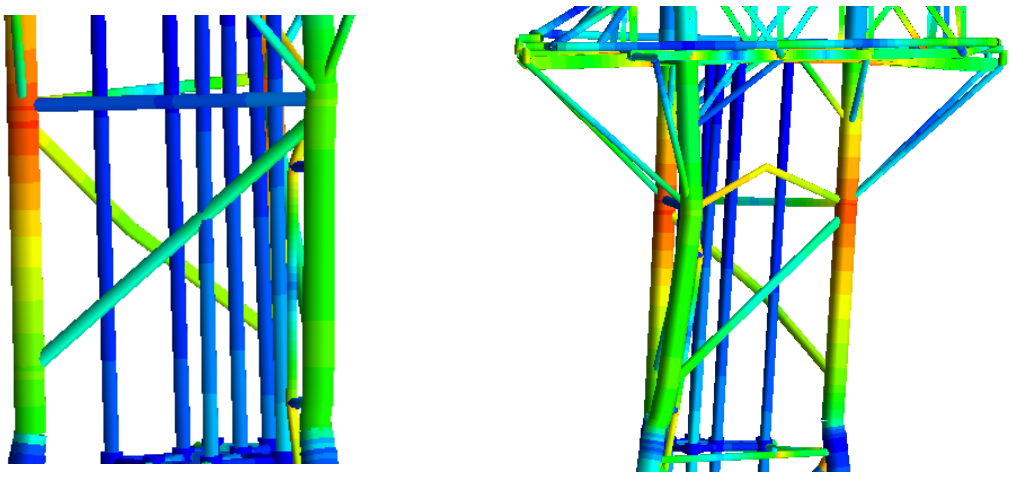

Figure 7.7: Comparison, braces above water in USFOS

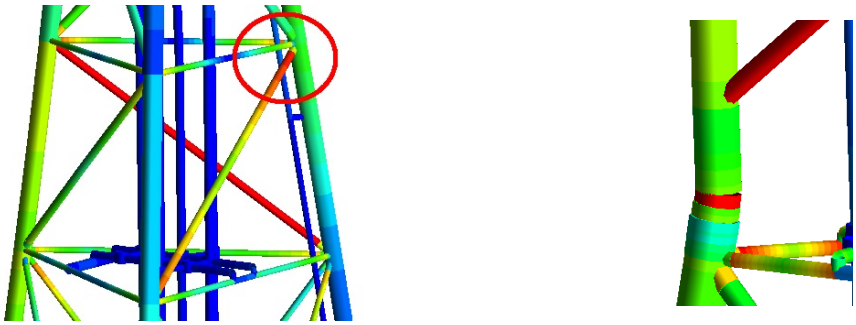

Figure 7.8: Left: braces in submerged level, -15m. Right: south leg -2m

The damages to the structure above the water line obtained from the dynamic analysis in USFOS were similar to the reported damage in many ways. Both the south and the northwest leg were bent south. The northeast leg was bent east and got a buckling at the collision point. This was the same as the reported damage in figure 7.4. The diagonal brace facing east was deformed as in the real situation, and the horizontal braces facing west got severe bending. The damage report from Conoco Phillips[Gjerstad, 2009] described a counter- clockwise rotation of the topside. The same counter-clockwise rotation was obtained in the dynamic analysis. This rotation happened because of the direction of the collision.

In the second underwater level (-15m), all of the three diagonal braces were close to max plastic utilization. The marked node in figure 7.8 was found to be detached in the damage survey. The same diagonal member was in high tension under the collision analysis and had max plastic utilization. The two other diagonal was both heavily loaded under the collision.

As illustrated in figure 7.8 the south leg joint at -2m was heavily compressed under the collision. Because of this the splice joint connecting the horizontal leg to the diagonal leg buckled. In the damage survey after the collision, the same local buckling was found in the same splice joint, illustrated in figure 7.9.

Figure 7.9: Buckling of splice joint at -2m

All of the collision analyses and the pushover analyses with south bound waves gave structural response with high compression force in the south leg near the crossover to the pile.

7.2 Discussion of methods in NORSOK 004, Appendix A

As discussed in section 3.1 the shared-energy method was used in this thesis, with both the vessel and the installation dissipating energy. The results were obtained by performing two separate uncoupled analyses in LS-DYNA and USFOS. The anticipated collision energy was calculated in section 6.2 based on NORSOK Appendix A[NORSOK, 2004], and was estimated to $E_s = 58.7MJ$.

By using the method described in section 6.2 and the results from the uncoupled analyses, the dissipated energy under the static ship collision analysis was found to be $58.62MJ$. The dissipated energy under the dynamic ship collision analysis was found to be $58.02MJ$. The deviation was 0.14% and 1.2% respectively. The results implies that the methods in NORSOK are accurate, even when using two uncoupled analyses to model the collision.

The NORSOK code also recommends a force-deformation relationship for collisions between ships with a displacement on approximately $5000mt$ and large diameter structures (D=10m), given in figure 7.10. Amdahl and Skallerud
[Amdahl and Skallerud, 2002] expected that this curve was overly conservative for collisions with jacket legs, (D $\sim$2m). They recommended other curves which were found by non-linear FEM simulations in LS-DYNA [Amdahl and Johansen, 2001]. The curves are given in figure 7.11 and figure 7.12.

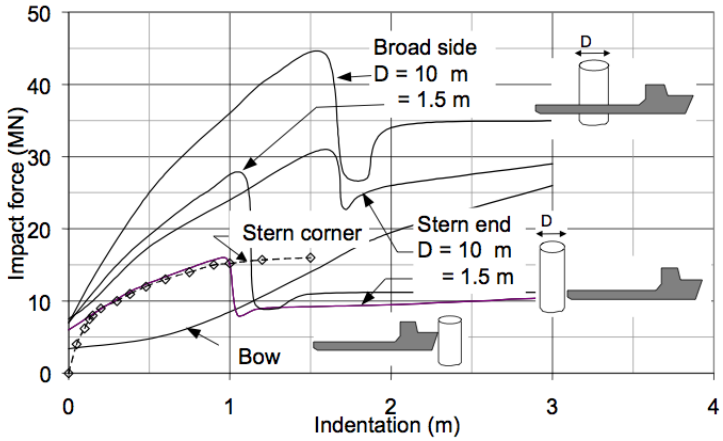

Figure 7.10: NORSOK load-deformation curve for beam/stern/bow impact

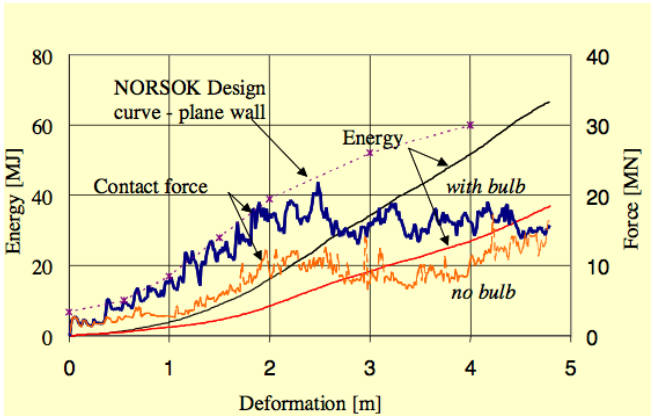

Figure 7.11: Load-deformation curve, bow impact with vertical leg, $D \simeq 2m$

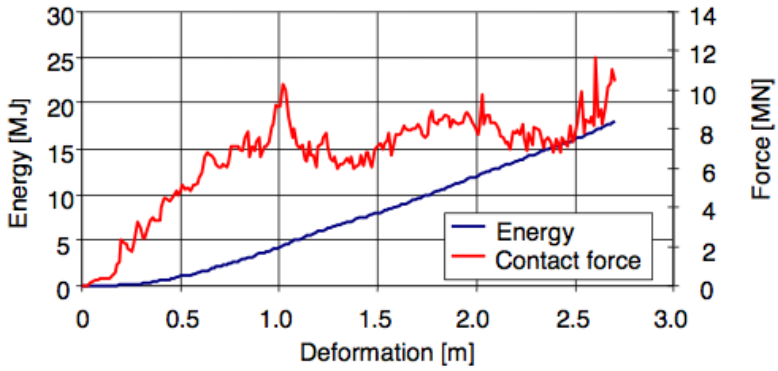

Figure 7.12: Load-deformation curve, bow impact with oblique brace, $D \simeq 1m$

Amdahl and Johansen did collision tests with and without bulb, and with a single oblique brace. The bow was considered to be strong and the model was made to be conservative. In the analysis in chapter 5 the bow was crashed into two separate legs with diameter $1067mm$ and two braces with diameter $450mm$.

Amdahl and Johansen only analyzed collision with one single member, while the collision model in this thesis included two legs and two braces with lesser diameters than for Amdahl and Johansens simulations. The results are therefor not trivial to compare.

The total force-deformation curve from the analyses in chapter 5 are for all members given in figure 7.13. Compared to the load curve without bulb in figure 7.11 and collision with oblique brace in figure 7.12 there were good accordance. The characteristics were the same, and the maximum value was also in the same range of $\simeq 12MN$ after the same displacement ($\simeq 3m$). The load-displacement curve in figure 7.13 starts when the two legs have contact with the bow.

Because of the difference in collision geometry there are some difficulties with the comparison of the curves, but it can be used as a good estimate and a can be used as a basis for comparison.

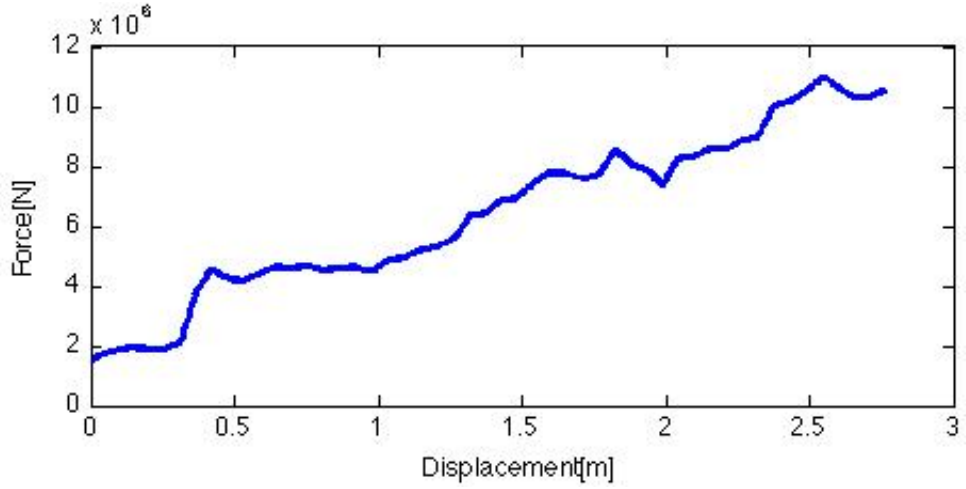

Figure 7.13: Total load-deformation from LS-DYNA

A suggestion to NORSOK Appendix A would be to update the design curves for collision with lower diameter columns than described in figure 7.10, because the curve overestimates the force for smaller diameter columns. It could also be suggested to describe collision design with several columns at other points than in the centre of the bow, which is the only collision characteristics described in NORSOK.

7.3 Sources of discrepancy

The results obtained in this theses were comparable and similar to the actual damage, but there will always be some errors and deviations because of sources of discrepancy. Because of the use of two separate FE models, errors are easily transferred in the analysis process.

7.3.1 FE models

A possible source of errors is the two FE models of the jacket and the vessel bow. The model of the bow was made after paper drawings, using ruler and pencil to calculate nodal points. These points were inserted into MSC.Patran, and lines were drawn between points. If the points were inserted wrong or if the scaling system was interpreted wrong, the model could deviate from the actual bow.

All of the member thicknesses on the plates and stiffeners were found in the same drawings. These drawings were from the time when the ship was constructed. No information regarding repairs or structural improvements were provided. This means that some parts of the bow model may have been less strong than the actual bow at the time of collision.

The USFOS model of Ekofisk 2/4W was provided by Atle Johansen at DNV and contained much information regarding soil data, grouting and structural repairs. This model was assumed to have a structural response close to that of the real installation. Possible deviations could be unreported corrosion on the jacket structure, badly fabricated members or joint fatigue. It is difficult to check these factors.

7.3.2 Collision modeling

In the LS-DYNA analysis, some input parameters were assumed. The boundary conditions behind the modeled bow were assumed to be fixed in all translations. It was also assumed that the collision could be modeled with a constant speed until the described deformation was obtained. This described deformation was based on the damage report and pictures taken after the accident. This could be more accurate if the precise deformation of the bow was known.

The ship collided with two of the 2/4W legs. The exact course of events are however not certain. If this was known, a better collision model could have been made. The collision model used in this thesis was based on assumptions from pictures and discussion with experts in ship collision.

The two non-linear springs imported from LS-DYNA to USFOS illustrated in figure 5.7 were simplified from the actual results, given in figure 5.6. The simplification

reduced the accuracy of the results, but because the LS-DYNA model itself had some inaccuracies this was a small source of discrepancy.

The springs from LS-DYNA were made for a certain deformation of the vessel bow. In the collapse analysis, both the mass and velocity was changed to increase the collision energy. This would also imply that the damage to the bow would be larger, and the springs could have different deformation characteristics. To better analyze the collapse, the input parameters would have to be changed in LS-DYNA as well as in USFOS to generate new non-linear springs. This was however not done in this thesis due to time issues.

7.3.3 Other sources of discrapency

All of the analyses done in this thesis were done by computer software. If undetected errors occur in the process, these errors will be transferred to most of the results.

Human errors are always a possible source of discrepancy. Mistakes like bad calculations and wrong assumptions could happen when working with this type of problems. Errors can be reduced by checking and ensuring correctness of calculations, and discuss methods and results with experts.

Chapter 8

Conclusion

The type of uncoupled analyses used in this thesis worked well for the collision analysis and gave good results. It gave reasons to believe that two different FE-programs can be used together and still give usable results. The damage obtained from the dynamic analysis was similar to the reported structural damage. The results were also similar to the design procedures described in NORSOK N-004 Appendix A.

The two FE models were able to give reasonable results. Many simplifications were made when modeling the bow of BOXVIII. Details as holes, bollards and deck equipment were neglected, which could have produced some in-accuracies. But because of the simplifications to the springs itself, these inaccuracies would not affect the final results.

The collision model which was supported by the two bridges was rejected due to the un-similarity to the reported damage, even though the crew on Ekofisk 2/4Q could feel the vibrations from the collision. This vibration could be because of transmitted impulse force through the bridge support in the initial part of the collision.

The collapse analyses were done to document what margins the structure had against total collapse, and were carried out by increasing the collision energy. The installation was analyzed in collision with an energy increase of 10%. Large structural deformations were induced, and the installation could have collapse because of the damages. 10% energy increase is equivalent to a velocity of $5.019 m/s$ or 9.76 knots. The actual collision speed was 9.3 knots. From figure 2.1 it is illustrated that the vessel accelerated from 6.7 knots to 9.3 knots on a distance no longer than $200m$. Had the vessel started the acceleration process $50m$ further from the installation, or if it had collided with the flare support, the accident could have had much worse consequences.

Collapse analyses with impact with only one leg was also performed, in both north and south direction. These analyses resulted in the structure getting severe rotational deformations. The two-leg collision between Big Orange XVIII and Ekofisk 2/4W probably prevented these more severe rotations to the structure, and may even have prevented the structure from collapsing.

8.1 Further work

There are several problems to be addressed to further improve the collision model. To check the correctness of the results, the analysis in LS-DYNA could be modified. Instead of using a described displacement of the jacket structure into the bow, the configuration could be changed with the bow given an initial speed into a fixed jacket structure. The mass behind the bow would had to be modeled correctly, and the work would have been tedious.

As discussed in section 7.3.2 the non-linear springs are not accurate for the collapse analyses, because the springs are configured for the given mass and velocity in the actual event. This problem could also be solved with changing the analysis configuration in LS-DYNA. If the configuration with initial speed was to be used and this gave good results, the mass and speed could also here be increased like in the collapse analysis in USFOS. The new non-linear springs would be implemented in USFOS and give a more accurate collapse analysis result.

The design procedures in NORSOK emphases on collisions between vessels and large diameter columns. They also mention collision with jacket legs, but these design curves are overly conservative. This is because the entire bow is not subjected to uniform deformation like in collision with large diameter columns. Based on the results described in section 7.2 and in Ship Collision Analysis, chapter 7 [Amdahl and Skallerud, 2002] a more accurate design procedure could be implemented in NORSOK for columns with smaller diameters.

Bibliography

[Alsos, 2008] Alsos, H. S. (2008). *Ship Grounding*. NTNU.

[Amdahl, 2011] Amdahl, J. (2011). Professor at institute of marine technology.

[Amdahl and Johansen, 2001] Amdahl, J. and Johansen, A. (2001). High-energy ship collision with jacket leg. Technical report, ISOPE stavanger.

[Amdahl and Skallerud, 2002] Amdahl, J. and Skallerud, B. (2002). *Ship Collision Analysis*.

[C.J.F.Clausen et al., 2006] C.J.F.Clausen, P.M.Aas, and K.Karlsrund (2006). Bearing capacity of driven piles in sand and clay, the ngi approach.

[DNV, 2003] DNV (1976-2003). Structural drawings of ekofisk 2/4 whisky.

[DNV, 2006] DNV (2006). Lifetime ekow struct integrity study. Technical report.

[dynasupport.com, 2011] dynasupport.com (2011). Dyna support.

[Gjerstad, 2009] Gjerstad, V.-A. (2009). Ekow boat impact- above water structural damages rev02. Technical report, Conoco Phillips.

[Gjerstad, 2011] Gjerstad, V.-A. (2011). Employee at conocco phillips.

[Hallquist, 2006] Hallquist, J. O. (2006). *LS-DYNA Theory Manual*. Livermore Software Technology Corporation.

[Johansen et al.,] Johansen, A., Solland, G., and Reitan, A. Employee at dnv.

[Liu, 2011] Liu, Z. (2011). Phd at institute of marine technology.

[Logan, 2007] Logan, D. L. (2007). *A first course in the finite element method*. 4 edition.

[Moan, 2003] Moan, T. (2003). *Finite Element modeling and analysis of offshore structures*.

[Moan, 2004] Moan, T. (2004). *Design of Offshore Structures*. Institute of Marine Technology.

[mscsoftware.com, 2011] mscsoftware.com (2011). Msc.software.

[NORSOK, 2004] NORSOK (2004). Norsok n-004 appendix a ship collisions.

[NPD, 2009a] NPD (2009a). Investigation report after the collision between ekofisk 2/4w and big orange xviii.

[NPD, 2009b] NPD (2009b). Investigation reports of offshore collisions.

[Schlumberger, 2009] Schlumberger (2009). Main dimensions of big orange xviii.

[Søreide et al., 1993] Søreide, T. H., Amdahl, J., Eberg, E., Holmås, T., and Hellan, Ø. (1993). Usfos theory manual. SINTEF Marintek.

[Subsea7, 2009] Subsea7 (2009). Ekow damage survey. Technical report.

[Ulstein, 1983a] Ulstein (1983a). Shell expansion drawing of boxviii.

[Ulstein, 1983b] Ulstein (1983b). Structural drawings of upper bow, boxviii.

[Weight.and.Sea.AS, 2006] Weight.and.Sea.AS (2006). Weight report; ekofisk 2/4 whisky.

[wikipedia.org, 2011] wikipedia.org (2011). Wikipedia.

Appendix A

LS-DYNA analyses

A.1 Deformed bow, 450mm mesh

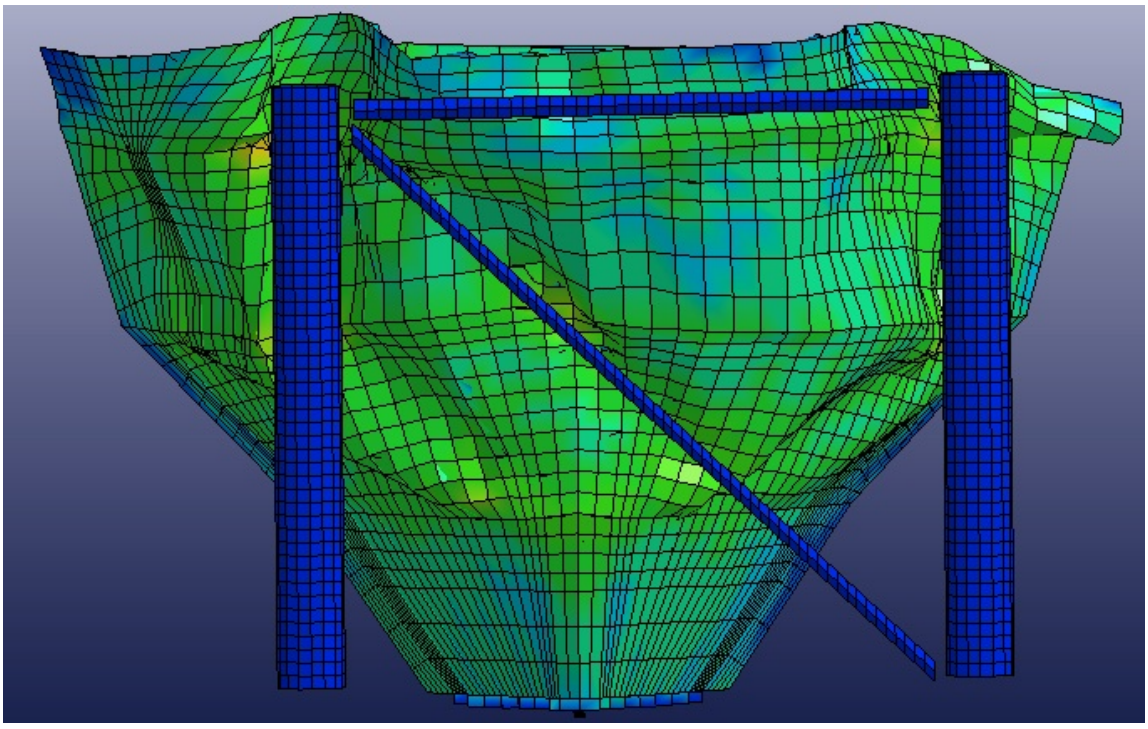

Figure A.1: 450mm front

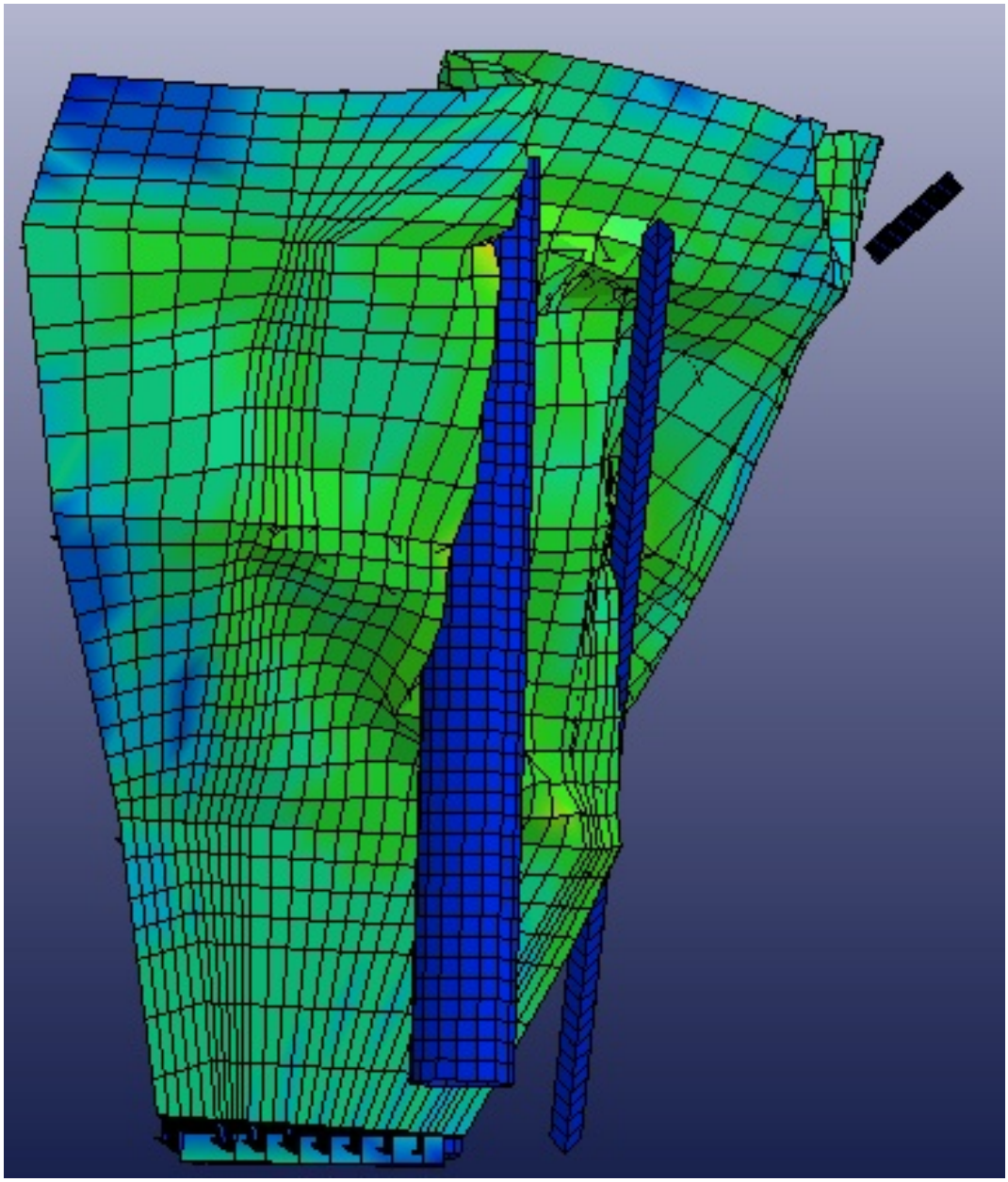

Figure A.2: 450mm side

A.2 Deformed bow, 200mm mesh

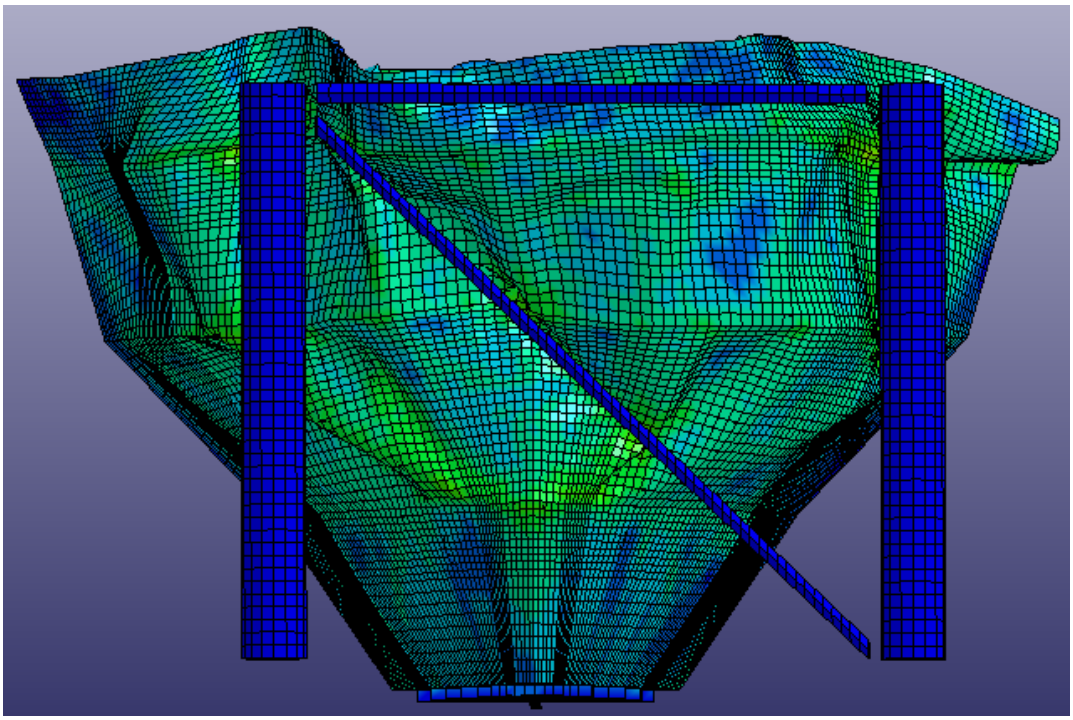

Figure A.3: 200mm front

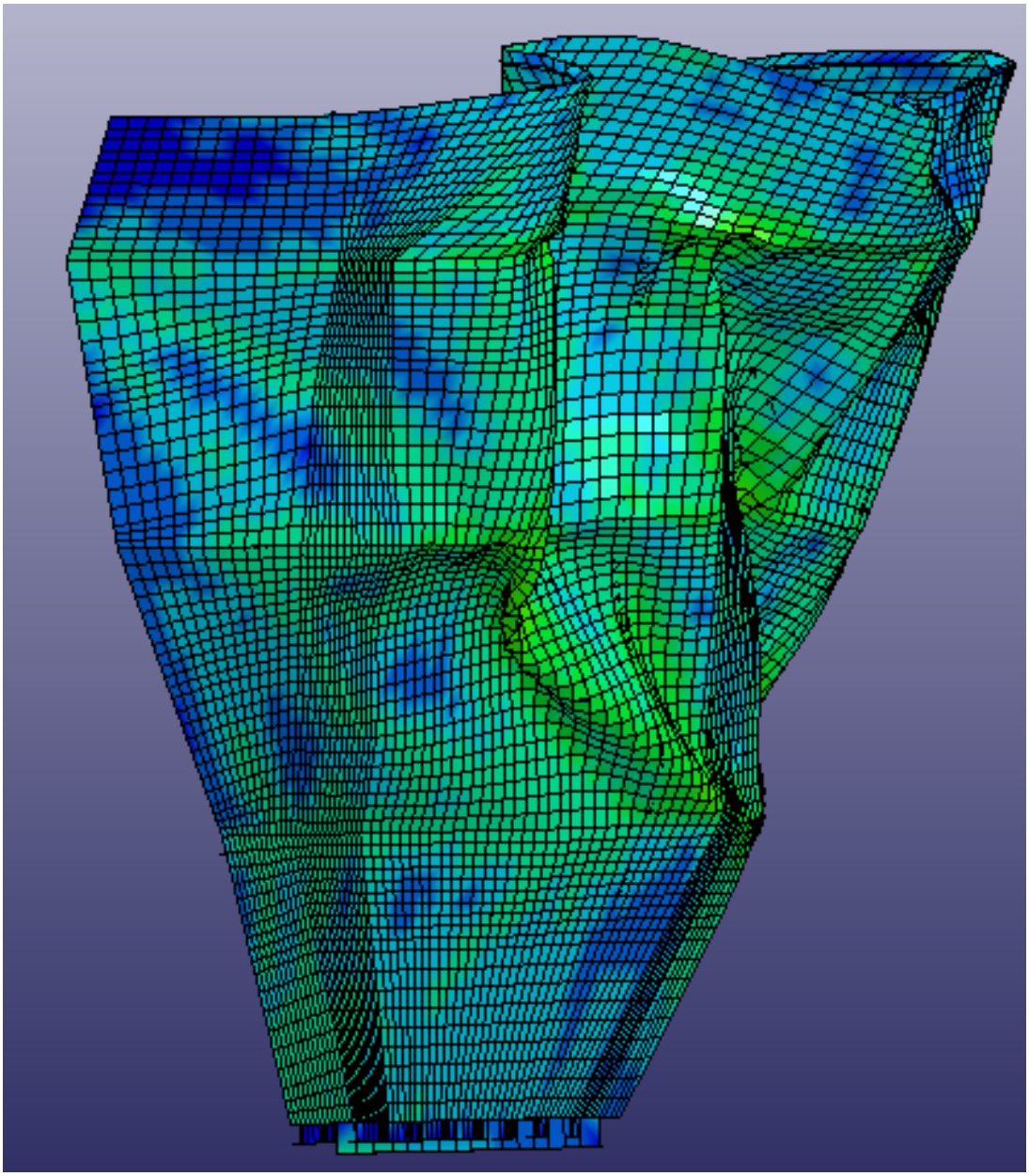

Figure A.4: 200mm side

Appendix B

USFOS analyses

B.1 Structural response, dynamic ship collision

B.1.1 Unsupported model

Structural response of dynamic ship collapse analysis. 0-5.5 seconds. δs=0.5:

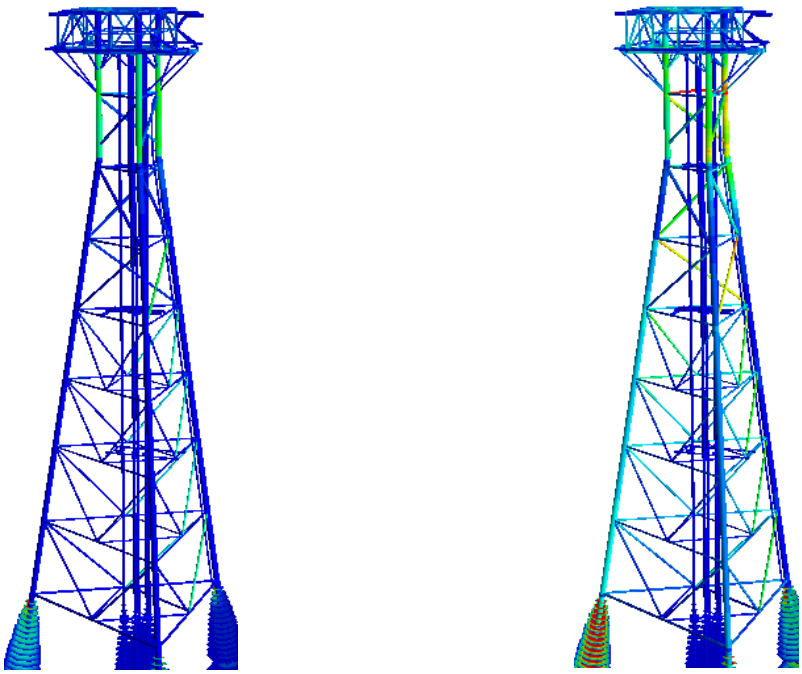

Figure B.1: 0.0s-0.5s

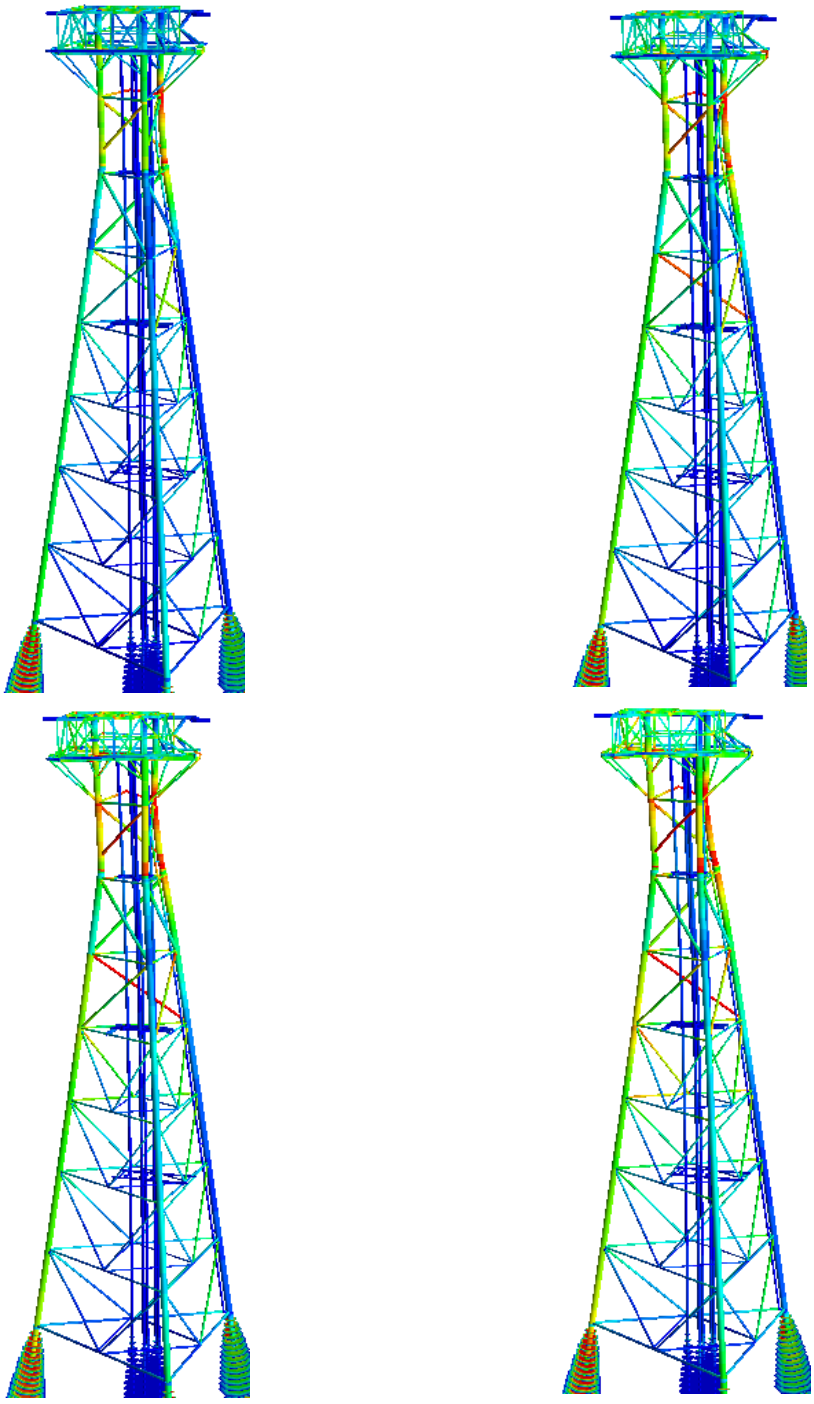

Figure B.2: 0.5s-2.0s

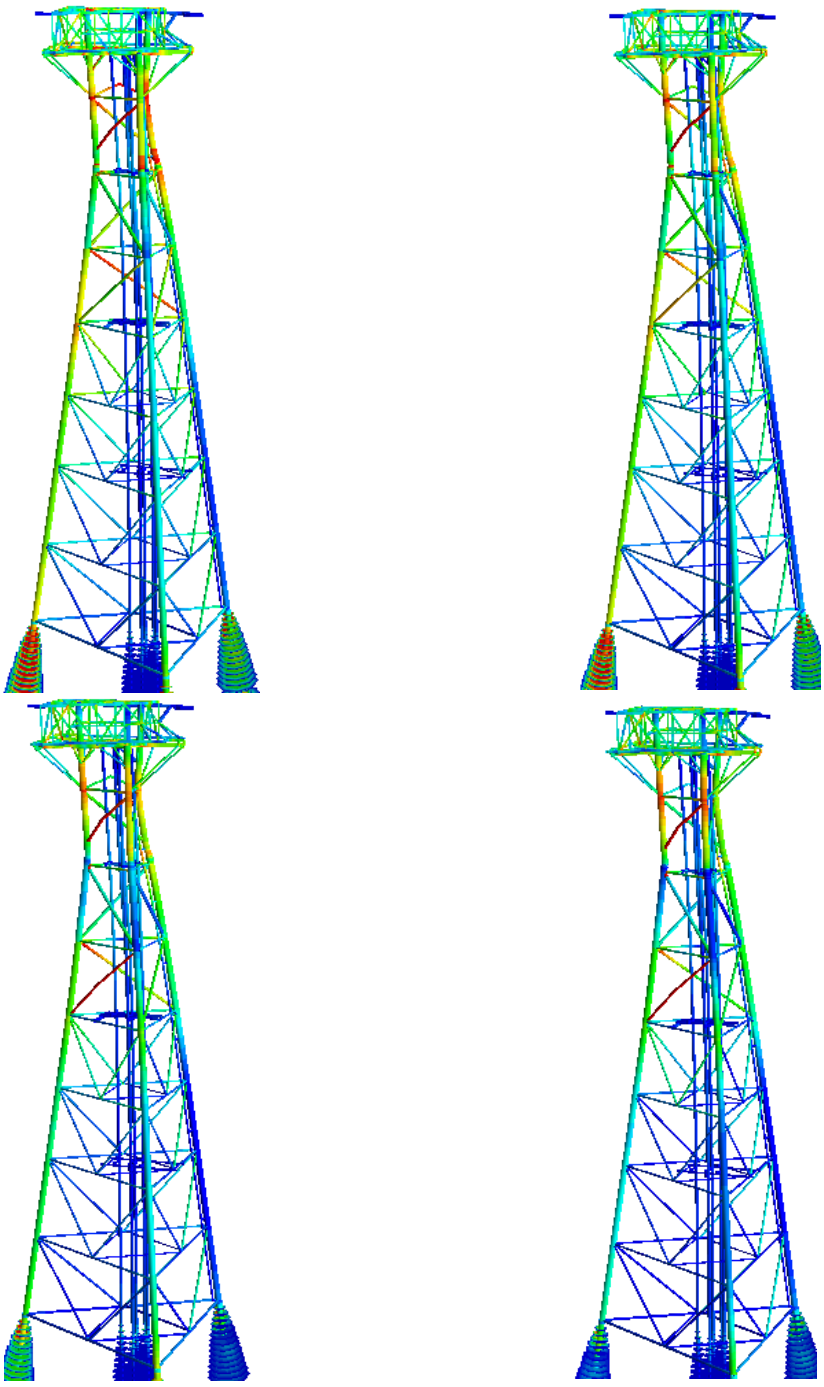

Figure B.3: 2.5s-4.0s

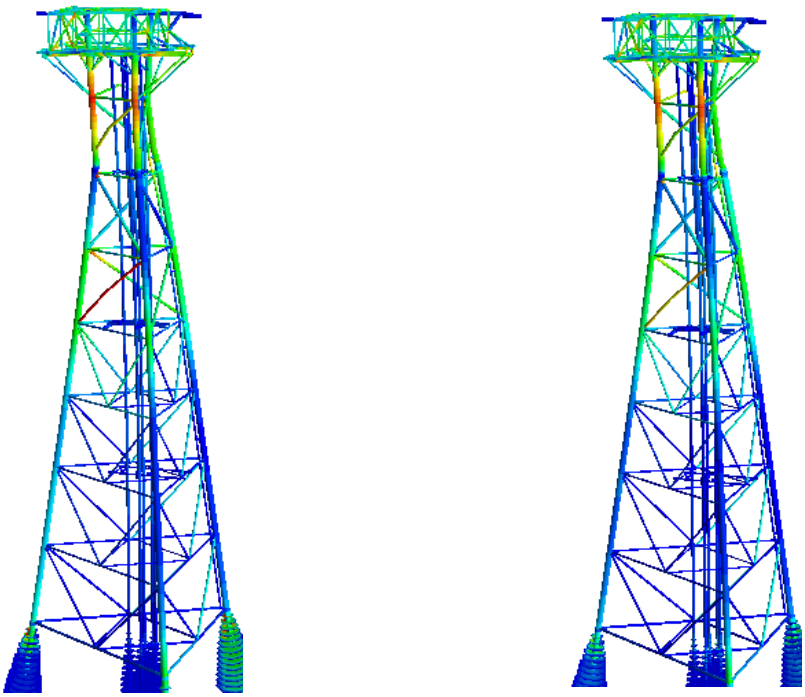

Figure B.4: 4.5s-5.0s

B.1.2 Collapse model, 10%

Structural response of dynamic ship collapse analysis. 0-5.5 seconds. δs=0.5:

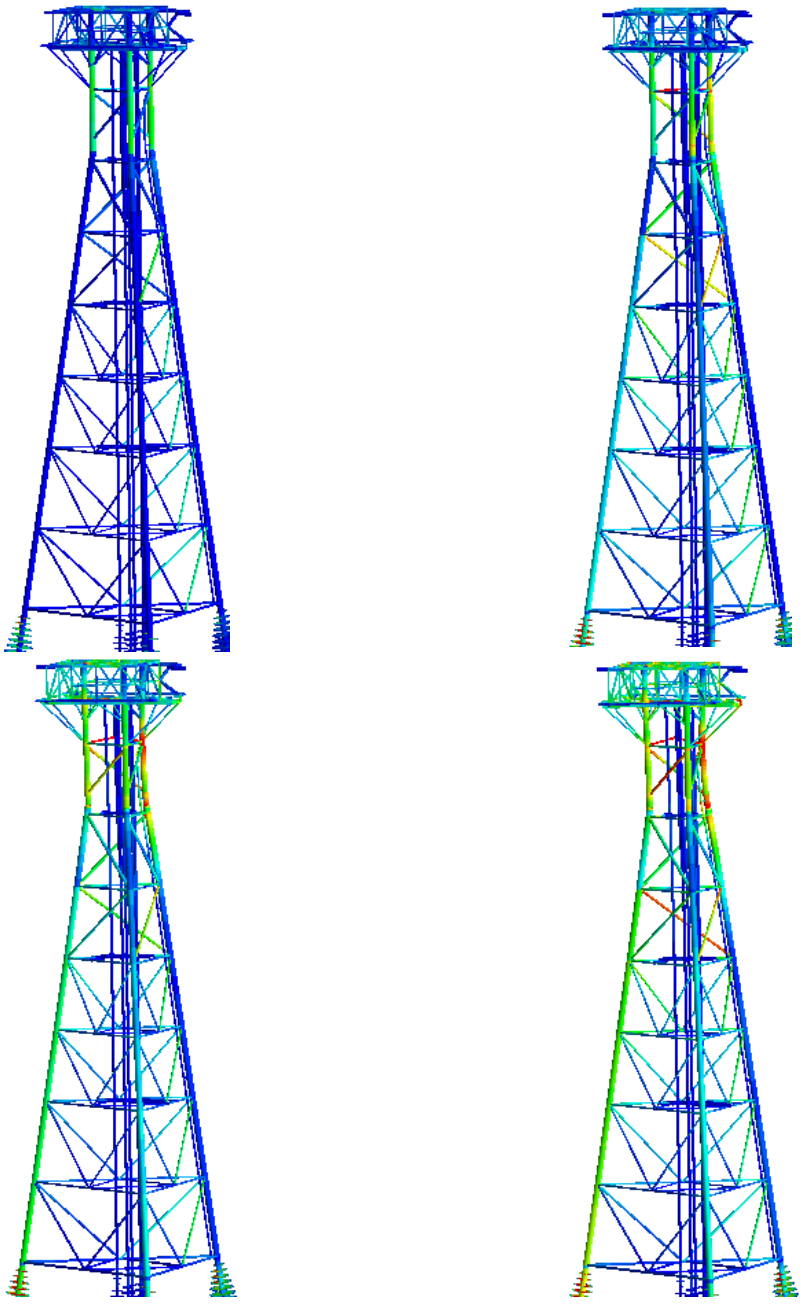

Figure B.5: 0.0s-1.5s

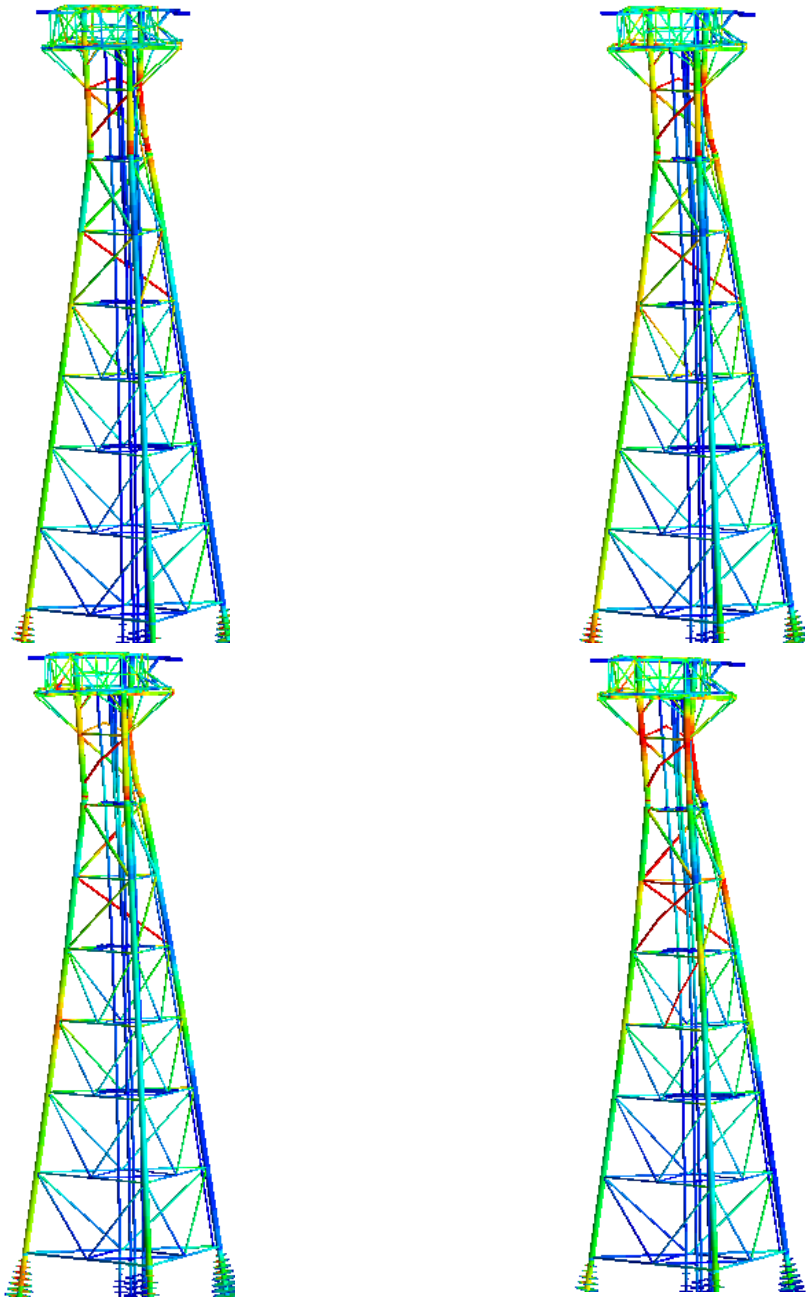

Figure B.6: 2.0s-3.5s

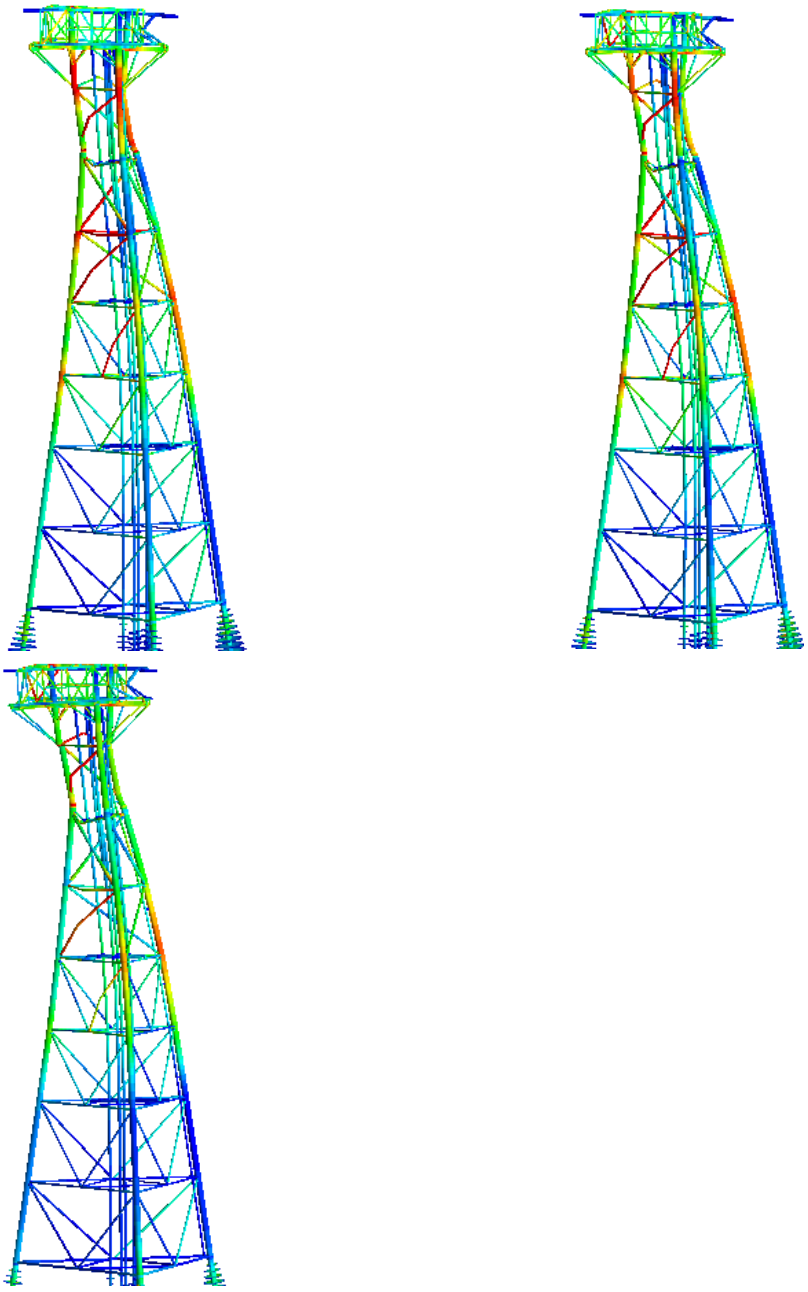

Figure B.7: 4.0s-5.0s

B.2 Load-deformation curves, ship collision in USFOS

B.2.1 Static collision analysis

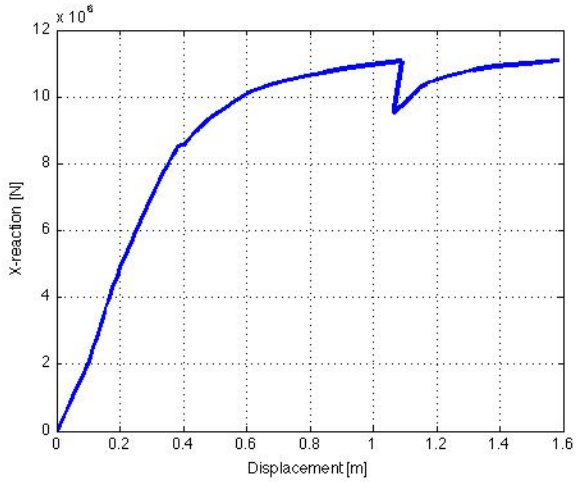

Figure B.8: Force-displacement, 2/4W

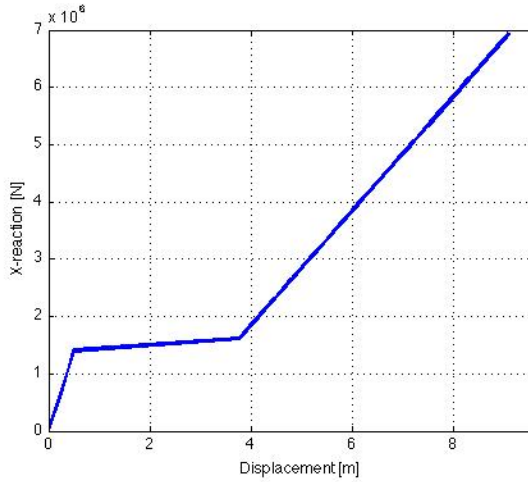

Figure B.9: Force-displacement, starboard spring

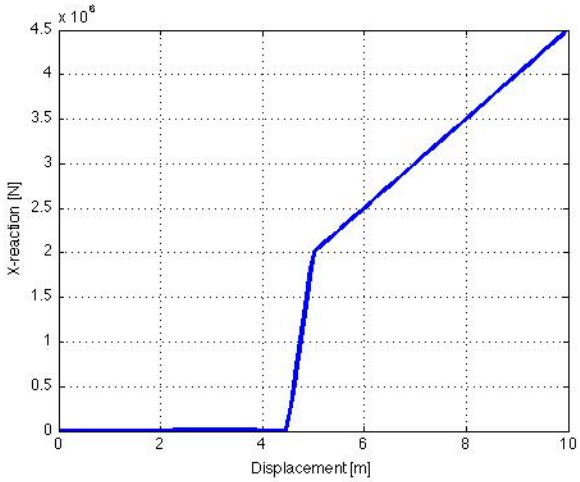

Figure B.10: Force-displacement, port spring

B.2.2 Dynamic collision analysis

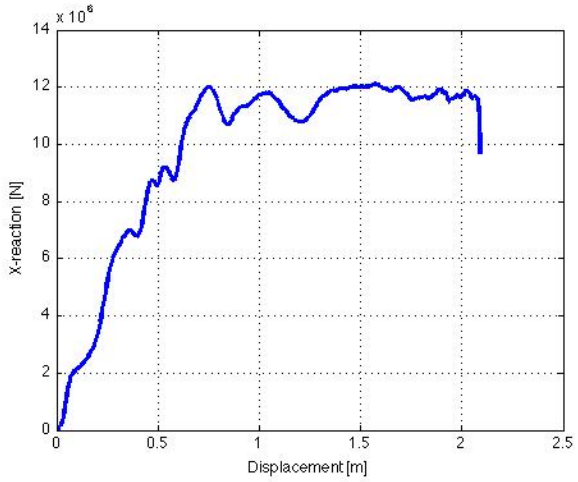

Figure B.11: Force-displacement, 2/4W

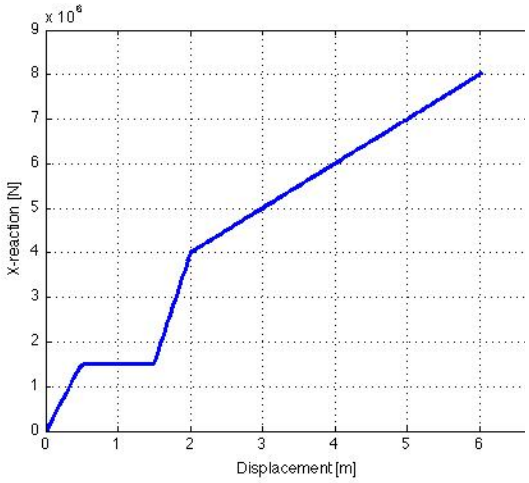

Figure B.12: Force-displacement, starboard spring

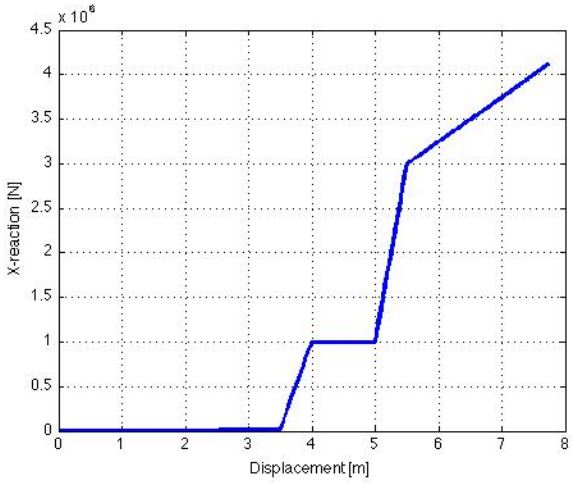

Figure B.13: Force-displacement, port spring

B.2.3 Dynamic collision analysis, bridge supported

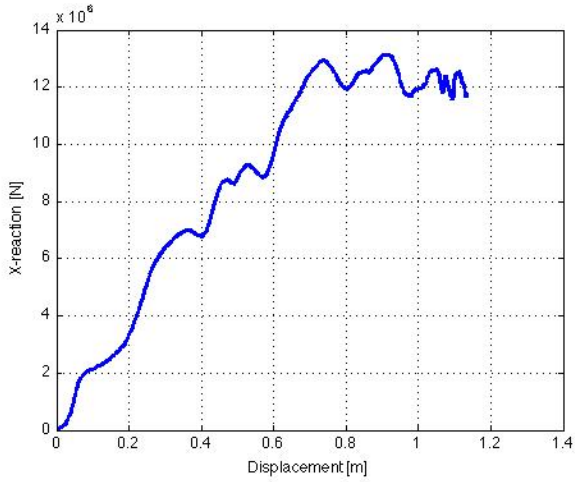

Figure B.14: Force-displacement, 2/4W

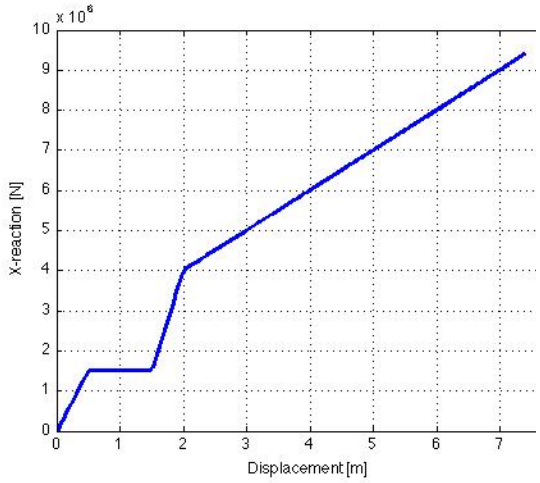

Figure B.15: Force-displacement, starboard spring

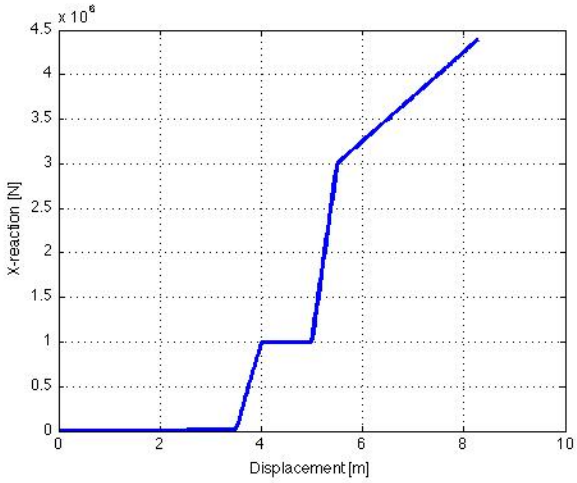

Figure B.16: Force-displacement, port spring

B.2.4 Collapse analysis, 5% energy increase by velocity

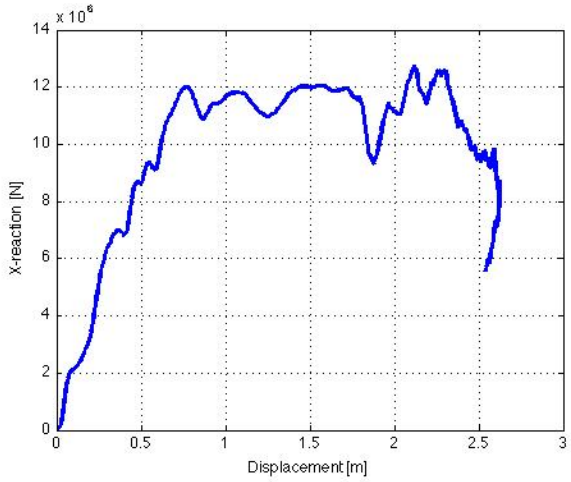

Figure B.17: Force-displacement, 2/4W

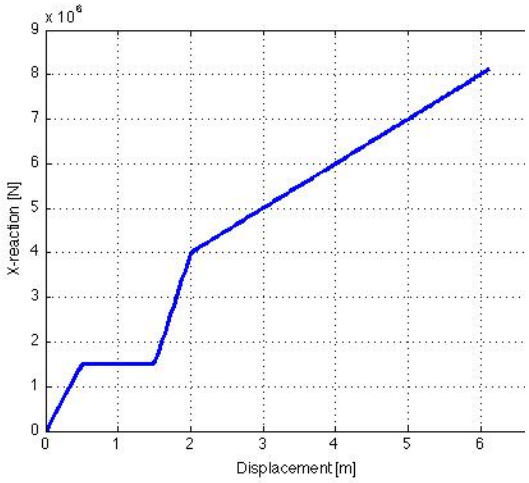

Figure B.18: Force-displacement, starboard spring

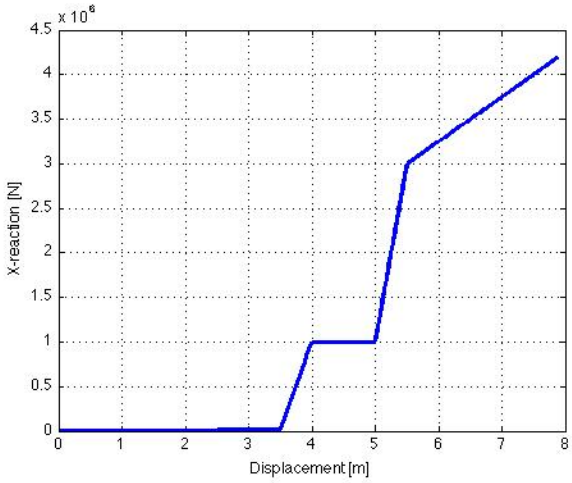

Figure B.19: Force-displacement, port spring

B.2.5 Colapse analysis, 5% energy increase by mass

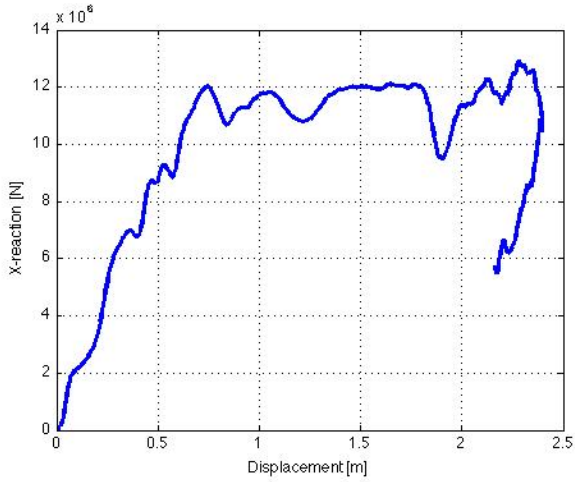

Figure B.20: Force-displacement, 2/4W

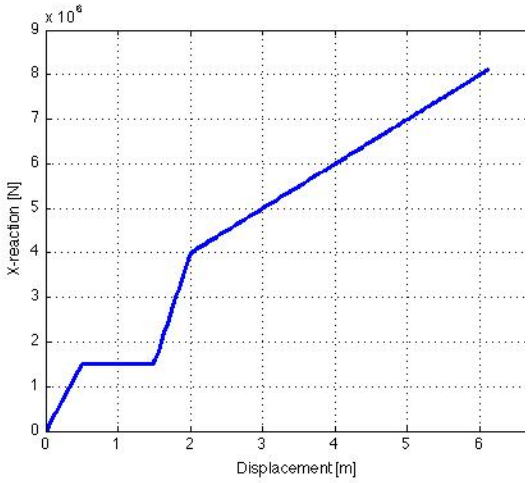

Figure B.21: Force-displacement, starboard spring

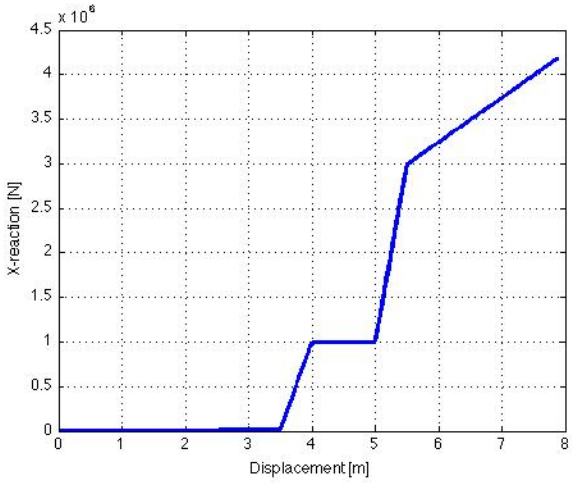

Figure B.22: Force-displacement, port spring

B.2.6 Collapse analysis, 7% energy increase by velocity

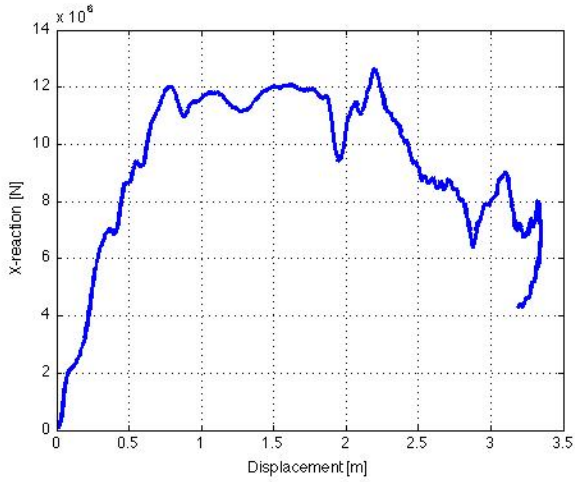

Figure B.23: Force-displacement, 2/4W

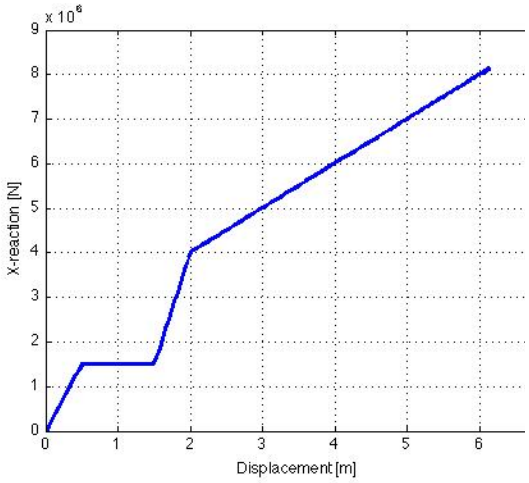

Figure B.24: Force-displacement, starboard spring

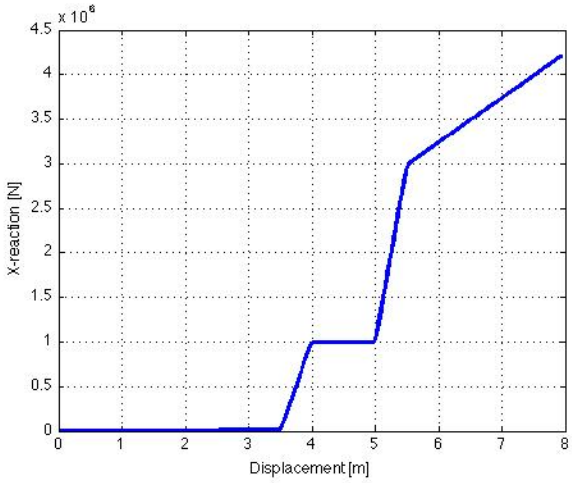

Figure B.25: Force-displacement, port spring

B.2.7 Collapse analysis, 7% energy increase by mass

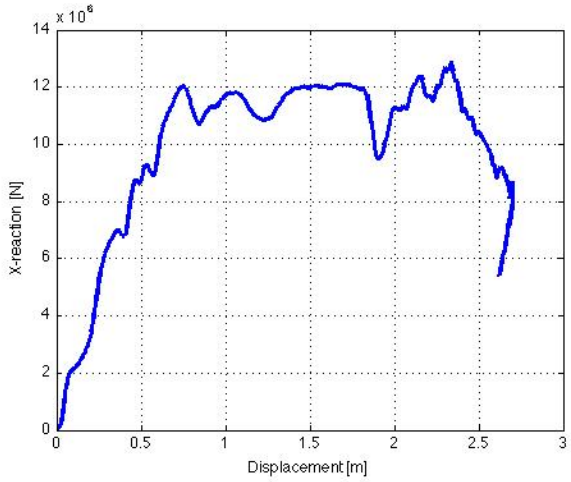

Figure B.26: Force-displacement, 2/4W

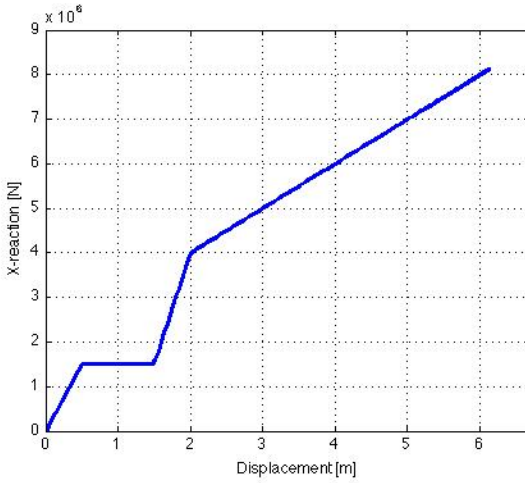

Figure B.27: Force-displacement, starboard spring

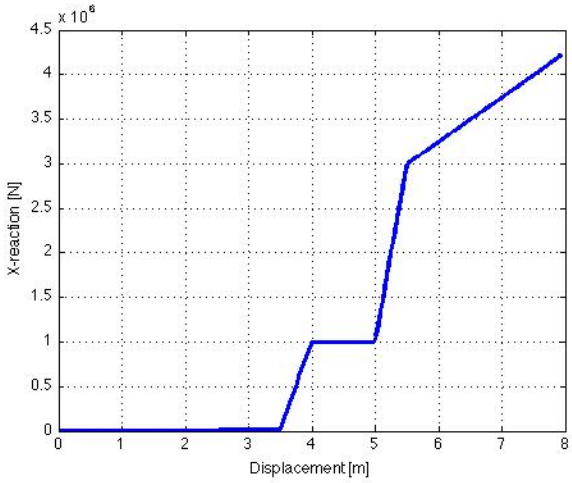

Figure B.28: Force-displacement, port spring

B.2.8 Collapse analysis, 10% energy increase by velocity

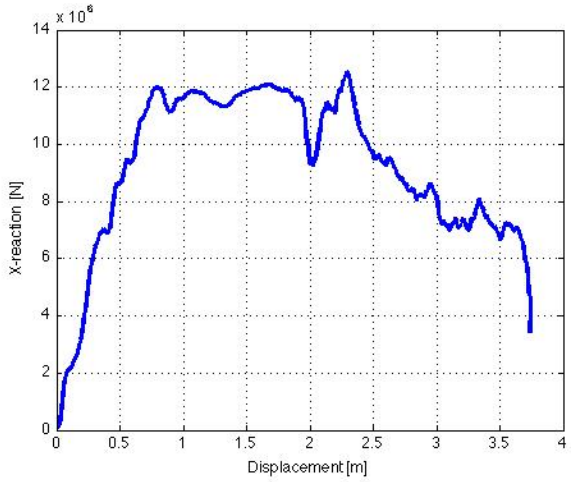

Figure B.29: Force-displacement, 2/4W

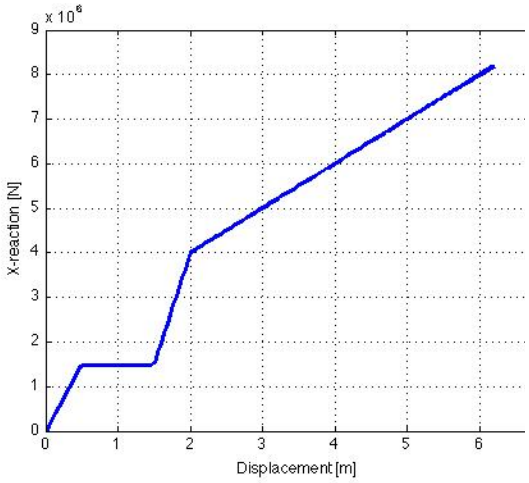

Figure B.30: Force-displacement, starboard spring

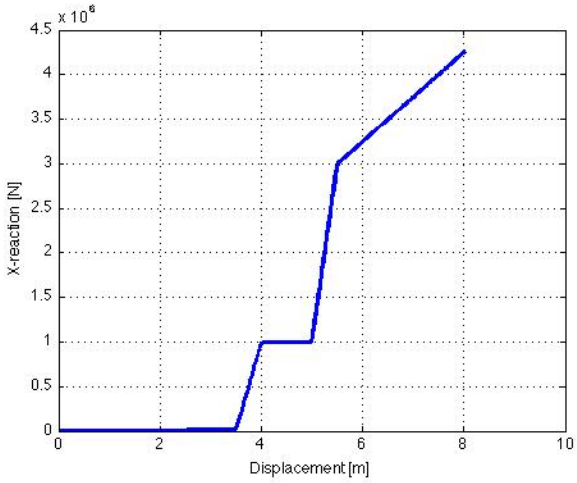

Figure B.31: Force-displacement, port spring

B.3 Velocities, dynamic ship collision

B.3.1 Unsupported

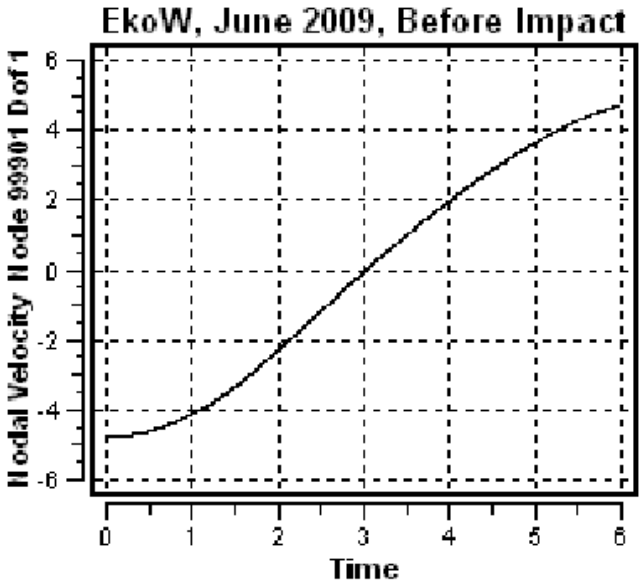

Figure B.32: Ship velocity

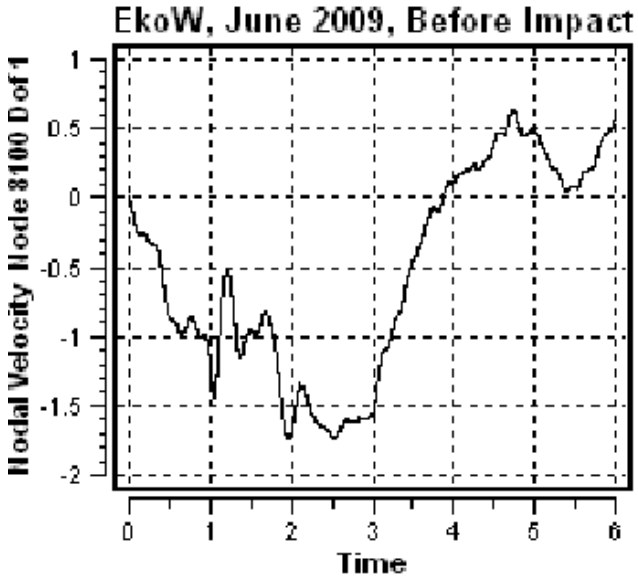

Figure B.33: Structure velocity

B.3.2 Bridge supported

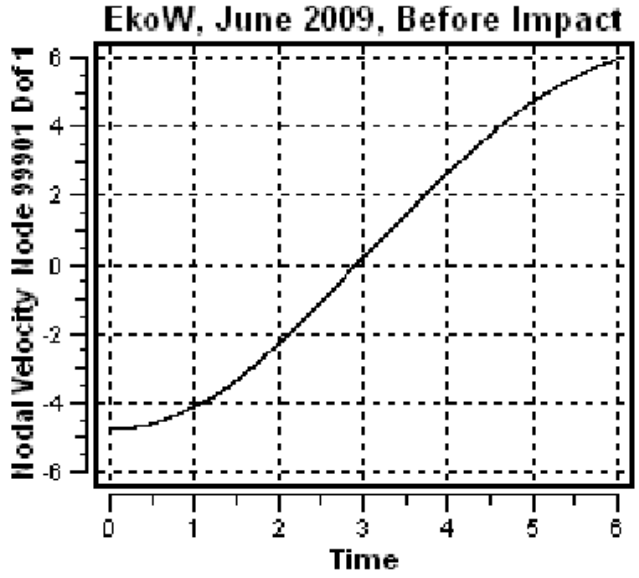

Figure B.34: Ship velocity

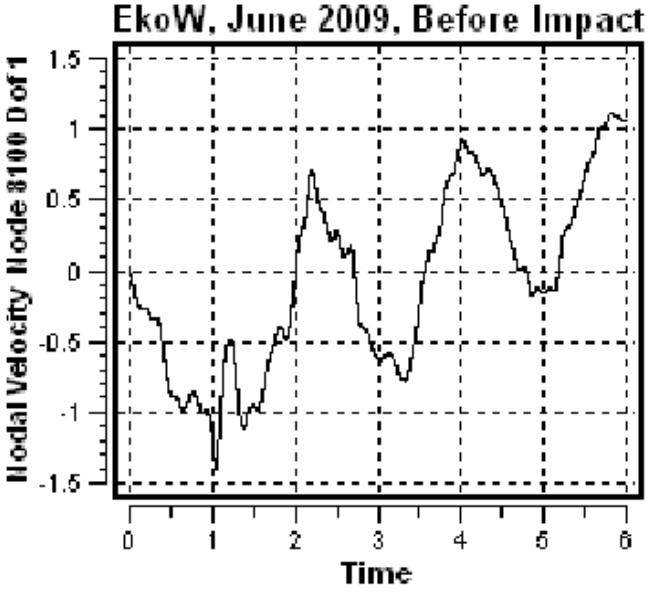

Figure B.35: Structure velocity

B.3.3 Collapse analysis, 10% energy increase

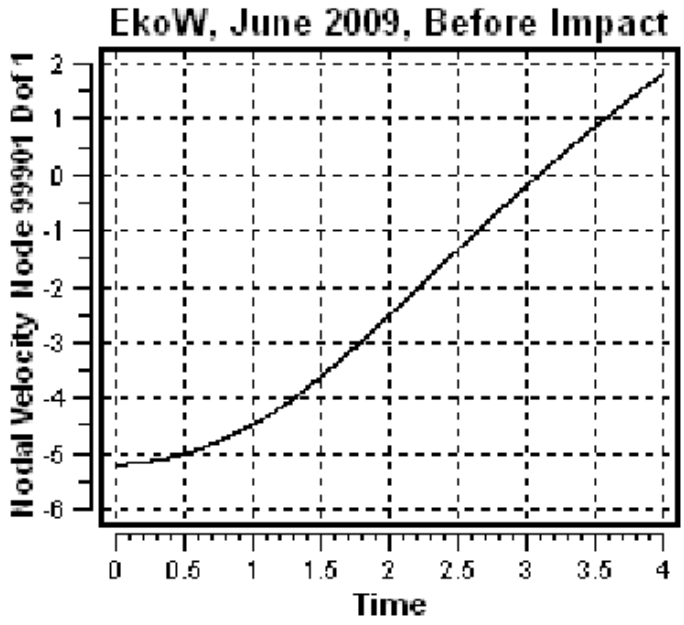

Figure B.36: Ship velocity

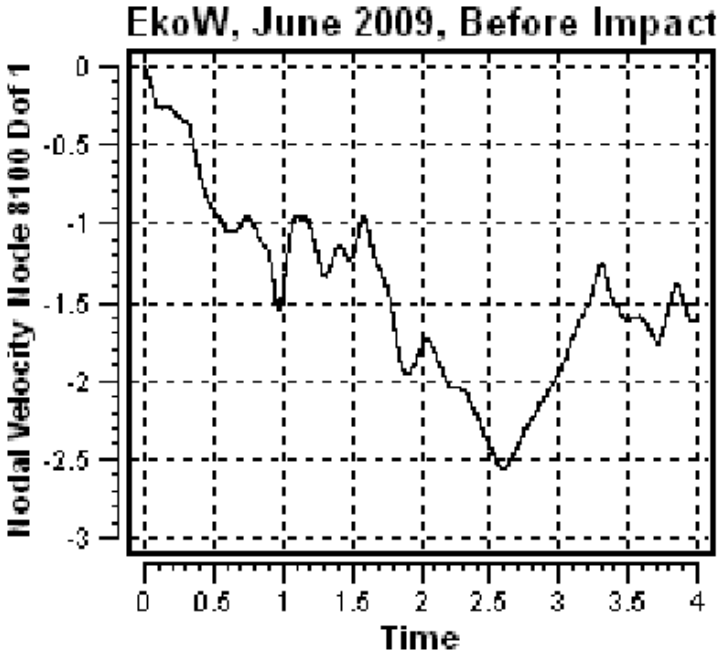

Figure B.37: Structure velocity

B.4 Accelerations, dynamic ship collision

B.4.1 Unsupported

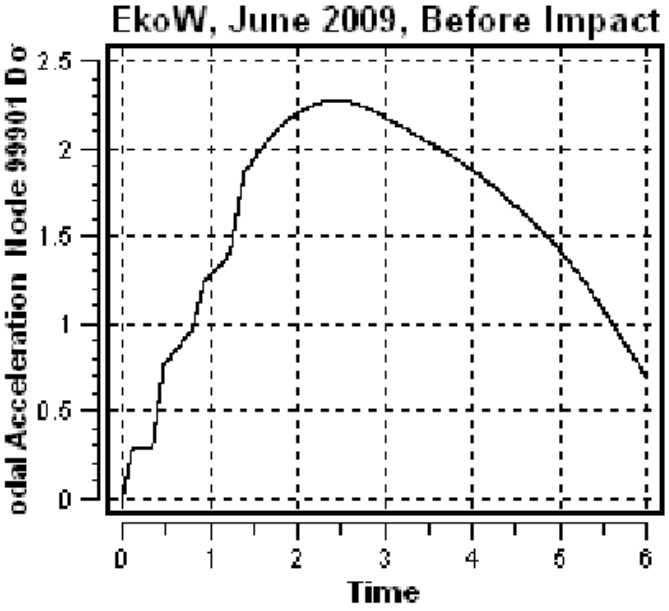

Figure B.38: Ship acceleration

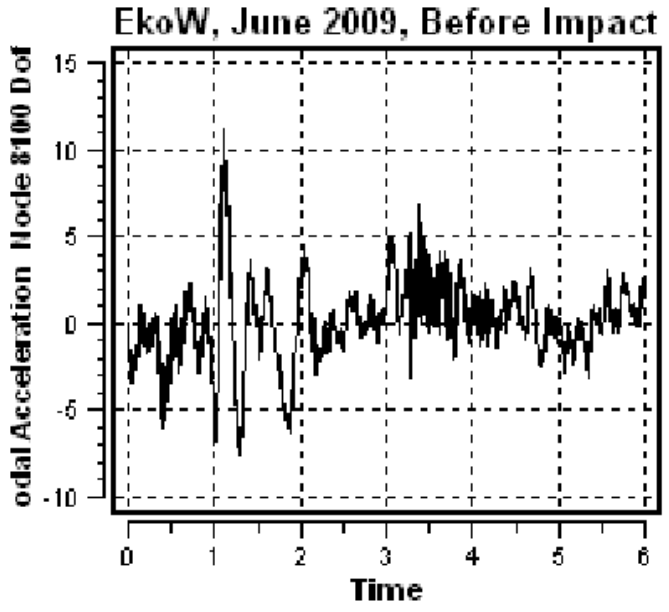

Figure B.39: Structure acceleration

B.4.2 Bridge supported

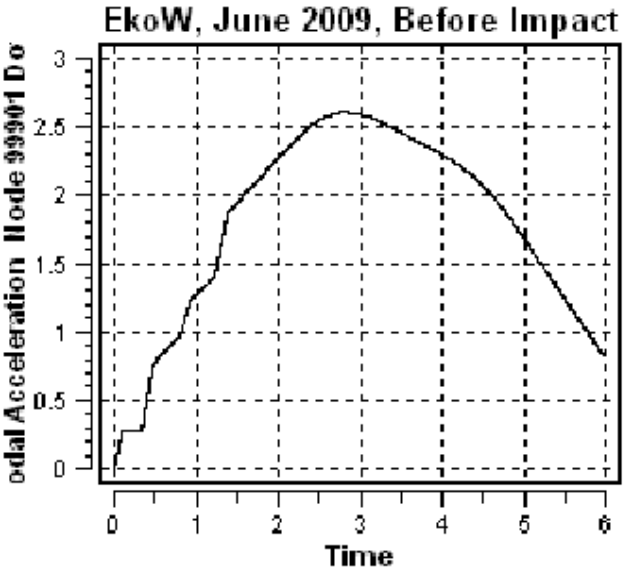

Figure B.40: Ship acceleration

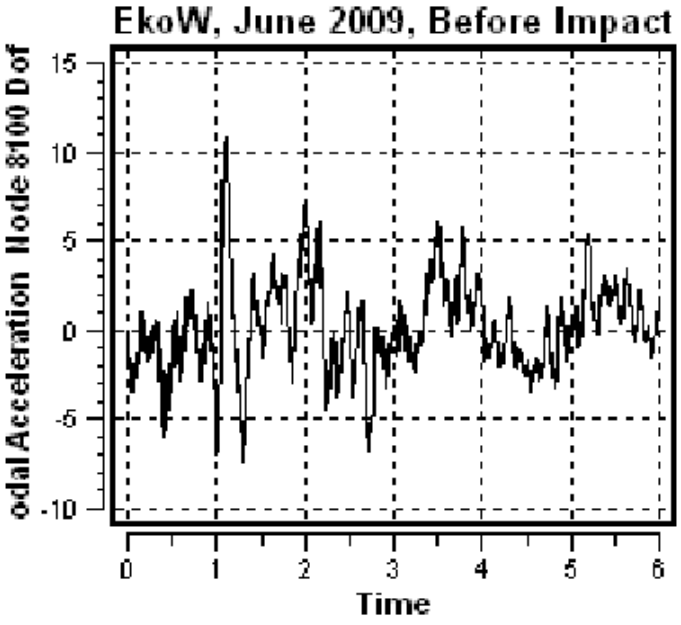

Figure B.41: Structure acceleration

B.4.3 Collapse analysis, 10% energy increase

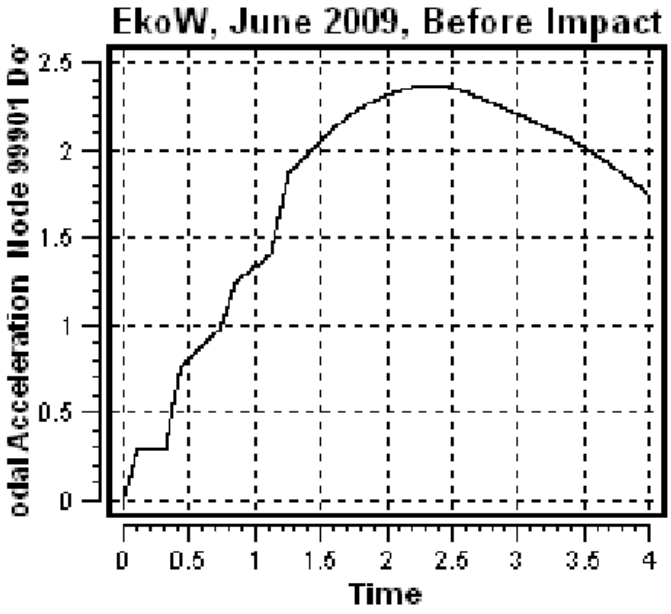

Figure B.42: Ship acceleration

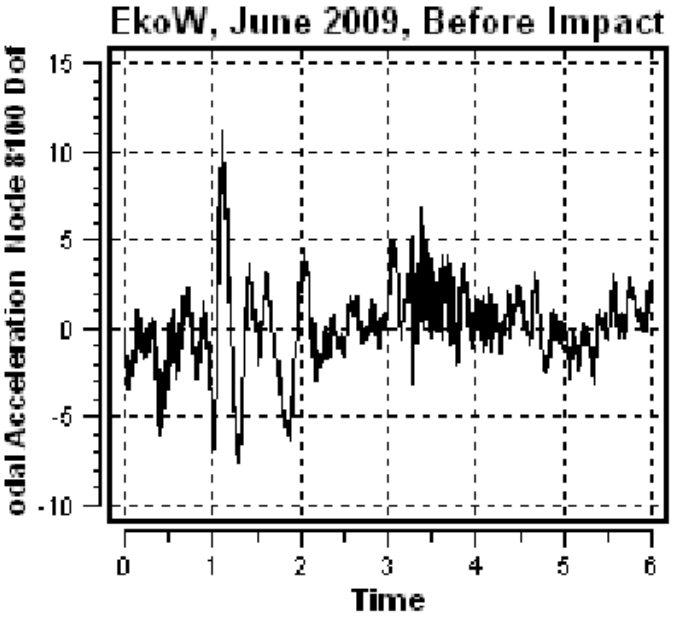

Figure B.43: Structure acceleration

Appendix C

Matlab analyses

The different input files for the matlab analyses are found in appendix D. The input files must be located in the same folder as the matlab code for the program to run.

```
%   Erik Paulsen, Master Thesis 2011
%
%   Script for calculating energy from load-deformation curve. The code
%   has been used to post process results from both USFOS and LS-DYNA.
%
%   filename: energy_ld.m
%
%
%%%%%%%%%%%%%%%%%%%%%%%%%%%%%%%%%%%%%%%%%%%%%%%%%%%%%%%%%%%%%%%%%%%%%%%%%%%%%%%
clc;
%clear all;
disp('Erik Paulsen. Master Thesis 2011 ');
disp(' ');
disp(' ');
%%%%%%%%%%%%%%% Opening the .txt- file, converting to data %%%%%%%%%%%%%%%%
file=uigetfile('*.*','Select txt-files');
fid=fopen(file);
varX=fscanf(fid,'%f %f',[2 inf]);
varX=varX';
disp(['Filename:  ',file])
%%%%%%%%%%%%%%% Make sure all the values are positive %%%%%%%%%%%%%%%%%%%%%%
varX=abs(varX);
%%%%%%%%%%%%%%% Make sure displacement are in meters %%%%%%%%%%%%%%%%%%%%%%%
if varX(30,1)>1
    varX(:,1)=.001*varX(:,1);
end
%%%%%%%%%%%%%%% Integrating to find energy %%%%%%%%%%%%%%%%%%%%%%%%%%%%%%%%
energy=trapz(varX(:,1),varX(:,2));
MJ=energy/1e6;
disp(['The absorbed energy is:  ',num2str(energy),' J = ',num2str(MJ),...
    ' MJ'])
%%%%%%%%%%%%%%% Plotting result %%%%%%%%%%%%%%%%%%%%%%%%%%%%%%%%%%%%%%%%%%%
plot(varX(:,1),varX(:,2),'linewidth',3);
xlabel('Displacement [m]');
ylabel(' X-reaction [N]');
grid on;
%%title('Starboard Leg, 200mm');

%%%%%%%%%%%%%%% Curves introduced to USFOS %%%%%%%%%%%%%%%%%%%%%%%%%%%%%%%%
%m_200sl=[4 1e4;.01 1e4;-.01 -1e4;-.5 -1.5e6;-1.5 -1.5e6;-2. -4.0e6;...
%-3.5 -5.5e6];
%m_200pl=[4 1e4;3 1e4;-3 -1e4;-3.5 -1e6;-4.5 -1e6;-5.0 -3.0e6;...
%-6.0 -3.5e6];
```

Appendix D

Digital files

D.1 USFOS

- Input files, static and dynamic analyses
- Animation, dynamic collision

D.2 LS-DYNA

- Input files, 450mm 250mm 200mm mesh
- Animation, 200mm mesh

D.3 MSC.Patran

- Database file, bow model

D.4 Matlab

- Matlab script file
- Matlab input files for post processing LS-DYNA results